University of Alberta

Supercritical Fluid Chromatography and High Temperature Liquid Chromatography for the Group-Type Separation of Diesel Fuels and Heavy Gas Oils

by

Richard Edmund Paproski 

A thesis submitted to the Faculty of Graduate Studies and Research
in partial fulfillment of the requirements for the degree of

Doctor of Philosophy

Department of Chemistry

Edmonton, Alberta
Fall, 2007

Your file Votre référence
ISBN: 978-0-494-33043-2
Our file Notre référence
ISBN: 978-0-494-33043-2

ABSTRACT

The group-type composition of fossil fuels affects their performance and environmental properties. Supercritical fluid chromatography (SFC) and normal phase high performance liquid chromatography (HPLC) are commonly applied to the determination of the proportion of saturates, mono-, di-, tri-, and polyaromatic hydrocarbons in these samples, but often fail to achieve adequate group-type resolution.

This thesis investigates the use of unconventional columns for separating diesel fuels by SFC and heavy gas oils (boiling range >350°C) by high temperature normal phase HPLC to improve group-type resolution. Higher mobile phase flow rates and unconventional column dimensions were also studied to obtain faster analysis times with both SFC and HPLC.

The highest group-type resolutions with SFC were obtained by serially coupling bare titania and bare silica columns. Short (5 to 15 cm) packed columns and monolithic silica columns were compared at high carbon dioxide flow rates for reducing SFC analysis time, with short packed columns achieving 7-fold lower separation times (as a low as 2 min) while maintaining significant resolution. Three diesel samples were studied to demonstrate the improvements in both resolution and analysis time.

A thermally stable bare zirconia column for normal phase HPLC was studied at temperatures up to 200°C. Increasing temperatures significantly decreased the retention of twenty five aromatic model compounds according to the van't Hoff equation (>30-fold decrease for some compounds). Large improvements in peak

shape, efficiency (>2.2-fold), group-type selectivity, and column re-equilibration times (>5-fold) were obtained at elevated temperatures. The thermal decomposition of two polar nitrogen compounds (indole and carbazole) was observed in a hexane/dichloromethane mobile phase at temperatures greater than 100°C. The first order decomposition of carbazole was studied in further detail.

Titania, zirconia, carbon, silica, and aminopropyl bonded silica columns were compared for the group-type separation of heavy gas oils with normal phase HPLC. Better group-type selectivity and faster separations were obtained at elevated temperatures. A high resolution method was developed using titania and silica columns with valve-switching and dual gradients to separate three heavy gas oils. A fast analysis time method using a titania column at high flow rates achieved separations in only 3 min.

ACKNOWLEDGEMENTS

I would like to thank my supervisor Dr. Charles Lucy for his guidance, support, and teachings during my time at the University of Alberta. His advice and direction have been truly outstanding. I wish to thank Dr. Jean Cooley, Dr. Vince Nowlan, and Brenda Crickmore from Syncrude Canada Ltd. for their guidance, support, and inspiration in pursuing this field of research. Heartfelt thanks go to my wife Mandy and our son Ryan for their tremendous loving support. I thank present and past group members for their continued support and efforts in making life in the Lucy group a truly enjoyable experience. I am grateful to Chen Liang for her effort and commitment in the lab. Her hard work made my role as a supervisor effortless and rewarding. I am indebted to the machine shop and electronics shop at the University of Alberta for their heroics in repairing key pieces of equipment in a timely manner.

This thesis research was supported by the Natural Sciences and Engineering Research Council of Canada, the University of Alberta, Syncrude Canada Ltd., the Canada Foundation for Innovation, and The Society for Analytical Chemists of Pittsburg. Special thanks to Syncrude Canada Ltd. for the use of their supercritical fluid chromatography instrument and facilities at Syncrude Research.

TABLE OF CONTENTS

CHAPTER THREE. Fast Supercritical Fluid Chromatography Hydrocarbon Group-Type Separations of Diesel Fuels Using Packed and Monolithic Columns

CHAPTER FOUR. High Temperature Normal Phase Liquid Chromatography on Bare Zirconia

CHAPTER FIVE. Zirconia, Titania, Silica, and Carbon Columns for the Group-Type Characterization of Heavy Gas Oils using Normal Phase High Temperature Liquid Chromatography

CHAPTER SIX. Conclusions and Future Work

LIST OF TABLES

LIST OF FIGURES

LIST OF NOMEMCLATURE

Symbol	Parameter
2D	Two dimensional separation
A	Multipath band broadening term of van Deemter equation
[A]	Reactant concentration
Abs.	Absorbance
AFD	Acoustic flame detection
ASTM	American Society for Testing and Materials
B	Longitudinal diffusion term of van Deemter equation
b	Path length of an absorbance flow cell
C	Resistance to mass transfer term of van Deemter equation
$C_{i,m}$	Concentration of i in the mobile phase
$C_{i,s}$	Concentration of i in the stationary phase
Const	Constant of arbitrary value
[C]	Analyte concentration
Di	Diaromatic
D_M	Diffusion coefficient
DNAP	Dinitroanilinopropyl bonded silica
d_p	Particle diameter
ELSD	Evaporative light scattering detection
F	Flow rate
FID	Flame ionization detection
f(p,k)	Function of pressure and retention

GC	Gas chromatography
H	Plate height
H_A	Plate height contribution from the A-term
H_B	Plate height contribution from the B-term
H_C	Plate height contribution from the C-term
HGO	Heavy gas oil
HGS	Hydrocarbon Group Separation column from Agilent (bare silica)
H_M	Plate height due to the resistance to mass transfer in the mobile phase
HP	Hewlett-Packard (now Agilent)
HPLC	High performance liquid chromatography
H_S	Plate height due to the resistance to mass transfer in the stationary phase
H_{SM}	Plate height due to the resistance to mass transfer in the stagnant mobile phase
i.d.	Internal diameter
i_M	Component i in the mobile phase
i_S	Component i in the stationary phase
k	Retention factor
k_i	Retention factor of component i
k_j	Retention factor of component j
k_R	Rate constant
LC	Liquid chromatography
L_C	Column length
Mono	Monoaromatic
MS	Mass spectrometry

N	Efficiency
$n_{i,M}$	Moles of i in the mobile phase
$n_{i,S}$	Moles of i in the stationary phase
NMR	Nuclear magnetic resonance
PAH	Polycyclic aromatic hydrocarbons (two or more aromatic rings)
P_c	Critical pressure
Penta	Pentaaromatic
Poly	Polyaromatic (four or more aromatic rings)
R	Universal gas constant
R^2	Correlation coefficient
RID	Refractive index detection
R_S	Resolution
RSD	Relative standard deviation
SEC	Size exclusion chromatography
SFC	Supercritical fluid chromatography
T	Temperature
t	Time
T_c	Critical temperature
t_D	Time required for analyte desorption from the stationary phase
Tetra	Tetraaromatic
t_r	Retention time
Tri	Triaromatic
t_o	Dead time

t_1	Retention time of peak 1
t_2	Retention time of peak 2
UV	Ultraviolet
V_M	Volume of the mobile phase
V_S	Volume of the stationary phase
w	Peak width at half-height
W_S	Weight of the stationary phase
w_1	Peak width at half-height of peak 1
w_2	Peak width at half-height of peak 2
$\alpha_{i,j}$	Separation factor between i and j (formerly selectivity factor)
β	Phase ratio
ΔH	Enthalpy for the transfer of the analyte from the mobile phase to the stationary phase
ΔP	Pressure drop across a column
ΔS	Entropy for the transfer of the analyte from the mobile phase to the stationary phase
ε	Extinction coefficient
γ_o	Obstruction factor
γ_t	Tortuosity factor
κ_i	Distribution coefficient of i
η	Viscosity
σ	Standard deviation
$\sigma^2_{V,cell}$	Variance due to detector cell volume
$\sigma^2_{V,inj}$	Variance due to injection volume

$\sigma^2_{V,R}$	Variance due to detector response time
$\sigma^2_{V,T}$	Variance due to connective tubing
$\sigma^2_{X,i}$	Variance of i in distance units
ω_A	Packing factor (A-term)
ω_C	Packing factor (C-term)
υ	Linear velocity
υ_{ave}	Average linear velocity

CHAPTER ONE. Introduction

1.1 Motivation and Thesis Overview

Fossil fuels such as jet and diesel fuel are the most important source of energy for our society today, providing the bulk of our global energy requirements for transportation, construction, heating, and agriculture. The group-type composition of these fuels (saturates, mono-, di-, tri-, and polycyclic aromatic compounds) influence what properties these fuels will possess. Performance properties (e.g. cetane number, pour point, smoke point, heat content)[1-4] and emission properties (e.g. particulate matter, polycyclic aromatic hydrocarbon (PAH), nitrogen oxides, carbon monoxide)[5-15] have been linked to the total aromatic and PAH content (dicyclic aromatic compounds and higher) in diesel fuels. Specifically, PAH content in diesel fuels increases particulate matter,[9,10,14] PAH,[12,13,15] and nitrogen oxide[9,10,14] emissions. Given the widespread use of diesel fuels, government limits on the PAH content of diesel fuels are becoming increasingly stringent.

Chromatography is a commonly used analytical method for the determination of hydrocarbon group-types.[16,17] Chromatography involves the separation of a sample into its different components. Here, it is desirable to separate the sample into different groups according to the number of aromatic rings. Once the compounds are separated, each group is then quantified by a detector to determine the relative amount (percent mass) of each hydrocarbon group-type in the sample.

Often the boiling range of a fossil fuel sample dictates which form of chromatography is most appropriate for the analysis. Light boiling materials such as

gasoline (<200°C) are often analyzed by gas chromatography (GC). Materials boiling in the jet and diesel fuel range (175-350°C) are commonly analyzed by supercritical fluid chromatography (SFC) or high performance liquid chromatography (HPLC), while materials boiling higher than 350°C are typically analyzed by HPLC. A problem with these methods is that insufficient resolution between the group-types is often achieved. This results in overlap of the different group-types, making their determination difficult. As a result, the accuracy of the results can be negatively affected.[17,18]

Another problem with these methods is the long analysis times required which limits the sample throughput. When performing real-time industrial process monitoring, the analysis time needs to be smaller than the time constant of the process being monitored.[19] Time constants are often on the order of minutes.[19]

This thesis explores various approaches for improving the group-type resolution provided by SFC and HPLC. It also examines different ways of decreasing SFC and HPLC analysis times. In Chapter 2, unconventional zirconia and titania based columns are compared with conventional silica based columns for the group-type separation of diesel fuels by SFC. In Chapter 3, short (5 to 15 cm) packed columns and monolithic columns are studied as two approaches for decreasing the SFC analysis time. In Chapter 4, the use of high column temperatures (up to 200°C) is studied with a thermally stable bare zirconia column for improving HPLC group-type separations and decreasing analysis time. In Chapter 5, titania, zirconia, and carbon based columns are compared with conventional silica-based columns for

separating heavy gas oils (>350°C) with higher group-type resolution and shorter analysis time using high temperature HPLC.

1.2 Chromatography

1.2.1 Separation[20-22]

Chromatography is a family of analytical techniques that separates samples into their various components. A sample is carried by a fluidic mobile phase through a column containing an immiscible stationary phase. The different sample components (analytes) equilibrate between the mobile phase and stationary phase to different extents. While sorbed onto the stationary phase, the analytes are immobile. Analytes in the mobile phase travel through the column at the same velocity as the mobile phase. Analytes that do not sorb onto the stationary phase are eluted from the column first and are said to be unretained. Analytes that undergo sorption onto the stationary phase are eluted from the column at a later time and are said to be retained by the column. The amount of sorption is often different for different analytes. Thus, different sample components can be separated based on the time it takes for them to elute from the column (retention time).

The stationary phases studied in this thesis were commercially prepared columns packed with solid porous particles (3 to 5 μm diameter particles with pore sizes ranging from 60 to 300 Å). The particles are held in place with porous frits. The mobile phases studied in this thesis were hexane and dichloromethane for HPLC, and supercritical carbon dioxide for SFC.

1.2.2 Chromatography Theory[20-22]

The mechanism for a chromatographic separation is based on the equilibration of an analyte, *i*, between a fluid mobile phase (M) and an immiscible stationary phase (S). The thermodynamic equilibrium that is established can be expressed by the following:

$$i_M \rightleftarrows i_S \qquad \text{(Equation 1-1)}$$

The further this equilibrium is shifted to the right, the more strongly an analyte will be retained by the column. The distribution coefficient, κ_i, for this process is described as follows:

$$\kappa_i = \frac{C_{i,S}}{C_{i,M}} \qquad \text{(Equation 1-2)}$$

where $C_{i,S}$ and $C_{i,M}$ are the concentration of the analyte in the stationary phase and mobile phase respectively. A more convenient way of quantifying retention is to use the retention factor, k_i:

$$k_i = \frac{n_{i,S}}{n_{i,M}} = \frac{\kappa_i}{\beta} \qquad \text{(Equation 1-3)}$$

where $n_{i,S}$ and $n_{i,M}$ are the moles of analyte in the stationary phase and mobile phase respectively, and β is the phase ratio. The phase ratio is the ratio of the mobile phase to the stationary phase:

$$\beta = \frac{V_M}{V_S} \qquad \text{(Equation 1-4)}$$

where V_M is the volume of the mobile phase (dead volume) and V_S is the volume of the stationary phase. The weight of the stationary phase (W_S) is more convenient to

measure and can be used instead of *Vs* providing the units are not omitted. The benefit of using the retention factor for quantifying retention is that it can be conveniently calculated by the following equation:

$$k_i = \frac{t_r - t_o}{t_o} \qquad \text{(Equation 1-5)}$$

where t_r is the retention time of analyte and t_o is the time it takes an unretained compound to elute from the column (dead time).

It is important to not only quantify to what extent an analyte is retained by a column but also how different the retention of two different analytes are. The term used to quantify the difference in retention is called the separation factor (formerly selectivity factor), $\alpha_{i,j}$,:

$$\alpha_{i,j} = \frac{k_j}{k_i} \qquad \text{(Equation 1-6)}$$

where k_j is the retention factor of the later eluting analyte, j, and k_i is the retention factor for the earlier eluting analyte, i.

It is also important to measure how narrow the analyte bands are as they elute from the column. Narrow analyte bands that lead to sharp Gaussian shaped peaks are easier to separate and quantify than broader bands. A measure of this band broadening is called plate height, H, and is given by the following equation:

$$H = \frac{\sigma^2_{X,i}}{L_C} \qquad \text{(Equation 1-7)}$$

where $\sigma^2_{X,i}$ is the variance of i in distance units squared and L_C is the length of the column. Narrower analyte bands will have smaller plate heights. Another term for measuring band broadening is called the efficiency, N:

$$N = \frac{L_C}{H} = \frac{{L_C}^2}{\sigma^2_{X,i}} \qquad \text{(Equation 1-8)}$$

The benefit of using plate height rather than efficiency to measure band broadening is that plate heights are corrected for column length. This allows the plate heights of columns with differing length to be compared directly.

Overall, the retention factor, the separation factor, and the efficiency determine how well two analytes will be separated with chromatography. The amount of separation is quantified by the resolution, R_S:

$$R_S = \frac{\sqrt{N}}{4} \cdot \frac{(\alpha_{j,i} - 1)}{\alpha_{j,i}} \cdot \frac{k_j}{(k_j + 1)} \qquad \text{(Equation 1-9)}$$

This equation demonstrates how resolution can be improved by increasing efficiency (decreasing plate height), increasing the separation factor, or by increasing the retention factor. Generally, when the resolution is greater than a value of 1.5, two equally sized Gaussian peaks are considered baseline resolved. This means that the signal intensity between the two peaks reaches the baseline value.

Due to the square root dependence, a 2-fold improvement in resolution will require a 4-fold increase in the efficiency. Such increases in efficiency can be difficult to achieve without excessively long columns and analysis times. Increases in the retention factor result in diminishing gains in resolution as the retention term in

Equation 1-9 approaches a value of one at very high values of k_j. Large retention factors also result in long analysis times. Generally, the best way to improve resolution is to improve the separation factor. This can be achieved by changing the stationary phase, the mobile phase, or the column temperature.

Resolution is often calculated directly from two Gaussian chromatographic peaks of interest using the following equation:

$$R_S = \frac{2(t_j - t_i)}{1.699(w_j + w_i)} \qquad \text{(Equation 1-10)}$$

where t_j and t_i are the retention times of later and earlier eluting analytes j and i respectively and w_j and w_i are the peak widths at half height for the same analytes.

1.2.3 Band Broadening[20-22]

The band broadening that occurs within the column can be described by the three terms of the van Deemter equation:

$$H = A + \frac{B}{\upsilon} + C\upsilon \qquad \text{(Equation 1-11)}$$

where A, B, and C describe different band broadening processes and υ is the linear velocity of the mobile phase (proportional to flow rate).

The A-term in the van Deemter equation is often referred to as the multipath band broadening term. It describes the band broadening that occurs when the analyte molecules take different paths through the column. Some analyte molecules may take a very straight path through the column, eluting sooner than the average analyte molecule. Likewise, some analyte molecules may take a very tortuous path through

the column, eluting later than most analyte molecules. Anything that contributes to a non-uniform flow profile through the column will contribute to multipath band broadening. Poorly packed columns or columns with a non-uniform build-up of particulate matter at the inlet of the column often display non-uniform flow profiles. The A-term is independent of flow rate and is present in all packed columns. The plate height contribution from the A-term, H_A, can be calculated as follows:

$$H_A = 2\omega_A d_p \qquad \text{(Equation 1-12)}$$

where ω_A is the packing factor and d_p is the particle diameter. The packing factor is larger for poorly packed columns. The particle diameter dependence shows how column efficiency can be improved by using smaller particles.

The B-term is referred to as the longitudinal diffusion term. It describes the diffusion of analyte molecules away from the center of the analyte band axially along the column. The longer the analyte band spends in the column, the more diffusion will occur. As a result, longitudinal diffusion scales with the inverse of flow rate. The plate height contribution from longitudinal diffusion, H_B, is calculated as follows:

$$H_B = \frac{2\gamma_o D_M}{\upsilon} \qquad \text{(Equation 1-13)}$$

where γ_o is the obstruction factor and D_M is the diffusion coefficient of the analyte in the mobile phase. Given the low diffusion coefficients in liquids, H_B can generally be ignored in conventional HPLC. However, H_B can be a significant source of band broadening in SFC and high temperature HPLC when operating at relatively low flow rates.

The C-term is referred to as the resistance to mass transfer term. The mass transfer of the analyte molecules within the column is not instantaneous. As a result, three band broadening processes occur due to limited mass transfer. The first is the time required for the analyte molecules to transfer from the stationary phase to the stagnant mobile phase within the pores of the particle. The plate height contribution from the resistance to mass transfer in the stationary phase, H_S, can be expressed as:

$$H_S = \frac{2k}{(1+k)^2} t_D \upsilon \qquad \text{(Equation 1-14)}$$

where k is the retention factor and t_D is the time that the analyte spends bound to the stationary phase before desorbing back into the mobile phase. The analytes in the stationary phase lag behind those in the mobile phase as the band moves down the column. Figure 1-1 depicts this process. At higher flow rates, the band moves further down the column before the analytes bound to the stationary phase are transferred to the mobile phase. This results in higher band broadening at higher flow rates.

The second resistance to mass transfer term is caused by the slow diffusion of analyte molecules within the stagnant mobile phase of the pores. The plate height contribution from the resistance to mass transfer in the stagnant mobile phase, H_{SM}, is given by the following:

$$H_{SM} = \frac{f(p,k) d_p^2}{\gamma_t D_M} \upsilon \qquad \text{(Equation 1-15)}$$

where $f(p,k)$ is a function of pressure and retention and γ_t is the tortuosity factor. The resistance to mass transfer in the stagnant mobile phase decreases with decreasing flow rate, decreasing particle diameter, and increasing analyte diffusion coefficient.

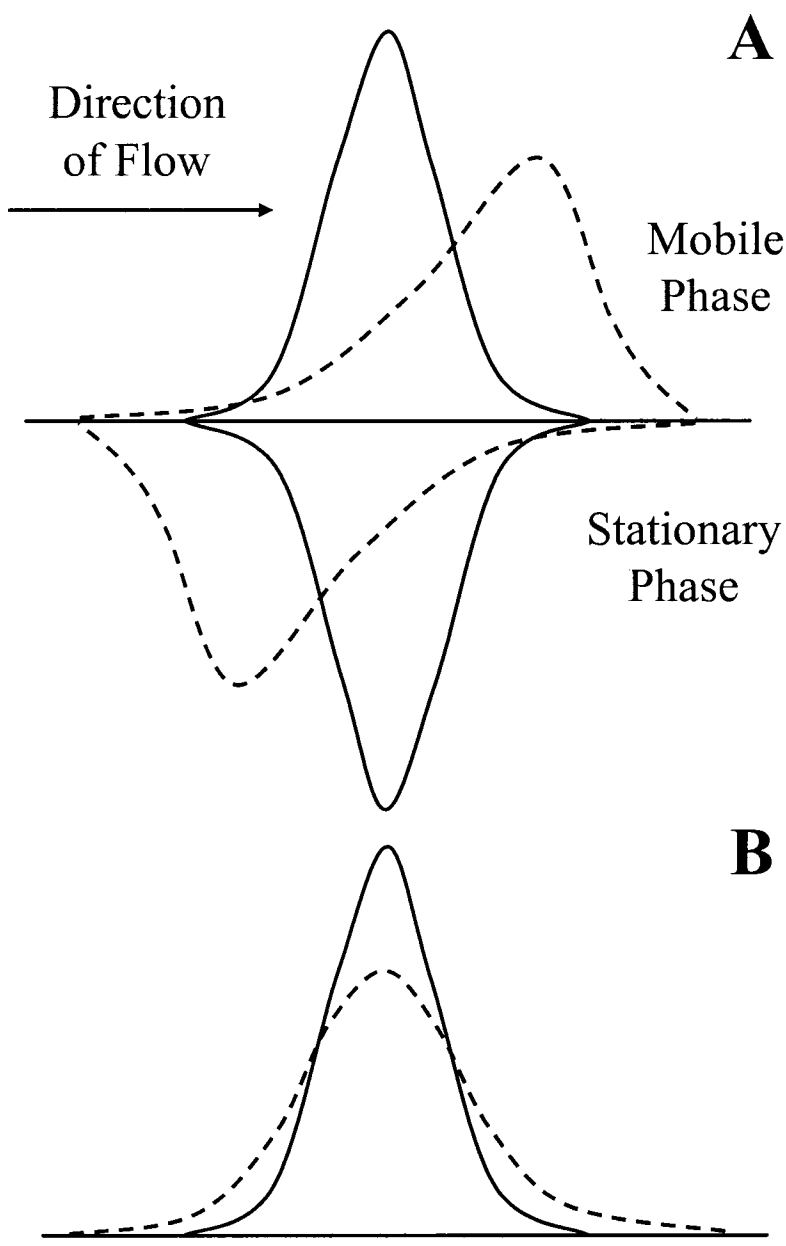

Figure 1-1. Diagram showing (A) the effect of the resistance to mass transfer in the stationary phase and (B) the resulting band broadening on a Gaussian peak. The area under the curves is proportional to the number of moles of analyte. Solid lines represent an ideal case where infinitely fast mass transfer occurs. Dotted lines represent the non-ideal case where resistance to mass transfer occurs. Adapted from reference.[20]

The third resistance to mass transfer term results from slow transfer of analyte molecules within the flowing mobile phase between the particles. The plate height contribution from the resistance to mass transfer in the mobile phase, H_M, is expressed as follows:

$$H_M = \frac{\omega_C d_p^2}{D_M} \upsilon \qquad \text{(Equation 1-16)}$$

where ω_C is the packing factor, which is smaller for uniformly packed beds. Similarly to H_{SM}, H_M decreases with decreasing flow rate, decreasing particle diameter, and increasing analyte diffusion. Because all three resistance to mass transfer terms have the same dependence on flow rate, they can be treated as a single resistance to mass term in the van Deemter equation.

When the plate height is plotted versus linear flow velocity (or flow rate), a van Deemter plot is obtained. Figure 1-2 shows the contributions of each band broadening term in the van Deemter equation. At low flow rates, the plate height is dominated by longitudinal diffusion (B-term). At high flow rates, the plate height is dominated by the resistance to mass transfer (C-term). At an intermediate flow rate, a minimum in the van Deemter plot is obtained. This is considered the optimum flow rate and is where the least band broadening (highest efficiency) is obtained. The minimum plate height is typically 2 to 3-fold larger than the particle diameter for a well packed column. When elevated temperatures are used to enhance diffusion, the optimum linear velocity increases proportionally with the diffusion coefficient, as shown in Figure 1-2.

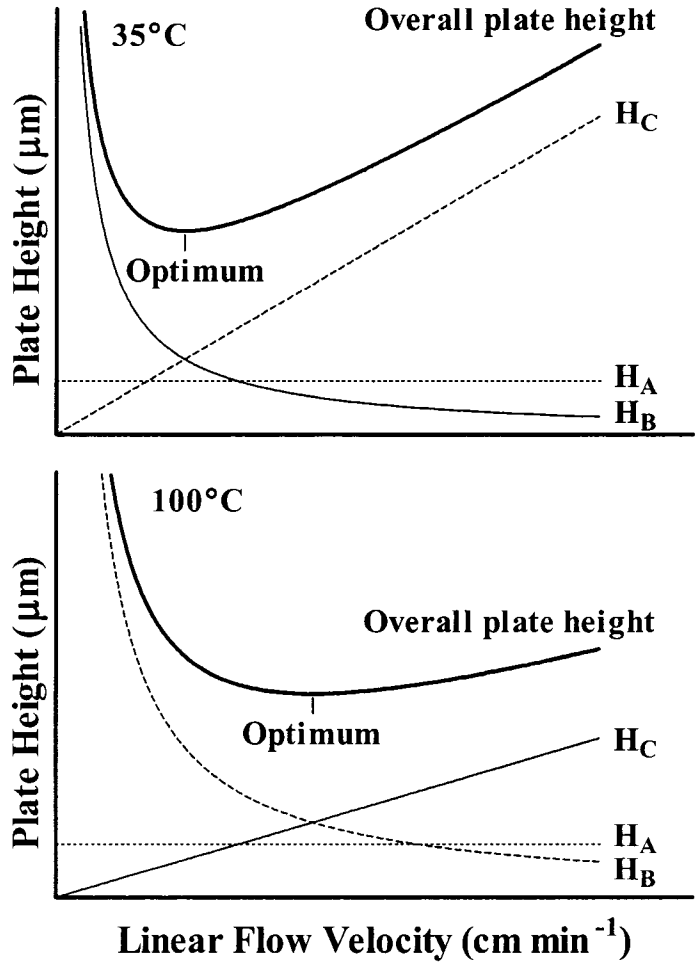

Figure 1-2. Plot of plate height versus linear flow velocity (proportional to flow rate) depicting the contributions from the three band broadening terms of the van Deemter equation. At 100°C, the diffusion coefficient is increased 2-fold compared to 35°C, resulting in a 2-fold faster optimum linear velocity.

Additional sources of band broadening can occur that originate from outside of the column (extra-column band broadening). Injection loops, connective tubing, detectors, and detector response time can all contribute to band broadening. However, problems with extra-column band broadening can be avoided with careful instrument design. Minimizing extra-column volumes associated with the injector, connective tubing, and detector, and the use of fast detector response times (0.1 seconds) is important.

1.2.4 Improving Efficiency and Analysis Time[20-22]

By using smaller particles, the minimum in the van Deemter curve is lowered. The use of smaller particles also reduces the resistance to the mass transfer term (Equations 1-15 and 1-16), thus lowering the slope of the van Deemter curve at high flow rates. This also results in an increase in the optimum flow rate. As a result, faster flow rates can be used to achieve lower analysis times without sacrificing efficiency. The limit to how small the particles that can be used is dictated by the maximum operating pressure of the pump. The relationship between the pressure drop across the column, ΔP, the average linear velocity of the mobile phase (proportional to flow rate), υ_{ave}, the viscosity, η, and the particle diameter, d_p, is given by the following equation:

$$\Delta P = \upsilon_{ave} \frac{\eta L_C Const}{d_p^2} \qquad \text{(Equation 1-17)}$$

The pressure supplied by the pump must increase 4-fold for every 2-fold reduction in particle diameter. Standard HPLC pumps do not operate reliably above a pressure of 4000 psi (276 bar). As a result, most HPLC columns of standard length (10 to 25 cm)

are packed with 3 to 5 μm particles. This represents the limit of conventional HPLC instruments. As discussed in Section 1.3.3, faster analysis times can be obtained through the use of supercritical fluid mobile phases with SFC and the use of elevated column temperatures with HPLC.

1.3 Normal Phase Separations

1.3.1 Normal Phase High Performance Liquid Chromatography[20-22]

Normal phase separations involve the use of polar stationary phases (e.g., bare silica) with relatively non-polar mobile phases (e.g., hexane). Analytes of low polarity (e.g., alkanes) form weak interactions with the polar stationary phase and are weakly retained as a result. Analytes of higher polarity or higher polarizability (e.g., aromatic hydrocarbons) form stronger interactions with the polar stationary phase and are more strongly retained as a result. Mobile phases of higher polarity (e.g., dichloromethane) are used to elute highly retained analytes.

A schematic of the normal phase HPLC instrument used in Chapters 4 and 5 is shown in Figure 1-3. Two high pressure pumps are used to deliver hexane or dichloromethane to the column at flow rates up to 5.0 ml min^{-1}. An autosampler is used to make automated injections of a sample into the mobile phase stream. An oven uniformly heats the column to the desired temperature (up to 200°C). The column separates the sample into individual group-types. The group-types are then measured by the two detectors as they elute from the column. A backpressure regulator is used to prevent the effluent mobile phase from boiling during experiments when the column is heated above the boiling point of the mobile phase.

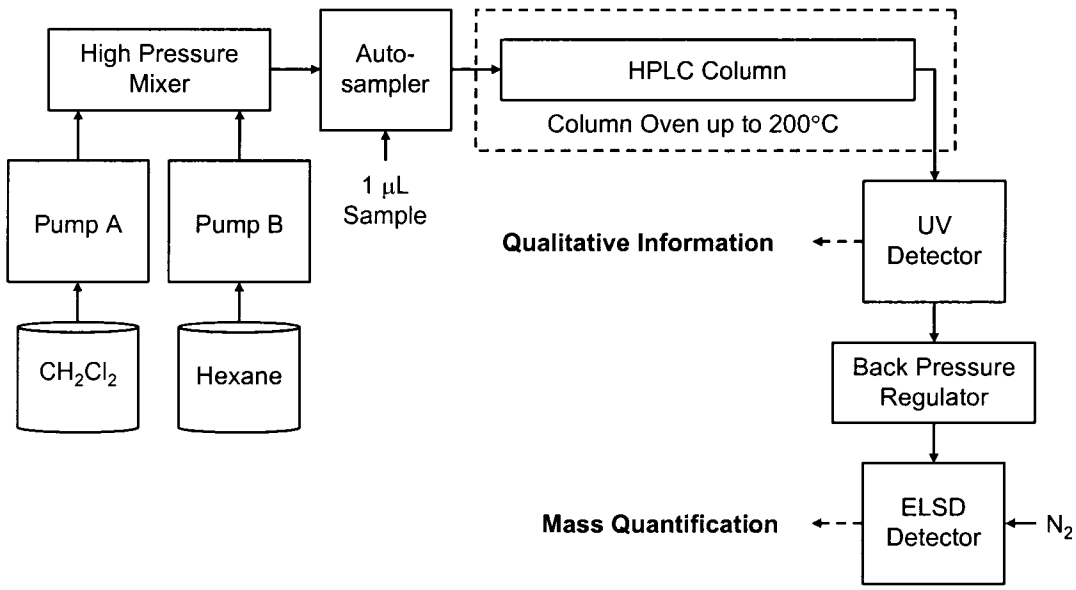

Figure 1-3. Schematic of the Varian ProStar HPLC instrument used in Chapters 4 and 5. Varian ProStar 210 pumps, Varian ProStar 410 autosampler, Metalox 200°C high temperature column heater, Knauer Smartline 2500 UV detector, and Alltech 500 ELSD detector.

1.3.2 Normal Phase Supercritical Fluid Chromatography[20,22,23]

In normal phase SFC, the stationary phase is again a polar sorbant (e.g., silica) and the mobile phase is pure supercritical carbon dioxide. The critical pressure and temperature for carbon dioxide are 74 bar and 31°C respectively. The elution strength of the mobile phase can be increased by increasing the supercritical carbon dioxide density (by lowering temperature and/or increasing pressure). However, the maximum mobile phase strength of supercritical carbon dioxide is similar to hexane using commercial SFC instruments. As a result, high boiling materials (>350°C) and high polarity compounds may yield excessively long elution times. Figure 1-4 shows a schematic for the SFC instrument used in Chapters 2 and 3. SFC instrumentation is very similar to HPLC instrumentation except that the supercritical mobile phase is both pressurized and heated to conditions beyond the critical point of the mobile phase.

A backpressure regulator is used to prevent depressurization of the carbon dioxide within the column. Carbon dioxide is pressured by the pump until the desired flow rate is achieved through the column. The backpressure regulator is set at the desired minimum pressure (typically 150 bar) to maintain supercritical conditions throughout the system. An autosampler is used to make sample injections. The oven maintains the column temperature (typically 35°C). The detectors measure the sample group-types as they elute from the column. Figure 1-5 shows a typical group-type separation of a diesel fuel separated on a conventional bare silica column. Baseline separation between the various group-types is rarely obtained.

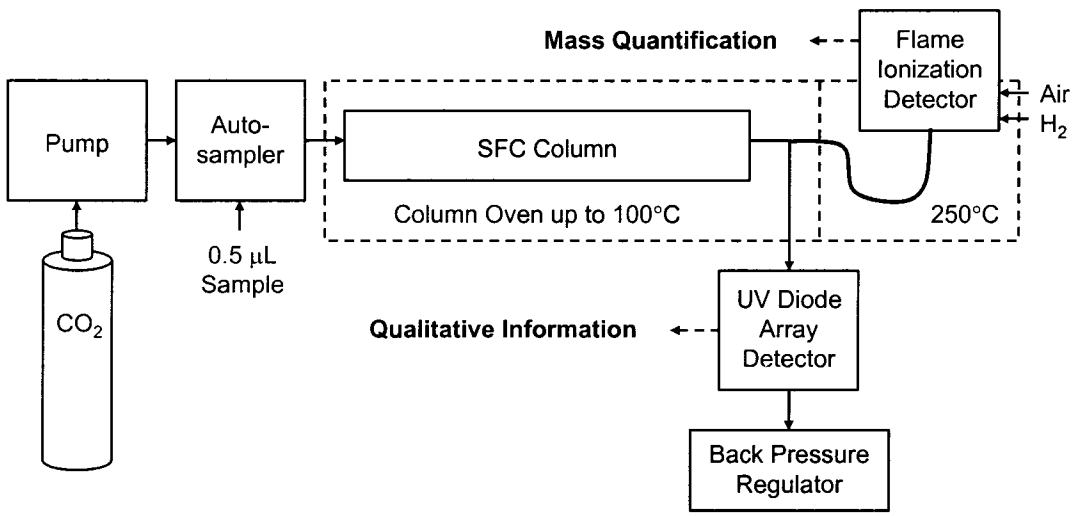

Figure 1-4. Schematic of the Hewlett-Packard SFC instrument used in Chapters 2 and 3. HP G1205A SFC pump module, HP 7673B automatic sampler, HP 5890 series II column oven, HP SFC FID, and HP Series 1050 UV diode array detector.

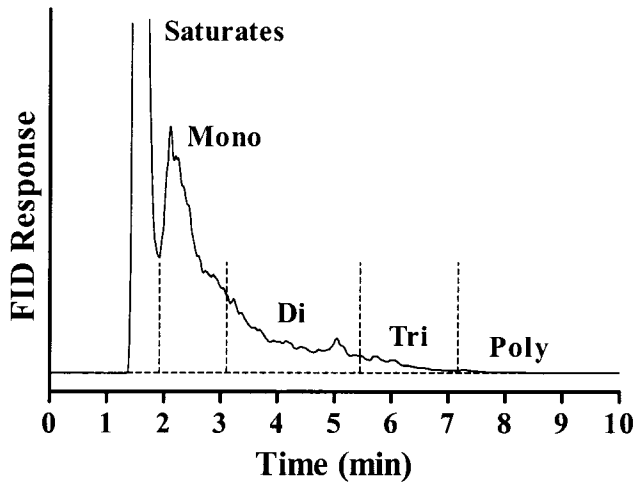

Figure 1-5. Chromatogram of a diesel blending feedstock separated by SFC at 35°C, 150 bar, and 2.0 ml min^{-1} on a 150 x 4.6 mm bare silica Hydrocarbon Group Separation column. Cut-points made according to the retention times of model compounds (Section 2.2.4).

As a result, the chromatogram is divided into separate group-types based on the retention time of model compounds.

1.3.3 Mobile Phase Comparison[20,22,23]

Supercritical carbon dioxide and hexane provide similar mobile phase strengths in normal phase separations based on solvent polarity studies using solvatochromic dyes.[23] However, Table 1-1 shows how the viscosity for supercritical carbon dioxide is 4.5-fold lower compared to hexane at 35°C and 200 bar (2900 psi). This permits higher flow rates to be used with SFC without exceeding the pressure limit of the pump. Further, analyte diffusion is expected to be 2.8-fold higher in supercritical carbon dioxide compared to hexane under the same conditions. This represents significant decreases in the H_{SM} and H_M resistance to mass transfer terms (Section 1.2.3). As a result, we would expect a flatter van Deemter curve at high flow rates in SFC compared to conventional HPLC. Higher diffusion rates and lower viscosity are the reasons why SFC inherently provides 3-fold faster analysis times over conventional HPLC.[24]

The arrival of thermally stable HPLC stationary phases[25,26] along with sophisticated high temperature column ovens has allowed temperatures up to 200°C to be used with HPLC. Table 1-1 shows how hexane's viscosity decreases 2.6-fold at 200°C compared to 35°C. A 4.2-fold increase in diffusion is expected at 200°C vs. 35°C. This shows how high temperature HPLC provides similar improvements in viscosity and diffusion compared to SFC. As a result, we would expect both techniques to provide similarly short analysis times when compared to conventional HPLC.

Table 1-1. Comparison of hexane and supercritical carbon dioxide mobile phases.

Mobile Phase	Temperature (°C)	Viscosity[a] (10^{-5} Pa s)	Diffusion Improvement[b]
Hexane	35	30.0	1.0
Hexane	100	20.9	2.0
Hexane	200	11.4	4.2
Carbon dioxide	35	6.59[c]	2.8

[a]Hexane viscosity based on 200 bar values from reference[27]

[b]Relative increase in diffusion coefficient compared to hexane at 35°C and 200 bar, based on Wilke-Chang equation (temperature, viscosity, and mobile phase molecular weight taken into account)[28]

[c]Carbon dioxide viscosity calculated using EOS-SCx version 2 free software.[29] Software viscosity values were found to be within 2% of literature values.[30]

1.3.4 Phase Behavior of Carbon Dioxide[23,31,32]

Figure 1-6 shows the pressure-temperature projection of the phase diagram for pure carbon dioxide. A proper understanding of carbon dioxide phase behavior allows one to avoid conditions that would result in phase separation of the mobile phase. Multiple phases flowing through the column would lead to a non-uniform flow profile and significant band broadening. This can occur when a polar modifier (e.g., methanol) is added to the mobile phase to increase eluent strength.

Figure 1-7 shows the pressure-temperature projection for a two component mobile phase (e.g., carbon dioxide and methanol). The region where multiple phases may occur is shown. The relative amount of the two components will determine whether phase separation will occur at a given temperature and pressure within this region. By using the loss of chromatographic efficiency of the sample solvent as an indication of the onset of multiphase behavior, Chester mapped out the critical loci separating the supercritical single phase region from the two-phase region for carbon dioxide and several common organic solvents.[31] Other researchers have investigated the critical loci for mixtures of carbon dioxide and different organic solvents by visual inspection of a fixed volume cell.[33] These results show that phase separation can be avoided by working at temperatures below 50°C and pressures higher than 100 bar for all solvents studied. In Chapter 2, temperatures higher than 50°C and pressures lower than 100 bar are studied. However, the combination of temperature and pressure studied in Chapter 2 result in conditions outside of the possible two-phase region. In Chapter 3, temperature is kept at 35°C while pressure is kept at or above 100 bar, outside of the possible two-phase region.

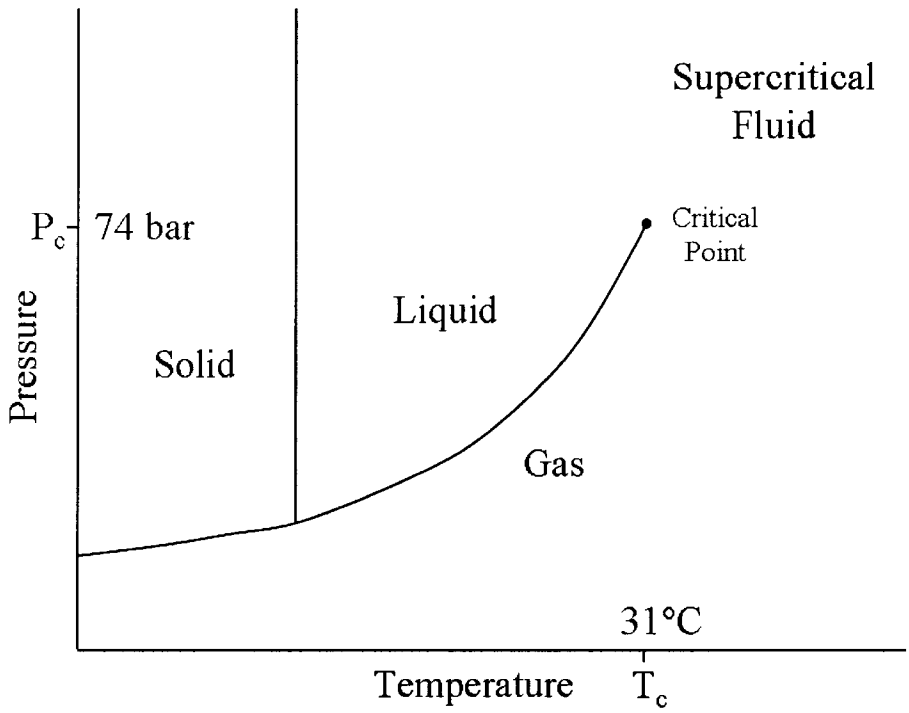

Figure 1-6. Pressure-temperature phase behavior projection for carbon dioxide. Critical pressure, P_c and critical temperature, T_c, are indicated.

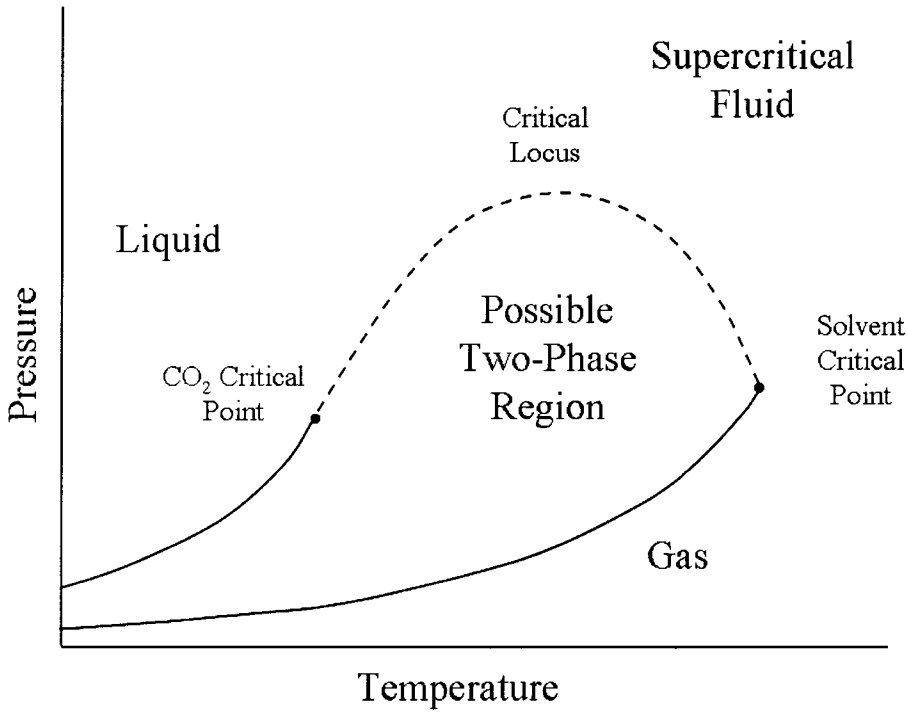

Figure 1-7. Pressure-temperature phase behavior projection for a two component system of carbon dioxide and an organic solvent such as methanol or hexane. For methanol, P_c = 80 bar and T_c = 240°C. For hexane, P_c = 30 bar and T_c = 234°C. For carbon disulfide, P_c = 79 bar and T_c = 279°C. Adapted from reference.[32]

Another source of band broadening can occur when the temperature and pressure are relatively close to the critical point, even when using a pure carbon dioxide mobile phase. At these conditions, a dense layer of carbon dioxide forms on the surface of the stationary phase, resulting in an increased resistance to mass transfer and poor efficiency.[23] Maintaining a pressure higher than 100 bar is sufficient to avoid this issue. When pressures less than 100 bar are studied in Chapter 2, no significant loss of efficiency is observed. This suggests that even if phase separation or dense carbon dioxide layer formation are occurring, they are not detrimental to the separation.

1.3.5 Stationary Phases[20,21]

Amorphous, porous bare silica is one of the oldest and most widely used stationary phases in normal phase chromatography. Its surface is covered with hydroxyl groups known as silanols (Si-OH). These silanols allow the formation of hydrogen bonds, dipole-dipole, and dipole-induced dipole interactions with analytes, thus making silica's surface highly polar. However, silanols are heterogeneous in nature, with some silanols displaying very high activity. Very strong interactions with basic analytes (e.g., amines) result, yielding poor efficiencies and peak tailing. Also, the water content of the mobile phase can strongly affect the activity of adsorption phases such as silica. This results in poor retention time precision if the water content is not carefully controlled.

To avoid these problems, bonded phases were developed using silane chemistry. The bonded phase that is studied in this thesis is aminopropyl bonded silica. The aminopropyl groups provide a homogenous surface that is less sensitive to

water concentration. As a result, retention time precision is generally better with bonded phases compared to bare silica. Further, it is easier to elute basic analytes with good efficiencies and good peak shapes with bonded phases. One problem with conventional silica based columns is that they dissolve in mobile phases containing water when the column temperature is increased beyond 65°C. As a result, conventional silica-based columns are rarely used with high temperature HPLC.

To avoid this problem, columns based on crystalline porous zirconia (ZrO_2) were developed.[26,34] Bare zirconia exhibits excellent chemical and thermally stability up to 200°C. This allows high column temperatures to be used to reduce analysis time. Crystalline porous bare titania (TiO_2) columns have also recently become commercially available.[26,35] Bare titania exhibits excellent chemical stability. However, its thermally stability has not yet been thoroughly established in the literature. Similar to bare silica, bare zirconia and bare titania also possess hydroxyl groups on their surface (zirconols and titanols), making them highly polar stationary phases.

A major difference between metal oxides (zirconia and titania) and bare silica is that metal oxides possess Lewis acid sites.[26,34] These sites are the result of coordinatively unsaturated metal centers that can form strong interactions with Lewis bases. These provide an additional interaction with analytes that silica cannot provide, resulting in differences in separation selectivity between metal oxide and silica columns. Unfortunately, Lewis acid-Lewis base interactions tend to be very strong and can result in poor efficiency and peak tailing for highly retained analytes.

In this thesis, zirconia and titania columns are studied to evaluate their ability to perform hydrocarbon group-type separations in comparison to silica-based columns.

1.3.6 Hydrocarbon Group-Type Separations[16,17]

As stated in Section 1.1, the distribution of saturates, mono-, di-, tri-, and polyaromatic aromatic compounds influence the fuel performance[1-4] and emission properties.[5-15] The objective of the group-type separation of fuels by chromatography is to baseline separate each of the group-types from all other group-types, rather than to separate each individual chemical compound from all other compounds. This allows accurate quantification of each group-type. The group-type resolution of a particular chromatographic approach will be assessed using model compounds representing each of the group-types, as detailed in Section 2.2.3.

Since the 1970s, bare silica columns have been widely used for hydrocarbon group-type separations. Bare silica is currently the preferred column for diesel group-type separations with SFC.[36] While bare silica columns provide excellent saturate vs. monoaromatic separations, they provide limited separation between the aromatic group-types as shown with SFC in Chapter 2 and HPLC in Chapter 5. Others have shown that higher column temperatures can improve aromatic group-type resolutions on silica with SFC, but at the expense of the saturate vs. monoaromatic resolution.[37]

Bonded phases, such as aminopropyl bonded silica, have become the most commonly used columns for group-type separations with HPLC. In addition to the benefits described in Section 1.3.5, bonded phases generally provide higher aromatic group-type resolutions compared to bare silica columns. This is especially true for charge-transfer columns.[38-40] These columns possess electron deficient bonded

phases that form strong interactions with π-electron rich analytes. Studies comparing various charge-transfer columns have shown that dinitroanilinopropyl bonded silica (DNAP) columns provide the highest aromatic group-type resolutions.[38,39] Despite this, DNAP columns yield lower retention for non-planar aromatics compared to planar aromatics.[39,41] This complicates the separation of aromatic group-types according to aromatic ring number rather than physical shape. Further, charge-transfer columns generally provide lower saturates vs. monoaromatics resolution compared to other columns.[42] Due to these limitations, the use of zirconia and titania based columns for hydrocarbon group-type separations is studied here for the first time. The highly polar hydroxyl groups on the surface of these columns are expected to provide good saturate vs. monoaromatic separations, similar to bare silica columns. Meanwhile, the presence of Lewis acid sites is expected to provide high aromatic group-type resolutions, similar to charge-transfer columns.

1.3.7 Detection[22,43,44]

In this thesis, three modes of detection are used. The first, flame ionization detection, is a universal detector that responds to all analytes that contain reduced carbon.[17,18,45,46] The column effluent is guided into a hydrogen-air flame. Reduced carbon burns in the flame, producing CHO^+ ions as a side reaction to combustion (1 in 10^5 reactions). The conductivity of the flame is measured with electrodes to determine the concentration of these ions in the flame. Flame ionization detection provides a very uniform signal for hydrocarbons, which makes it an excellent detector for the group-type analysis of fossil fuels. The one drawback of using this detector is that it will also respond to any reduced carbon in the mobile phase. As a result, it

cannot be used directly with most normal phase HPLC mobile phases due to the high background noise that would result. However, it can be used with the carbon dioxide mobile phase used with SFC.

Evaporative light scattering detection allows for the detection of non-volatile compounds in SFC and HPLC.[47] The column effluent is nebulized with a nebulizer gas (e.g., nitrogen), producing small droplets of mobile phase. These droplets are introduced into a heated drift tube where they undergo evaporation. Analytes that do not evaporate produce small particles in the drift tube. At the end of the drift tube is a light scattering cell. Here, laser light is scattered by the dried analyte particles towards a light sensitive detector (typically a photomultiplier tube or photodiode). Any non-volatile analyte will yield a signal. ELSD detectors are not nearly as sensitive or universal as FID detectors. However, ELSD can be used with volatile organic mobile phases such as hexane. Because the ELSD detector does not respond to volatile analytes, it can only be used reliably for the detection of high boiling materials such as heavy gas oils (boiling range >350°C).

UV absorbance detection is the most widely used form of detection in HPLC. Any analytes that possess a chromophore provide a signal that is proportional to concentration. A broad spectrum of UV light shines through the column effluent as it travels through a flow cell. Analyte molecules absorb some of the UV light. The amount of light absorbed is described by Beer's Law:

$$Abs. = \varepsilon b[\mathrm{C}] \qquad \text{(Equation 1-18)}$$

where *Abs.* is the absorbance, ε is the extinction coefficient (varies with different analytes and wavelengths), b is the pathlength of the flow cell, and $[C]$ is the

concentration of the analyte. Many detectors only allow a single wavelength to be monitored at one time. However, diode array detectors permit a large section of the spectrum to be monitored simultaneously. The main drawback of UV detection for the group-type analysis of hydrocarbons is that the saturates (e.g., alkanes) do not appreciably absorb UV light. Also, because the extinction coefficient varies for different analytes, reliable quantification can be difficult for those group-types that do provide a response. As a result, UV detection was used in this thesis for solely qualitative characterization of samples.

Flame ionization detection (FID) is used with SFC in Chapters 2 and 3 to provide reliable mass quantification of hydrocarbon group-types in diesel samples. The FID chromatogram is used to determine the retention time and peak width at half-height of model compounds in Chapters 2 and 3. UV absorbance detection is used to qualitatively characterize the aromatic group-types with both SFC and HPLC in Chapters 2-5. The UV absorbance chromatogram is also used with HPLC in Chapters 4 and 5 to measure the retention time and peak width at half-height for aromatic model compounds. In Chapter 5, evaporative light scattering detection (ELSD) is used to monitor the saturated model compounds and to quantify the group-types in heavy gas oil samples with HPLC.

1.4 References

(1) Cookson, D. J.; Lloyd, C. P.; Smith, B. E., *Energy & Fuels* **1988**, *2*, 854-860.

(2) Cookson, D. J.; Iliopoulos, P.; Smith, B. E., *Fuel* **1995**, *74*, 70-78.

(3) Sato, S.; Sugimoto, Y.; Sakanishi, K.; Saito, I.; Yui, S., *Fuel* **2004**, *83*, 1915-1927.

(4) Sjögren, M.; Li, H.; Rannug, U.; Westerholm, R., *Fuel* **1995**, *74*, 983-989.

(5) de Lucas, A.; Durán, A.; Carmona, M.; Lapuerta, M., *Fuel* **2001**, *80*, 539-548.

(6) Karonis, A.; Lois, E.; Zannikos, F.; Alexandridis, A.; Sarimveis, H., *Energy & Fuels* **2003**, *17*, 1259-1265.

(7) Zannis, T. C.; Hountalas, D. T., *J. Energy Inst.* **2004**, *77*, 16-25.

(8) Ohtsuka, A.; Hashimoto, K.; Akutsu, Y.; Arai, M.; Tamura, M., *J. Jpn. Petrol. Inst.* **2002**, *45*, 24-31.

(9) Li, X.; Gülder, Ö. L., *J. Can. Pet. Technol.* **1998**, *37*, 56-60.

(10) Shimazaki, N.; Tsuchiya, K.; Morinaga, M.; Shibata, M.; Shibata, Y., *SAE Technical Paper* **2002**, *2002-01-2824.*

(11) Mitchell, K., *SAE Technical Paper* **2000**, *2000-01-2890.*

(12) Tanaka, S.; Takizawa, H.; Shimizu, T.; Sanse, K., *SAE Technical Paper* **1998**, *982648.*

(13) Andrews, G. E.; Ishaq, R. B.; Farrar-Khan, J. R.; Shen, Y.; Williams, P. T., *SAE Technical Paper* **1998**, *980527.*

(14) Signer, M.; Heinze, P.; Mercogliano, R.; Stein, H. J., *SAE Technical Paper* **1996**, *961074.*

(15) Mitchell, K.; Steere, D. E.; Taylor, J. A.; Manicom, B.; Fisher, J. E.; Sienicki, E. J.; Chiu, C.; Williams, P. T., *SAE Technical Paper* **1994**, *942053.*

(16) Lundanes, E.; Greibrokk, T., *J. High Resol. Chromatogr.* **1994**, *17*, 197-202.

(17) Barman, B. N.; Cebolla, V. L.; Membrado, L., *Crit. Rev. Anal. Chem.* **2000**, *30*, 75-120.

(18) Thiébaut, D. R. P.; Robert, E. C., *Analusis* **1999**, *27*, 681-690.

(19) Honigs, D. E., *Am. Lab.* **1987**, *19*, 48-51.

(20) Cantwell, F. F., *Analytical Separations Class Notes*, University of Alberta: Edmonton, 2003.

(21) Snyder, L. R., *Principles of Adsorption Chromatography*, Marcel Dekker, Inc., New York, 1968.

(22) Skoog, D. A.; Holler, F. J.; Nieman, T. A., *Principles of Instrumental Analysis, Fifth Edition*, Harcourt Brace & Company, Orlando, 1998.

(23) Berger, T. A., *Packed Column SFC*, The Royal Society of Chemistry, Cambridge, 1995.

(24) Chester, T. L.; Pinkston, J. D., *Anal. Chem.* **2002**, *74*, 2801-2812.

(25) Greibrokk, T.; Andersen, T., *J. Chromatogr. A* **2003**, *1000*, 743-755.

(26) Nawrocki, J.; Dunlap, C.; McCormick, A.; Carr, P. W., *J. Chromatogr. A* **2004**, *1028*, 1-30.

(27) Kiran, E.; Sen, Y. L., *Int. J. Thermophys.* **1992**, *13*, 411-442.

(28) Wilke, C. R.; Chang, P., *AICHE J.* **1955**, *1*, 264-270.

(29) http://hp.vector.co.jp/authors/VA030090/.

(30) Sovova, H.; Prochazka, J., *Ind. Eng. Chem. Res.* **1993**, *32*, 3162-3169.

(31) Chester, T. L., *Microchem. J.* **1999**, *61*, 12-24.

(32) Zou, X.-Y.; Shaw, J. M., *Phase Behavior: An Overview*, University of Alberta: Edmonton, 2005.

(33) Reaves, J. T.; Griffith, A. T.; Roberts, C. B., *J. Chem. Eng. Data* **1998**, *43*, 683-686.

(34) Nawrocki, J.; Rigney, M. P.; McCormick, A.; Carr, P. W., *J. Chromatogr. A* **1993**, *657*, 229-282.

(35) Winkler, J.; Marmé, S., *J. Chromatogr. A* **2000**, *888*, 51-62.

(36) *Method D 5186-03, Annual Book of ASTM Standards*, American Society for Testing and Materials, West Conshohocken, PA, USA, 2003.

(37) Shariff, S. M.; Robson, M. M.; Myers, P.; Bartle, K. D.; Clifford, A. A., *Fuel* **1997**, *77*, 927-931.

(38) Grizzle, P. L.; Thomson, J. S., *Anal. Chem.* **1982**, *54*, 1071-1078.

(39) Welch, K. J.; Hoffman, N. E., *J. Chromatogr.* **1992**, *591*, 75-88.

(40) Ghosh, P.; Chawla, B.; Joshi, P. V.; Jaffe, S. B., *Energy & Fuels* **2006**, *20*, 609-619.

(41) Sander, L. C.; Parris, R. M.; Wise, S. A.; Garrigues, P., *Anal. Chem.* **1991**, *63*, 2589-2597.

(42) Robbins, W. K., *J. Chromatogr. Sci.* **1998**, *36*, 457-466.

(43) Lucy, C. A., *Instrumental Analysis Class Notes*, University of Alberta: Edmonton, 1999.

(44) Yeung, E. S.; Synovec, R. E., *Anal. Chem.* **1986**, *58*, 1237A-1256A.

(45) DiSanzo, F. P.; Yoder, R. E., *J. Chromatogr. Sci.* **1991**, *29*, 4-7.

(46) M'Hamdi, R.; Thiébaut, D.; Caude, M., *J. High Resol. Chromatogr.* **1997**, *20*, 545-554.

(47) Young, C. S.; Dolan, J. W., *LCGC* **2003**, *21*, 120-128.

CHAPTER TWO. Comparison of Titania, Zirconia, and Silica Stationary Phases for Separating Diesel Fuels According to Hydrocarbon Group-Type by Supercritical Fluid Chromatography*

2.1 Introduction

In North America, the American Society for Testing and Materials (ASTM) method D 5186-03 is used to determine the aromatic and polycyclic aromatic hydrocarbons (PAH, two or more aromatic rings) content of diesel and aviation turbine fuels.[1] This method uses supercritical fluid chromatography (SFC) with a carbon dioxide mobile phase to separate diesel fuels according to group-type followed by flame ionization detection (FID). Other techniques used for diesel group-type separations include high performance liquid chromatography (HPLC),[2-7] gas chromatography (GC),[2,8-10] LC-GC,[11,12] SFC-GC,[13] and SFC-MS (mass spectrometry).[14] However, HPLC detectors yield a non-uniform response for saturates and aromatics,[2,15-17] necessitating complex calibrations. In contrast, FID provides reliable mass quantification of each hydrocarbon group-type.[2,15-17] GC separations often require two dimensional (2D) separations or mass spectrometric detectors that give non-uniform responses to achieve group-type separations,[2,9] making GC less practical for routine group-type analysis.

The Hydrocarbon Group Separation (HGS) column from Agilent (250 x 4.6 mm i.d., 5 μm bare Lichrospher Si 60 silica spherical particles)[18] has been widely used with SFC to provide higher group-type resolutions compared to other bare

---

*A version of this chapter has been published. Paproski R. E., Cooley, J., Lucy C. A., *Journal of Chromatography A* **2005**, 1095, 156-163.

silicas. However, the results herein show that bare silica columns have difficulty separating the di- and triaromatic groups cleanly. Limited aromatic group-type resolutions restrict the accuracy of diesel group-type determinations with SFC.[2,15] Also, achieving high aromatic group-type resolutions while maintaining the resolution of saturates and aromatics has proven difficult.[2] For these reasons, several column packing materials offering different surface chemistries compared to bare silica are studied in this chapter. These include bare zirconia, polybutadiene coated zirconia, carbon coated zirconia, bare titania, and an aminopropyl-bonded silica. A high purity, low metals type B bare silica Kromasil column, a Lichrospher Si 60 bare silica column and an irregular version of the spherical Lichrospher Si 60 bare silica column were also studied for comparison purposes. The columns are assessed primarily on the basis of whether they can achieve high resolution between the different hydrocarbon groups: saturates, mono-, di-, tri-, and polyaromatics. Three diesel samples of increasing boiling range, density, and polycyclic aromatic hydrocarbon (PAH) content were used to assess the capabilities of the HGS column and a titania-silica coupled column.

2.2 Experimental

2.2.1 Apparatus

The columns listed in Table 2-1 were tested on a Hewlett-Packard (now Agilent, Palo Alto, CA, USA) SFC system at 35°C, 150 bar (downstream pressure), and 2.0 ml min^{-1} (flow rate at the pump). A schematic diagram of the SFC instrument is shown in Chapter 1 (Figure 1-4).

Table 2-1. Columns tested and group-type resolutions achieved at 35°C, 150 bar, 2.0 ml min^{-1}.

Column	Length (x 4.6 mm i.d.)	Diameter, Pore Size	Resolution Sat. vs. Mono.	Mono. vs. Di.	Di. vs. Tri.	Tri. vs. Poly.
Hydrocarbon Group Separation (HGS)[a,b]	250	5 μm, 60 Å	8.7	6.1	0	8.1
Bare Silica Lichrospher Si 60[c]	250	5 μm, 60 Å	11.6	6.3	0	8.6
Bare Silica Lichrosorb Si 60[c,d]	250	5 μm, 60 Å	6.0	2.9	0	5.2
Bare Silica Kromasil Si[c]	250	5 μm, 60 Å	7.5	3.3	0	5.8
Spherisorb-NH2[e]	150	3 μm, 80 Å	5.0	7.1	0.7	12.9
Bare Zirconia PHASE[f]	150	3 μm, 300 Å	1.4	7.1	2.9	2.3
Bare Titania Sachtopore-NP[f]	150	3 μm, 60 Å	5.4	11.8	1.4	8.9
Bare Zirconia-HGS[g]	400	-	9.9	8.1	3.2	6.8
Bare Titania-HGS[g]	400	-	13.4	10.7	3.6	11.0
Bare Titania-Lichrospher[g]	400	-	14.7	11.9	3.7	12.1

[a]Previously used for the group-type analysis of diesel fuels by SFC
[b]Agilent, Palo Alto, CA
[c]Thermo Electron, Waltham, MA
[d]Irregular version of spherical Lichrospher Si 60 packing
[e]Waters, Milford, MA
[f]Zirchrom, Anoka, MN
[g]Coupled columns
[h]Resolution RSD was typically less than 3%

An HP G1205A SFC pump module was used to pump SFC grade (>99.995%, <3 ppm water content) carbon dioxide (Air Liquide, Montreal, QC) through the test columns, heated in an HP 5890 series II column oven. An HP 7673B automatic sampler with 50 µl syringe was used to inject samples into a Rheodyne (Rohnert Park, CA) 7410 injection valve (0.5 µl full loop injection). Quantification was provided by an HP SFC FID. Qualitative diode array detection (DAD) was provided by an HP Series 1050 DAD. A T-joint was used to split the flow between the two detectors. The time shift between the FID and DAD signals was less than 5 seconds.

The Hewlett-Packard SFC controls downstream system pressure through the use of a backpressure regulator located after the DAD. A low flow fused silica integral restrictor (part number G1205-21400, Agilent)[17] was used to depressurize the carbon dioxide prior to the FID. Hydrogen gas for the FID was provided by a Whatman (Florham Park, NJ) Hydrogen Generator model 75-34 at a typical flow rate of 43.4 ml min^{-1}. Air was supplied by a Domnick Hunter (Mississauga, ON) Nitrox Z zero air generator at a typical flow rate of 347 ml min^{-1}. Data acquisition at 5 Hz was provided by a Vectra 486/66XM personal computer running HP-SFC ChemStation Rev. A.01.02 software.

2.2.2 Standards and Samples

Twenty model compounds (>97% purity, see Table 2-2) were studied on each test column. Model compound samples were prepared by dissolving each compound in ACS grade carbon disulfide (Fisher Scientific, Nepean, ON) at 0.1% w/w.

Table 2-2. Model compounds studied and retention times (min) shown under optimized conditions.

Compound	Hydrocarbon Group-Type	Titania-HGS coupled column	HGS column
Methane (dead time)	-	2.08	1.30
Octane[a]	Saturate, paraffin	2.20	1.42
Methylcyclohexane[b]	Saturate, naphthene	2.28	1.48
Hexadecane[c] (75% w/w)	Saturate, paraffin	2.29	1.46
Docosane[a]	Saturate, paraffin	2.36	1.49
Decahydronaphthalene[b]	Saturate, naphthene	CS_2 overlap	CS_2 overlap
Benzene[c]	Mono	3.06	2.08
n-Butylbenzene[b]	Mono	3.12	2.05
Toluene[c] (20% w/w)	Mono	3.12	2.11
2-Ethyltoluene[a]	Mono	3.35	2.24
Tetralin[a]	Mono	3.99	2.67
Naphthalene[c]	Di	5.07	3.17
Biphenyl[a]	Di	6.40	3.78
Acenaphthene[a]	Di	7.33	4.11
Fluorene[a]	Di	10.9	5.10
9,10-Dihydroanthracene[b]	Di	11.6	6.03
Dibenzothiophene[b]	Diaromatic, thiophene	12.2	5.28
Phenanthrene[a]	Tri	13.6	5.93
Anthracene[c]	Tri	14.0	5.62
Pyrene[a]	Poly	24.9	8.40
2-Naphthalenethiol[b]	Diaromatic, thiol	>60.0	5.84

[a]Sigma-Aldrich Canada Ltd., Oakville, ON
[b]Acros Organics, Morris Plains, NJ
[c]Fisher Scientific, Nepean, ON
[d]Retention time RSD was typically less than 0.4%

Due to overlap of docosane with the carbon disulfide solvent peak on some columns, an ASTM method D 5186-03[1] performance mixture consisting of 75% w/w hexadecane, 20% w/w toluene, 3% w/w tetralin, and 2% w/w naphthalene was also studied. Samples containing methane were prepared by gently bubbling methane (Air Liquide) for 30 seconds through 1.5 ml of carbon disulfide in a glass autosampler vial cooled with dry ice. The vial was quickly and tightly capped and used within three months of preparation.

Diesel samples were injected without dilution. A May 1997 oilsands derived ultra low sulfur (<10 ppm) Synfuel diesel, produced for onsite use at Syncrude Canada Ltd. in Fort McMurray, Alberta, Canada, was studied as a low boiling, low PAH content diesel sample (0.830 g cm^{-3} at 15°C). A 1998 commercial Ontario, Canada diesel was studied to represent a conventional diesel sample (0.839 g cm^{-3} at 15°C). A Shell Canada Ltd. diesel blending feedstock was studied as a high boiling, high PAH content diesel sample (0.871 g cm^{-3} at 15°C). The simulated distillation results for each diesel sample are shown in Table 2-3.

2.2.3 Calculations

Retention times and peak widths at half-height were determined using ChemStation Rev. A.01.02 software. Retention factors were calculated using methane as the dead time marker. Apparent plate heights, H, were calculated using peak widths at half height. Plate heights measured in SFC may have errors due to the compressible nature of the mobile phase.[19] Plate heights measured here are described as apparent to reflect this.

Table 2-3. Simulated distillation results for three diesel fuels studied.

	Synfuel	Commercial Diesel	Blending Feedstock
Initial Boiling Point (°C)	125	173	90
T10% (°C)	158	199	256
T50% (°C)	199	256	324
T90% (°C)	246	311	364
Final Boiling Point (°C)	284	337	400

[a]Simulated distillation results were obtained by Syncrude Canada Ltd. by integrating the FID signal of a sample eluted from a non-polar gas chromatography column using an increasing temperature ramp (ASTM D2887-04a).

Determining the resolution between the latest eluting model compound of one group-type versus the earliest eluting model compound of the next group-type is one way of quantifying the degree of separation between two group-types. Resolution combines the effects of retention, separation selectivity, and efficiency according to the Resolution Equation (Equation 1-9). Resolution, R_S, between two group-types such as mono- and diaromatics were calculated based on width at half height:

$$R_S = \frac{2(t_2 - t_1)}{1.699(w_2 - w_1)} \qquad \text{(Equation 2-1)}$$

where t_1 and t_2 are the retention time of the latest eluting monoaromatic and the earliest eluting diaromatic model compound studied. w_1 and w_2 are the peak widths at half-height of the latest eluting monoaromatic and the earliest eluting diaromatic model compound studied. Here, a resolution value of zero indicates that model compounds from different group-types are eluting in the wrong sequence. For example, hexadecane is a saturates model compound and toluene is a monoaromatic model compound. To achieve group-type separation between saturates and monoaromatics, all saturates should elute before all monoaromatics. Thus, if hexadecane elutes after toluene, the group-type resolution would be zero even if the two compounds were baseline resolved.

Because of overlap of docosane with the carbon disulfide sample solvent on several test columns, the resolutions between the saturates and monoaromatics were calculated from the hexadecane and toluene peaks from the ASTM D 5186-03 performance mixture. This may result in overestimation of the saturate and monoaromatic resolution, but it allows for direct comparison of all columns studied.

Carbon dioxide densities were calculated based on temperature and downstream pressure using EOS-SCx version 2 free software.[20] This software was found to produce carbon dioxide densities that were not statistically different from those reported in the literature over the entire range of temperature and pressure conditions studied here.[21]

2.2.4 Cut Points for Group-Type Analysis

The cut point between saturates and aromatics was determined as the minimum in the signal between the two groups. ASTM D 5186-03 method[1] cuts the mono- and diaromatic group-types at the beginning of the elution of the naphthalene peak. This was determined as 3.10 min for the HGS column and 4.96 min for the titania-HGS coupled column following inspection of the chromatograms containing naphthalene.

Although the ASTM method does not distinguish between di-, tri- and polyaromatics, they were determined here as follows. On the HGS column, the di- and triaromatic cut point was taken as 5.45 min based on the midpoint point between the dibenzothiophene and anthracene peaks. Note that this ignores the fact that on the HGS column, 9,10-dihydroanthracene (diaromatic) eluted after both of the triaromatic model compounds that were studied. On the titania-HGS coupled column, the midpoint between the dibenzothiophene and phenanthrene peaks was used, giving 12.9 min. On the HGS column the tri- and polyaromatic cut point was determined to be 7.16 min based on the midpoint between the phenanthrene and pyrene peaks. On the titania-HGS column the midpoint between the anthracene and pyrene peaks was used, giving 19.4 min. Due to differences in the elution order of the triaromatics on

the HGS and titania-HGS coupled column, different triaromatic model compounds were used for the cut-points. See Chapter 1 (Figure 1-5) for an example of an integrated diesel chromatogram using the cut-points for the HGS column.

2.3 Results and Discussion

2.3.1 Comparison of Conventional Silica Columns

Conventional Type A bare silica columns HGS, Lichrospher Si 60, Lichrosorb Si 60, as well as a low metals Type B bare silica Kromasil Si column were studied to determine how well bare silica columns perform group-type separations of diesel samples. A Spherisorb-NH2 column was also studied because aminopropyl columns have been used with HPLC to perform group-type separations of gasoline,[22] diesel,[3] gas oil,[23-25] crude oil,[26,27] and heavy distillates.[28] The twenty model compounds in Table 2-2 were studied on each column at 35°C, 150 bar, and 2.0 ml min^{-1} which was determined to be the optimal conditions for group-type separations on the HGS column (Figure 2-1).

For the aromatics, most of the silica columns produced apparent plate heights in the range of 8 to 20 μm. The exception was the HGS column, which yielded an apparent plate height of 36 μm for pyrene. The apparent plate heights for hexadecane were in the range of 14 μm for the aminopropyl-bonded silica column to 49 μm for the HGS column. These higher apparent plate heights are possibly the result of mass overloading of the columns due to the higher 75% w/w concentration of hexadecane in the ASTM performance mixture compared to the other model compounds at 0.1% w/w.

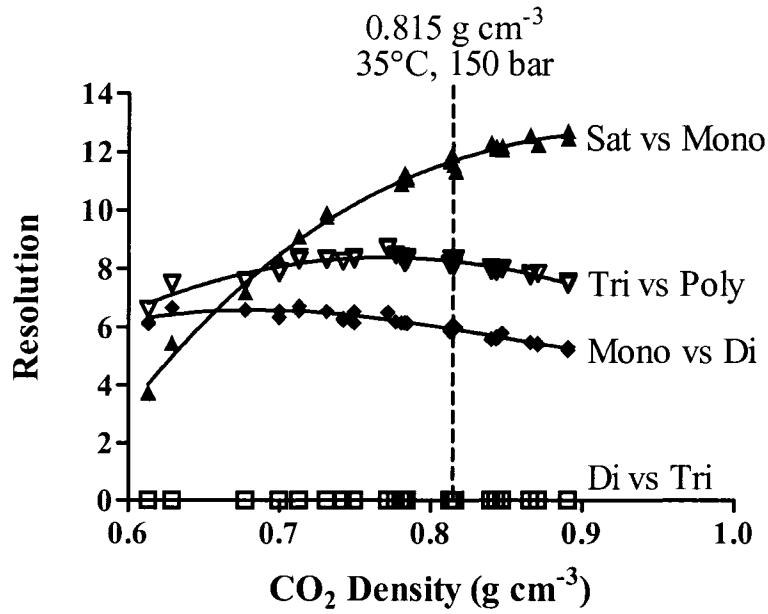

Figure 2-1. Group-type resolutions versus carbon dioxide density at temperatures from 35°C to 50°C and pressures from 100 to 200 bar at 2.0 ml min^{-1} on a bare silica HGS column. Note that the saturate vs. monoaromatic resolution shown in this particular graph is based on docosane and benzene peaks rather than hexadecane and toluene peaks as discussed in Section 2.2.3. See Table 2-1 for column dimensions. Resolution RSD was typically less than 3%.

Docosane at 0.1% w/w produced apparent plate heights between 9 and 12 μm when it was not overlapping with the CS_2 solvent peak.

When the group-type resolutions of the various silica columns are compared (Table 2-1), the highest saturate vs. monoaromatic resolution is achieved on the Lichrospher column with the aminopropyl-bonded silica column producing the lowest saturate vs. monoaromatic resolution. The Lichrospher, HGS, and aminopropyl-bonded silica columns produced high mono- vs. diaromatic and tri- vs. polyaromatic resolutions. The aminopropyl-bonded silica column was the only silica column to achieve any di- vs. triaromatic resolution, but it provided poor saturate vs. monoaromatic resolution. The trends observed on the aminopropyl-bonded silica column are similar to those reported previously.[17] The Lichrosorb and Kromasil columns performed poorly compared to the other silica columns.

None of the silica columns adequately separated all of the model compounds according to group-type, with the separation of di- and triaromatics proving to be the most difficult. Despite this, all of the silica columns studied met the ASTM D 5186-03 method[1] requirements of R_s(sat, mono) = 4 and R_s(mono, di) = 2 (see Table 2-1). These resolution requirements are easily met, but they fail to provide near baseline resolution of group-types in diesel samples. Alternative column materials offering different surface chemistries were studied in an effort to achieve the highest possible resolution of all group-types.

2.3.2 Comparison of Zirconia and Titania Columns

Bare zirconia was studied as it has a polar surface similar to silica, while possessing Lewis acid sites which provide additional interactions with π-electron rich

PAH compounds.[29-32] All of the aromatics eluted according to ring number on a bare zirconia column, but not without a significant loss in the saturate vs. monoaromatic resolution (Table 2-1). Most of the PAHs studied yielded poorer efficiencies on bare zirconia compared to silica. Significant improvements in efficiency were observed at higher temperatures and pressures (Figure 2-2A). However, even at 100°C and 250 bar (0.59 g cm^{-3} carbon dioxide density), anthracene's apparent plate height of 65 μm is still 3.6-fold higher than on bare silica at the milder conditions of 35°C and 150 bar (0.82 g cm^{-3}). Also, at these higher temperatures and pressures, the hexadecane and toluene peaks were unresolved, indicating a significant loss in the saturate vs. monoaromatic resolution. Improvements in the aromatic group-type resolutions were 6%, 27%, and 180% respectively at 100°C and 250 bar compared to 35°C and 150 bar.

Two reversed phase zirconia columns were also studied and found to be unsuitable for group-type separations in SFC. A carbon coated zirconia column was too retentive to elute saturates or aromatics within 60 min, even at the strongest eluent conditions studied of 35°C and 200 bar (0.87 g cm^{-3}). A polybutadiene coated zirconia column eluted docosane after the monoaromatics.

Although the retention of docosane could be reduced relative to the aromatic compounds by decreasing the temperature and increasing the pressure, docosane had a similar retention factor to biphenyl at the best conditions of 35°C and 200 bar. Thus the polybutadiene coated zirconia did not yield a saturates-monoaromatics separation.

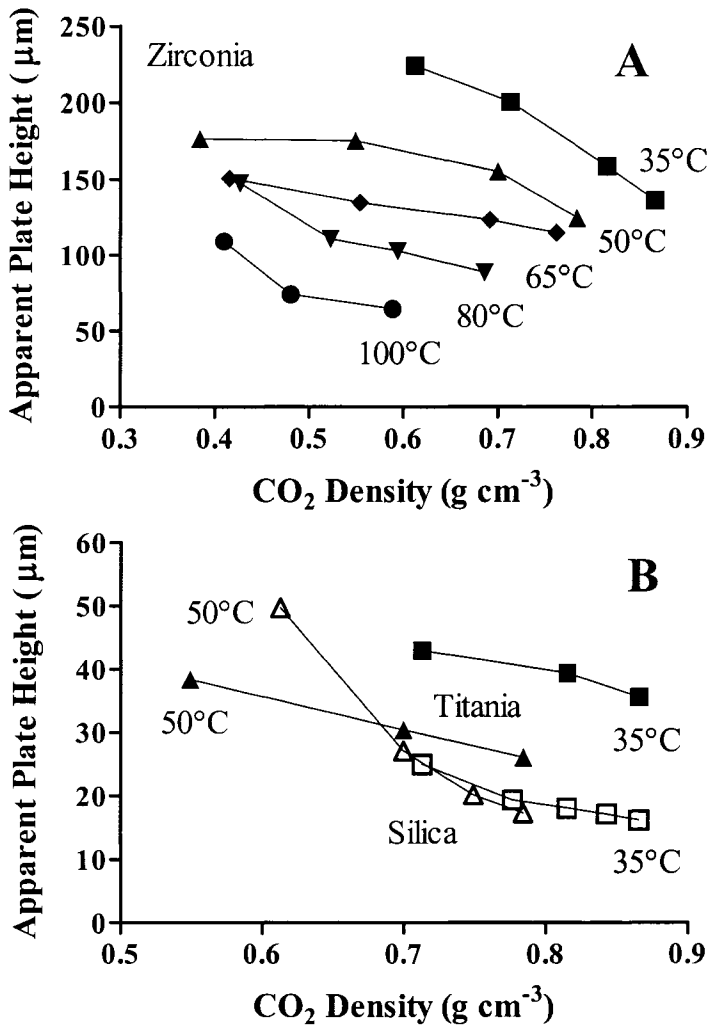

Figure 2-2. Apparent plate height of anthracene versus carbon dioxide density at temperatures from 35°C to 100°C and pressures from 85 to 250 bar at 2.0 ml min^{-1} on (A) a bare zirconia column, (B) a bare titania column (closed symbols) and a bare silica HGS column (open symbols). No significant loss in efficiency was observed for any studied compounds when pressures less than 100 bar[33,34] or temperatures higher than 50°C[33] were studied (see Section 1.3.4). See Table 2-1 for column dimensions. Apparent plate height RSD was typically less than 6%.

The polybutadiene coated zirconia column eluted all of the PAHs according to ring number, but also suffered from poorer PAH efficiencies than silica with apparent plate heights for anthracene in the range of 16 to 60 μm under the same conditions as Figure 2-2A.

Bare titania was studied because it has a similar surface chemistry to bare zirconia.[29-31,35] It is available with smaller pore sizes than zirconia. This leads to higher surface area and higher retention factors for improving the saturate vs. monoaromatic resolution. A bare titania column eluted all of the group-types in order, with more reasonable PAH efficiencies than bare zirconia (Figure 2-2B). Anthracene's apparent plate height on bare titania improved from 39 μm to 26 μm as temperature and pressure were increased from 35°C and 150 bar (0.82 g cm^{-3}) to 50°C and 200 bar (0.78 g cm^{-3}). The apparent plate heights for the saturate and monoaromatic model compounds on zirconia and titania were comparable or lower than on silica. At 50°C and 200 bar, the di- vs. triaromatic and tri- vs. polyaromatic resolutions on bare titania improved by 79% and 19% respectively compared to 35°C and 150 bar. The saturate vs. monoaromatic resolution decreased by 7%, while the mono- vs. diaromatic resolution did not change.

Comparison of the group-type resolutions on bare silica, aminopropyl-bonded silica, bare zirconia, and bare titania at 35°C and 150 bar (Figure 2-3) reveals that bare silica provides the highest saturate vs. monoaromatic resolution followed by bare titania, aminopropyl-bonded silica, and then bare zirconia. Bare titania produces the highest mono- vs. diaromatic resolution while bare zirconia produces the highest di- vs. triaromatic resolution.

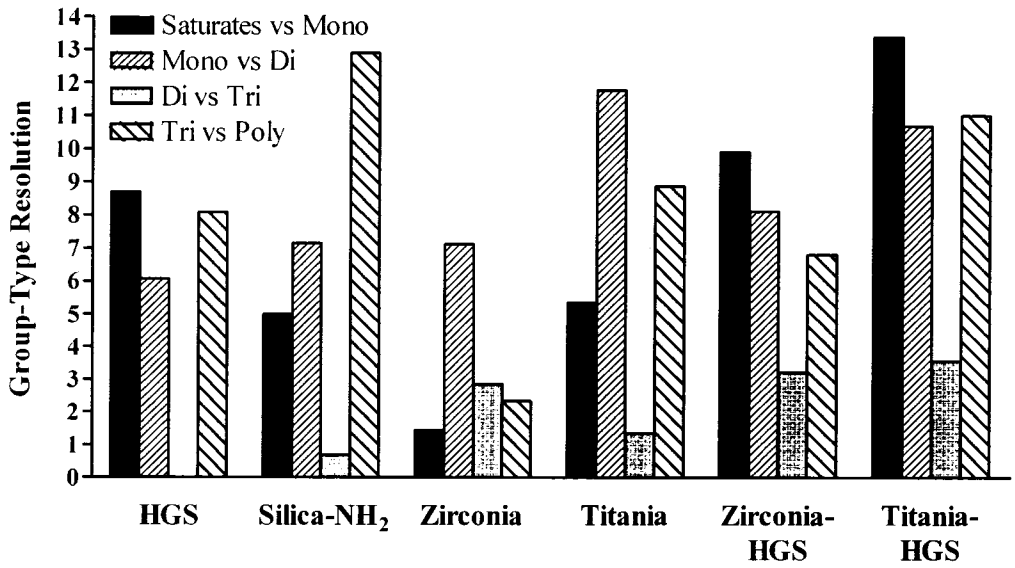

Figure 2-3. Group-type resolutions on various columns and coupled columns at 35°C, 150 bar, and 2.0 ml min^{-1}. See Table 2-1 for column dimensions and numerical resolution values. All saturate vs. monoaromatic resolutions were based on hexadecane and toluene. All mono- vs. diaromatic resolutions were based on tetralin and naphthalene. Remaining resolutions were based on: HGS (phenanthrene and pyrene); aminopropyl boned silica (dihydroanthracene and anthracene, phenanthrene and pyrene); zirconia, titania, titania-HGS (dibenzothiophene and phenanthrene, anthracene and pyrene); zirconia-HGS (dibenzothiophene and anthracene, phenanthrene and pyrene). Resolution RSD was typically less than 3%.

The aminopropyl-bonded silica column produced the highest tri- vs. polyaromatic resolution.

2.3.3 Coupled Titania-Silica and Zirconia-Silica Columns

Bare titania provides good aromatic group-type resolutions. Bare silica provides good saturate vs. monoaromatic resolution. A bare titania column was coupled to the bare silica HGS column to provide higher overall resolutions. The titania column was placed upstream of the silica column to provide a higher average carbon dioxide density across the titania column to help improve PAH efficiency. A bare zirconia and HGS coupled column was also studied.

At 35°C and 150 bar, both zirconia-HGS and titania-HGS coupled columns yield poor PAH efficiencies compared to bare silica (e.g., $H_{anthracene}$ of 79 μm and 43 μm respectively compared to 18 μm on the HGS column). When the elution conditions are increased to 100°C and 250 bar for the zirconia-HGS coupled column and 50°C and 200 bar for the titania-HGS coupled column, these apparent plate heights improve to 37 μm and 26 μm respectively.

The zirconia-HGS coupled column achieved comparable or better group-type resolutions at 35°C and 150 bar compared to the HGS column alone (Figure 2-3). At 100°C and 250 bar, the saturate vs. monoaromatic resolution on the zirconia-HGS column decreased by 38%, while the aromatic group-type resolutions increased by 1%, 31%, and 60% respectively. Note that changes less than the typical 3% RSD for resolution values reported here are not statistically significant.

At 35°C and 150 bar, the titania-HGS coupled column gave the highest group-type resolutions overall (Figure 2-3). At 50°C and 200 bar, saturate vs.

monoaromatic and mono- vs. diaromatic resolutions decreased by 6% and 8% respectively while the di- vs. triaromatic and tri- vs. polyaromatic resolutions increased by 1% (statistically insignificant) and 15% respectively. When the titania column was coupled to the new bare silica Lichrospher column instead of the HGS column, resolutions were further improved as shown in Table 2-1. These resolutions are higher than previously reported results using similar length columns,[17,36,37] and comparable or better than columns more than twice as long.[37,38]

2.3.4 Group-Type Analysis of Diesel Samples Using a Titania-Silica Coupled Column

Three diesel samples were analyzed on the bare titania-HGS coupled column and on the HGS column alone. As the HGS column has been used previously for diesel group-type analysis, our results are more indicative of typical column performance rather than new column performance. The first diesel sample studied was a Synfuel diesel that is representative of light diesels with relatively low PAH concentrations. The second sample was a commercial Ontario diesel with moderate PAH concentrations. The third sample was a Shell Canada Ltd. diesel blending feedstock that is representative of very heavy (dense) diesels with high PAH concentrations.

Figure 2-4A shows the FID and UV traces for the Synfuel diesel sample separated on the HGS column under standard conditions. The FID trace shows the elution of all group-types with the signal intensity being directly proportional to hydrocarbon mass. The UV response at 254 nm indicates that the monoaromatics begin to elute at 1.8 min.

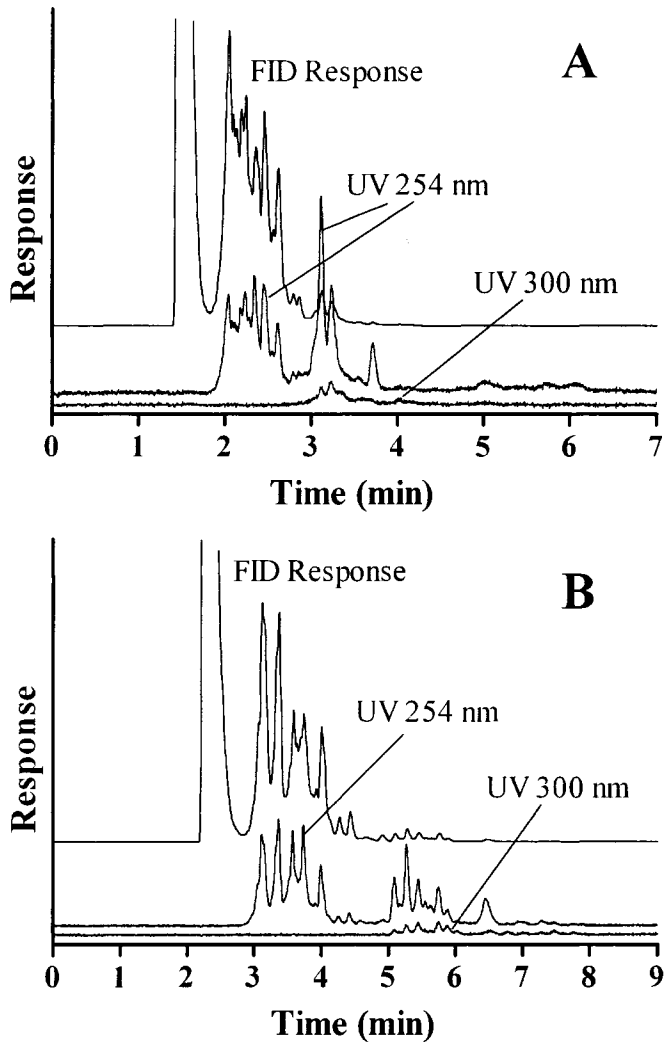

Figure 2-4. FID and UV traces of a Synfuel light diesel separated at 35°C, 150 bar, and 2.0 ml min^{-1} on (A) a bare silica HGS column and (B) a bare titania column coupled to a bare silica HGS column. See Table 2-1 for column dimensions.

The UV response at 300 nm shows that the diaromatics begin to elute at 2.8 min. Near baseline resolution is obtained between the saturates, mono-, and diaromatics on the HGS column.

Figure 2-4B shows the same separation on the bare titania-HGS column. Near baseline resolution between the saturates, mono-, and diaromatics is also obtained, with the monoaromatics beginning to elute at 2.9 min and the diaromatics at 5.0 min. It is clear from Figure 2-4A and Figure 2-4B that the diaromatics have different elution times on the two columns, with better resolution of the aromatic peaks observed on the titania-HGS coupled column.

Figure 2-5A shows the commercial Ontario diesel separated on the HGS column. With this commercial diesel there is less resolution between the group-types compared to the lighter Synfuel diesel (Figure 2-4A). Figure 2-5B shows the same separation on the titania-HGS coupled column. The higher mono- vs. diaromatic resolution on the titania-HGS coupled column can be observed by the lower signal intensity of the FID trace when the diaromatics begin to elute at 5.0 min compared to the HGS column at 2.8 min. Lower FID signal intensity near the cut-point indicates lower overlap of the two group-types. The PAH compounds require 40 min to elute from titania-HGS column, compared to 10 min from the HGS column. While this significantly increases the analysis time, it also provides much higher aromatic resolutions. A shorter titania column could be used to reduce the analysis time while still providing high aromatic group-type resolutions.

Figure 2-6A shows the diesel blending feedstock separated on the HGS column.

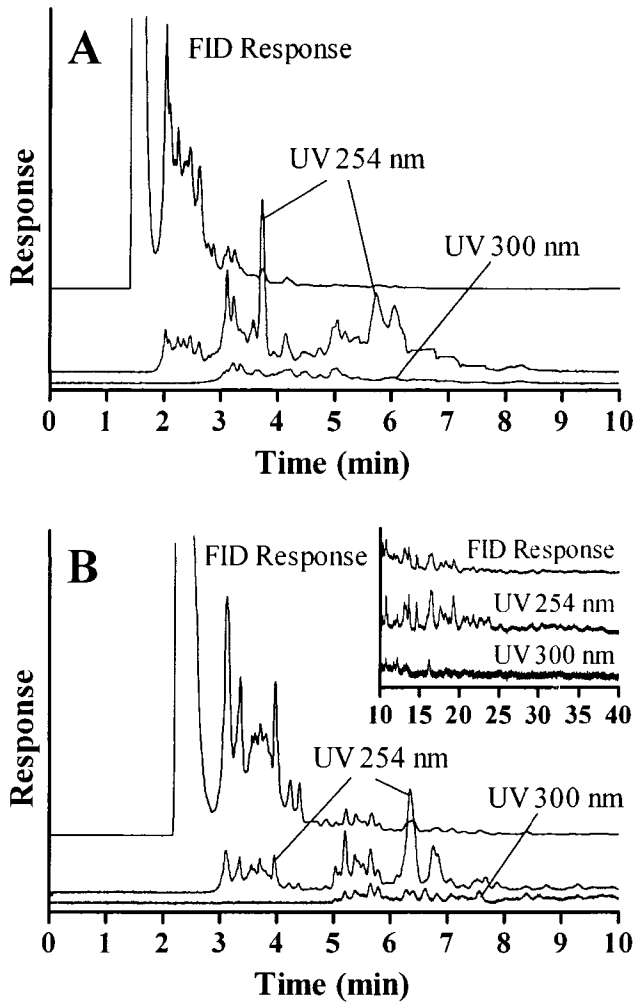

Figure 2-5. FID and UV traces of a commercial Ontario, Canada diesel separated at 35°C, 150 bar, and 2.0 ml min^{-1} on (A) a bare silica HGS column and (B) a bare titania column coupled to a bare silica HGS column. See Table 2-1 for column dimensions.

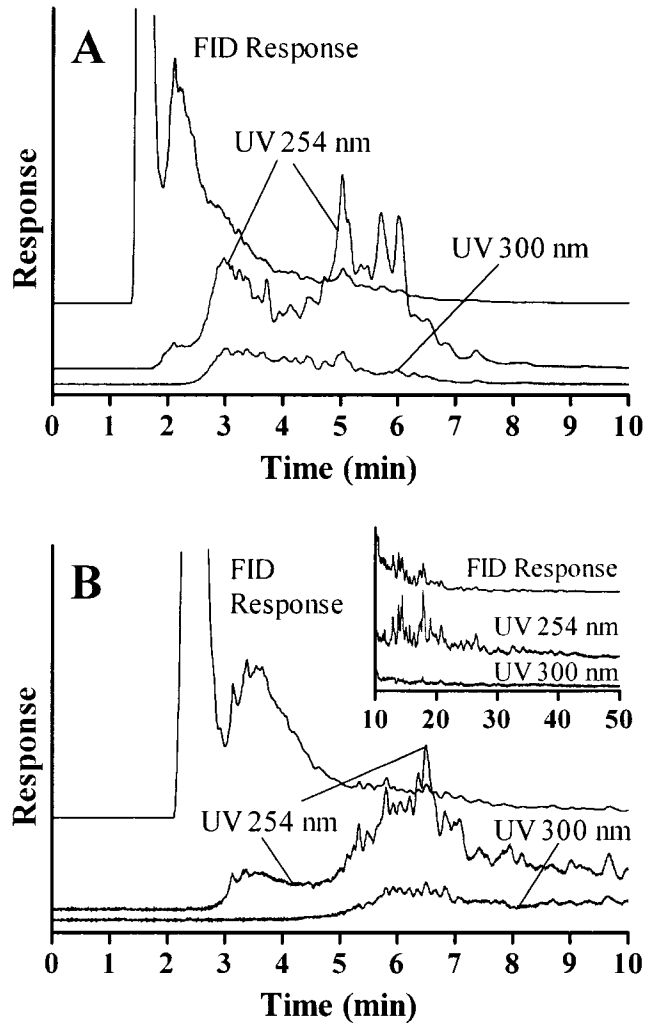

Figure 2-6. FID and UV traces of a diesel blending feedstock separated at 35°C, 150 bar, and 2.0 ml min^{-1} on (A) a bare silica HGS column and (B) a bare titania column coupled to a bare silica HGS column. See Table 2-1 for column dimensions.

With this heavier diesel sample there is much less resolution between the group-types compared to the lighter diesel samples (Figure 2-4A and Figure 2-5A). There is also much higher PAH content (Table 2-4). Figure 2-6B shows the same separation on the titania-HGS coupled column. Again, the higher mono- vs. diaromatic resolution on the titania-HGS coupled column is shown by the lower signal intensity of the FID trace when the diaromatics begin to elute at 4.2 min compared to the HGS column alone at 2.4 min. While all compounds have eluted from the HGS column by 10 min, they continue to elute from the titania-HGS column until 50 min.

The diesel group-type results from both columns are compared in Table 2-4. It should be noted that the di- and triaromatic determinations on the HGS column are somewhat suspect as there was overlap of the model compounds from the two groups on the HGS column (Table 2-2). For the Synfuel sample, the near baseline resolution on both columns makes the results less sensitive to column choice, yielding similar results (within 0.5 mass%) for both. However, significant differences in the commercial diesel results are observed between the two columns. The mono, di-, and polyaromatic results appear sensitive to column choice due to the lower resolution between group-types. For the diesel blending feedstock, significant differences are observed between the two columns for all of the group-types except the triaromatics.

2.3.5 Retention Time and Resolution Repeatability

Polar sample components could be irreversibly retained and may alter the column performance over time. For instance, naphthalenethiol did not elute within 60 min on Lichrospher silica, titania, and zirconia columns.

Table 2-4. Group-type content of diesel samples reported in mass% (RSD, %).

Sample	Column	Saturates	Mono.	Di.	Tri.	Poly.
Synfuel	HGS	63.5 (0.1%)	34.7 (0.4%)	1.8 (4%)[a]	0.04 (40%)[a]	-
Synfuel	Ti-HGS	63.5 (0.1%)	34.3 (0.1%)	2.2 (2%)	0.01 (40%)	-
Commercial Diesel	HGS	70.1 (0.1%)	24.6 (0.2%)	4.7 (0.6%)[a]	0.5 (7%)[a]	0.09 (26%)
Commercial Diesel	Ti-HGS	69.8 (0.1%)	23.5 (0.2%)	5.5 (0.6%)	0.6 (6%)	0.6 (9%)
Blending Feedstock	HGS	64.1 (0.1%)	22.7 (0.3%)	11.0 (0.3%)[a]	1.9 (1%)[a]	0.3 (10%)
Blending Feedstock	Ti-HGS	65.6 (0.1%)	19.3 (0.3%)	11.8 (0.2%)	2.0 (0.9%)	1.3 (3%)

[a]HGS results ignore 9,10-dihydroanthracene's (diaromatic) elution after triaromatic model compounds

To determine whether polar compounds in diesels affect titania column performance, the commercial Ontario diesel (350 ppm sulfur) and then the Synfuel diesel (<10 ppm sulfur, 0.4 mass% 2-ethylhexyl nitrate cetane improver, 110 ppm lubricity improver) were injected 100 times each on the titania column. The ASTM performance mixture and anthracene were run about every 20 injections to determine if the column retention characteristics were altered.

The RSD of the retention time was 0.1% for hexadecane, 0.3% for toluene, 0.6% for tetralin, 1.0% for naphthalene, and 4.8% for anthracene over the 200 diesel injections. Most of the variation occurred during the first 60 injections of the commercial diesel. The retention time RSD during the last 140 injections was less than 0.4% for all five model compounds. Resolution was stable throughout the test with R_S(hexadecane, toluene) = 5.2 (3% RSD) and R_S(tetralin, naphthalene) = 10.6 (2% RSD). The commercial diesel was rerun on the titania-HGS coupled column following the 200 repeat diesel injections. These results were within 0.3 mass% from the original results reported in Table 2-4 and were not statistically different. This demonstrates titania's applicability to diesel samples with significant amounts of naturally occurring sulfur as well as diesel additives.

2.4 Conclusions

A titania-silica coupled column was found to provide the highest overall group-type resolutions of the twenty model compounds studied, with the separation of di- and triaromatics proving to be the most difficult. The study of three diesel samples demonstrated that group-type separations become more difficult as the

boiling range and PAH content of the diesel samples increase. In turn, results become more sensitive to column choice with heavier samples. While there are no diesel standard reference materials to confirm which column yields the most accurate results, we are more confident in the results produced by the column with the highest group-type resolutions between model compounds.

2.5 References

(1) *Method D 5186-03, Annual Book of ASTM Standards*, American Society for Testing and Materials, West Conshohocken, PA, USA, 2003.

(2) Barman, B. N.; Cebolla, V. L.; Membrado, L., *Crit. Rev. Anal. Chem.* **2000**, *30*, 75-120.

(3) Šegudovic, N.; Tomic, T.; Škrobonja, L.; Kontic, L., *J. Sep. Sci.* **2004**, *27*, 65-70.

(4) Sink, C. W.; Hardy, D. R., *Anal. Chem.* **1994**, *66*, 1334-1338.

(5) McKerrell, E. H., *Fuel* **1993**, *72*, 1403-1409.

(6) *Method 391/95, IP Standard Methods for Analysis and Testing of Petroleum and Related Products and British Standard 2000 Parts*, The Institute of Petroleum (now Energy Institute), London, England, 1995.

(7) *Method D 6591-00, Annual Book of ASTM Standards*, American Society for Testing and Materials, West Conshohocken, PA, USA, 2000.

(8) Barman, B. N., *Anal. Chem.* **2001**, *73*, 2791-2804.

(9) Wang, F. C.-Y.; Qian, K.; Green, L. A., *Anal. Chem.* **2005**, *77*, 2777-2785.

(10) Briker, Y.; Ring, Z.; Iacchelli, A.; McLean, N.; Rahimi, P. M.; Fairbridge, C.; Malhotra, R.; Coggiola, M. A.; Young, S. E., *Energy & Fuels* **2001**, *15*, 23-37.

(11) Trisciani, A.; Munari, F., *J. High Resol. Chromatogr.* **1994**, *17*, 452-456.

(12) Davies, I. L.; Bartle, K. D.; Andrews, G. E.; Williams, P. T., *J. Chromatogr. Sci.* **1988**, *26*, 125-130.

(13) Pál, R.; Juhász, M.; Stumpf, Á., *J. Chromatogr. A* **1998**, *819*, 249-257.

(14) Qian, K.; Diehl, J. W.; Dechert, G. J.; DiSanzo, F. P., *Eur. J. Mass Spectrom.* **2004**, *10*, 187-196.

(15) Thiébaut, D. R. P.; Robert, E. C., *Analusis* **1999**, *27*, 681-690.

(16) DiSanzo, F. P.; Yoder, R. E., *J. Chromatogr. Sci.* **1991**, *29*, 4-7.

(17) M'Hamdi, R.; Thiébaut, D.; Caude, M., *J. High Resol. Chromatogr.* **1997**, *20*, 545-554.

(18) Berger, T. A., *Personal communication.* **2003**.

(19) Poe, D. P.; Martire, D. E., *J. Chromatogr.* **1990**, *517*, 3-29.

(20) http://hp.vector.co.jp/authors/VA030090/.

(21) Span, R.; Wagner, W., *J. Phys. Chem. Ref. Data* **1996**, *25*, 1509-1596.

(22) Kaminski, M.; Kartanowicz, R.; Przyjazny, A., *J. Chromatogr. A* **2004**, *1029*, 77-85.

(23) Woods, J. R.; Kung, J.; Pleizier, G.; Kotlyar, L. S.; Sparks, B. D.; Adjaye, J.; Chung, K. H., *Fuel* **2004**, *83*, 1907-1914.

(24) Robert, E.; Beboulene, J.-J.; Codet, G.; Enache, D., *J. Chromatogr. A* **1994**, *683*, 215-222.

(25) Pasadakis, N.; Gaganis, V.; Varotsis, N., *Fuel* **2001**, *80*, 147-153.

(26) Ali, M. A., *Pet. Sci. Technol.* **2003**, *21*, 963-970.

(27) Fan, T.; Buckley, J. S., *Energy & Fuels* **2002**, *16*, 1571-1575.

(28) Sarowha, S. L. S.; Sharma, B. K.; Sharma, C. D.; Bhagat, S. D., *Energy & Fuels* **1997**, *11*, 566-569.

(29) Grün, M.; Kurganov, A. A.; Schacht, S.; Schüth, F.; Unger, K. K., *J. Chromatogr. A* **1996**, *740*, 1-9.

(30) Nawrocki, J.; Dunlap, C.; McCormick, A.; Carr, P. W., *J. Chromatogr. A* **2004**, *1028*, 1-30.

(31) Kurganov, A.; Trüdinger, U.; Isaeva, T.; Unger, K., *Chromatographia* **1996**, *42*, 217-222.

(32) Nawrocki, J.; Rigney, M. P.; McCormick, A.; Carr, P. W., *J. Chromatogr. A* **1993**, *657*, 229-282.

(33) Chester, T. L., *Microchem. J.* **1999**, *61*, 12-24.

(34) Berger, T. A., *Packed Column SFC*, The Royal Society of Chemistry, Cambridge, 1995.

(35) Winkler, J.; Marmé, S., *J. Chromatogr. A* **2000**, *888*, 51-62.

(36) Richter, B. E.; Jones, B. A.; Porter, N. L., *J. Chromatogr. Sci.* **1998**, *36*, 444-448.

(37) Li, W.; Malik, A.; Lee, M. L.; Jones, B. A.; Porter, N. L.; Richter, B. E., *Anal. Chem.* **1995**, *67*, 647-654.

(38) Shariff, S. M.; Robson, M. M.; Myers, P.; Bartle, K. D.; Clifford, A. A., *Fuel* **1997**, *77*, 927-931.

CHAPTER THREE. Fast Supercritical Fluid Chromatography Hydrocarbon Group-Type Separations of Diesel Fuels Using Packed and Monolithic Columns*

3.1 Introduction

Supercritical fluid chromatography (SFC) is used to provide 3-fold[1] faster separations than high performance liquid chromatography (HPLC) in pharmaceutical, chiral, petroleum, polymer, natural product, and food-related applications.[1-3] Faster separations improve sample throughput, reduce costs, and make real-time process monitoring feasible.[4] Surprisingly, few publications have dealt with increasing the speed of SFC separations beyond the 3-fold improvement[1] that SFC inherently provides over HPLC. SFC separation times can be further reduced using methods similar to those used to decrease separation times in HPLC, such as using shorter columns with smaller diameter packing.[5]

This paper focuses on increasing the speed of a common industrial analysis performed by SFC – the separation of diesel fuels into hydrocarbon group-types (*i.e.* saturates, mono-, di-, tri-, and polyaromatics). Diesel and jet fuel environmental and performance properties have been associated with the group-type compositions of these fuels.[6-20] In particular, high polycyclic aromatic hydrocarbon (PAH) content increases particulate matter,[14,15,19] nitrogen oxides,[14,15,19] and PAH emissions.[17,18,20] Government regulations on PAH content are becoming ever more stringent to curb these emissions. ASTM method D 5186-03[21] uses SFC with a carbon dioxide mobile

*A version of this chapter has been published. Paproski R. E., Cooley, J., Lucy C. A.; *Analyst* **2006**, 131, 422-428.

phase and a packed silica column to separate diesel fuels according to hydrocarbon group-type.

In Chapter 2, coupling a 15 cm column of 3 μm bare titania in series with a conventional 25 cm column of 5 μm bare silica was shown to greatly increase group-type resolutions, especially between the di- and triaromatic model compounds. However, this coupled column increased the separation time for a commercial diesel sample from 10 min to 40 min.

Here, two different approaches for reducing separation time are compared. The first approach is to use shorter columns with smaller diameter packing.[5,22-26] Shortening the column reduces the separation efficiency. Using a smaller diameter packing helps offset this by improving the plate height. When the flow rate is increased, the overall effect is a drastic reduction in separation time while maintaining acceptable group-type resolutions.

The second approach is to use monolithic columns. These columns contain a single continuous macroporous (~2 μm pore diameter) and mesoporous (~13 nm pore diameter) rod of silica.[27-29] The large macropores allow mobile phase to flow through the column with about a tenth of the pressure drop compared to conventional particle packed columns.[27-29] This allows much higher flow rates to be used before the pressure limitations of the pump are met. The use of monolithic columns in HPLC has resulted in reduced analysis times while maintaining resolution.[25,26,28-31] In SFC, Lesellier et al. coupled five monolithic columns to a conventional packed column to permit the separation of β-carotene isomers.[32]

Both approaches are studied with an emphasis on determining what factors are limiting resolution at high flow rates. Diesel samples of increasing boiling range and PAH content are studied to determine whether increasing the speed of the analysis affects the quantitative diesel group-type results.

3.2 Experimental

3.2.1 Apparatus

The experimental conditions have been described in Chapter 2. Briefly, a Hewlett-Packard (now Agilent, Palo Alto, CA) SFC system pumped SFC grade (>99.995%, <3 ppm water content) carbon dioxide (Air Liquide, Montreal, QC) through the test columns at pump flow rates from 1.0 up to 5.0 ml min^{-1} and downstream pressures from 100 to 150 bar. The three test columns studied were: a 100 x 4.6 mm, 3 μm, 60 Å bare silica Lichrospher Si 60 packed column (Thermo Electron, Waltham, MA); a 50 x 4.6 mm, 3 μm, 60 Å bare titania Sachtopore-NP packed column (Zirchrom, Anoka, MN) coupled to the Lichrospher column; and a 100 x 4.6 mm, 2 μm macropores, 130 Å mesopores bare silica Chromolith Si monolithic column (Merck KGaA, Darmstadt, Germany). The columns were maintained at 35°C. An HP 7673B automatic sampler was used with a Rheodyne (Rohnert Park, CA) 7410 injection valve to provide 0.5 μl full loop sample injections. Quantitative flame ionization detection (FID) was provided by an HP SFC FID. Qualitative diode array detection (DAD) was provided by an HP Series 1050 DAD.

3.2.2 Standards and Samples

Standards and samples were prepared as described in Section 2.2.2.

3.2.3 Calculations

Retention factors, apparent plate heights, and group-type resolutions were calculated as described in Section 2.2.3.

3.2.4 Cut Points for Group-Type Analysis

The minimum in the signal between the saturates and aromatics was used as a cut-point. ASTM method D 5186-03[21] places the mono- and diaromatic cut point at the beginning of the elution of the naphthalene peak. This was 0.54 min for the Lichrospher silica column and 0.90 min for the titania-Lichrospher coupled column.

For the Lichrospher silica column, the di- and triaromatic cut point was 0.78 min, the midpoint point between the dibenzothiophene and anthracene peaks. This ignores that 9,10-dihydroanthracene (diaromatic) eluted after both of the triaromatic model compounds that were studied on the Lichrospher column. This is typical for conventional bare silica columns, while titania-silica coupled columns cleanly separate di- and triaromatic model compounds as shown in Chapter 2. For the titania-Lichrospher coupled column, the midpoint between the dibenzothiophene and phenanthrene peaks was used (1.95 min). For the Lichrospher column the tri- and polyaromatic cut point was 0.92 min based on the midpoint point between the phenanthrene and pyrene peaks. For the titania-Lichrospher coupled column, the midpoint between the anthracene and pyrene peaks was used (2.67 min).

For reasons discussed below in Sections 3.3.3 and 3.3.4, three coupled Chromolith columns were used to separate the Synfuel sample. The cut points between the aromatic groups were 1.30 min, 1.52 min, and 1.65 min.

3.3 Results and Discussion

Short analysis times are central to achieving high sample throughput, reduced costs, and real-time monitoring of industrial processes.[4] Short packed columns and monolithic columns are compared under high flow rates as two alternative approaches for reducing the time of a model SFC separation – the determination of diesel group-types.

3.3.1 Retention on Packed and Monolithic Columns

To determine whether conventional particle packed columns or monolithic columns would produce faster diesel separations while maintaining high group-type resolutions, a particle packed Lichrospher Si 60 bare silica column and a monolithic Chromolith Si bare silica column were studied.

Retention factors were substantially higher on the packed Lichrospher column than on the monolithic Chromolith column. For instance, at 2.0 ml min^{-1} and 150 bar, the retention factor of anthracene was 2.5 on the Lichrospher column and 0.56 on the Chromolith. This difference in retention is consistent with the higher surface area of the Lichrospher column (700 m^2g^{-1}) compared to the Chromolith column (300 m^2g^{-1}). Also, the higher porosity of the Chromolith column[26,29,32] further raises its phase ratio (mobile phase volume to stationary phase weight). This results in significantly lower retention factors for the Chromolith column compared to the Lichrospher column.

Figure 3-1 plots the retention factors of the representative model compound anthracene as a function of flow rate. Retention decreases with increasing flow rate for both the Lichrospher and Chromolith columns.

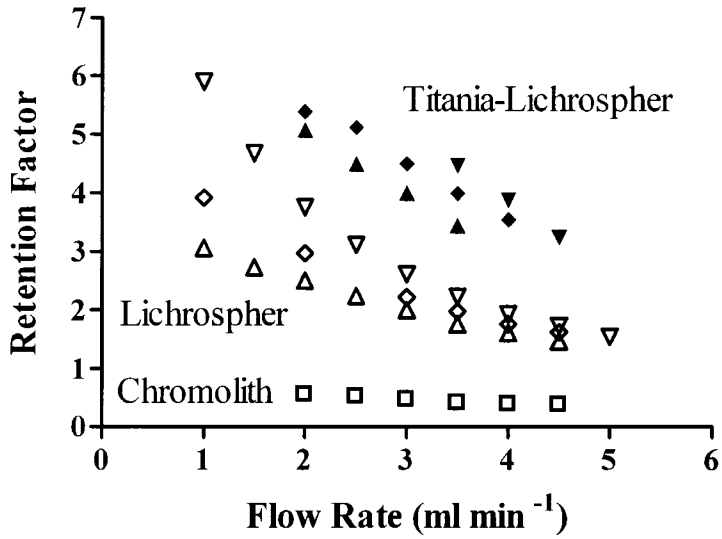

Figure 3-1. Retention of anthracene versus flow rate at 100 bar (▼), 125 bar (♦), and 150 bar (▲) at 35°C on a 15 cm titania-Lichrospher coupled column (closed symbols), 10 cm Lichrospher column (open symbols), and a 10 cm Chromolith column at 150 bar (□). Retention factor RSD was typically less than 1%.

A pressure limit of 300 bar at the pump head prevented flow rates up to the pump's limit of 5.0 ml min^{-1} from being studied. When the flow rate is increased from 2.0 to 4.0 ml min^{-1}, the retention factor for anthracene is reduced 1.6-fold on the Lichrospher column and 1.4-fold on the Chromolith column.

Retention factors decrease with increasing flow rate due to the increased column pressure. At higher flow rates, the pressure drop across the column and connective tubing increases. Because the pressure is controlled downstream, this results in a higher average carbon dioxide density across the column. This produces stronger eluting conditions at higher flow rates.[32] The lower retention factors at higher flow rates reduce both the separation time and resolution.

The Chromolith column produces about a tenth the pressure drop of the Lichrospher column when the pressure drop associated with the injector, connective tubing, and DAD flow cell are subtracted. However, the extra-column backpressure is significantly higher than the Chromolith backpressure. The Chromolith column itself accounts for less than 11% of the total system backpressure. The retention factors on the Chromolith column decrease with increasing flow rate largely due to the increase in the post-column contribution of the extra-column backpressure, rather than the backpressure across the Chromolith column. As will be discussed in Section 3.3.3, lowering the flow rate to 1.0 ml min^{-1} minimized the extra-column backpressure effects.

The elution time of the latest eluting model compound, pyrene, is reduced significantly when shorter columns are used at higher flow rates. At 4.5 ml min^{-1}, pyrene elutes in only 1.0 min on the 10 cm Lichrospher column and in 0.54 min on

the 10 cm Chromolith column at 125 and 150 bar respectively. These are much shorter than the 6.8 min on the conventional 25 cm Lichrospher column using 2.0 ml min^{-1} and 150 bar.

Titania columns provide greater aromatic group-type resolutions than silica, and coupling a titania and silica column together yields higher overall resolution. Thus, to improve group-type resolutions, a short 5 cm bare titania column was coupled to the 10 cm bare silica Lichrospher column. The closed symbols in Figure 3-1 show the retention of anthracene on the titania-Lichrospher coupled column as a function of flow rate. The addition of the titania column makes the titania-Lichrospher coupled column up to twice as retentive for anthracene compared to the Lichrospher column alone. Pyrene elutes in 3.3 min on the 15 cm titania-Lichrospher coupled column at 4.0 ml min^{-1} and 125 bar. This compares to 23.7 min on the previously studied 40 cm titania-Lichrospher coupled column at 2.0 ml min^{-1} and 150 bar.

Overall, the shorter Lichrospher and titania-Lichrospher coupled columns could reduce the retention time of pyrene up to 7-fold compared to conventional length columns run at typical flow rates. The Chromolith column yielded up to a 13-fold lower pyrene retention time compared to the 25 cm Lichrospher column.

3.3.2 Column Efficiency on Packed and Monolithic Columns

Figure 3-2 is a plot of the apparent plate height of anthracene at various flow rates for both the Lichrospher and Chromolith column.

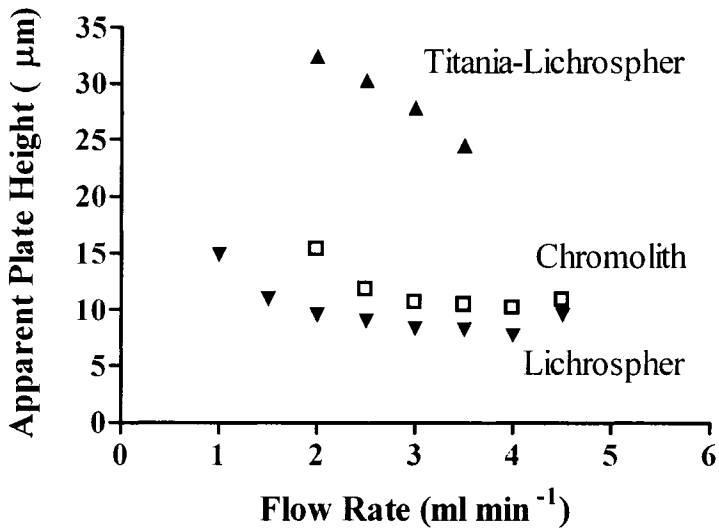

Figure 3-2. Apparent plate height of anthracene versus flow rate on a 15 cm titania-Lichrospher coupled column (▲), 10 cm Chromolith column (□), and a 10 cm Lichrospher column (▼) at 35°C and 150 bar. Apparent plate height RSD was typically less than 6%.

Optimum flow rates for both columns were near 4.0 ml min^{-1}, with the packed Lichrospher column yielding a slightly lower optimum apparent plate height of 8 μm compared to 10 μm on the Chromolith.

The apparent plate heights on the packed Lichrospher column were a few microns lower than on the monolithic Chromolith column for most of the model compounds except naphthalenethiol. This polar compound produced an optimum apparent plate height of 9 μm on the monolithic Chromolith column while it displayed strong tailing and poor efficiency on the packed Lichrospher column. Overall, both columns demonstrate low apparent plate heights and optimum flow rates near the 5.0 ml min^{-1} maximum flow rate of the pump. Therefore, efficiency is not being lost due to slow mass transfer at the highest flow rates achievable.

To achieve significantly faster separation times, some efficiency was sacrificed compared to the results on longer columns (Chapter 2). The apparent efficiency of anthracene is reduced from 22,200 to 10,900 plates when a shorter 10 cm Lichrospher column with 3 μm packing is run at 4.5 ml min^{-1} and 125 bar. These conditions produced the shortest pyrene elution time while maintaining significant resolution and were considered optimal. The apparent efficiency of anthracene on the 10 cm Chromolith column is 9,200 plates at 4.5 ml min^{-1} and 150 bar.

The apparent plate height of anthracene as a function of flow rate on the short titania-Lichrospher coupled column is shown in Figure 3-2. At 2.0 ml min^{-1}, the apparent plate height of anthracene is 32 μm. This improves to 25 μm at 4.0 ml min^{-1}. In Chapter 2, PAH apparent plate heights on titania improved with increasing carbon dioxide density. The apparent plate height of anthracene improves significantly with

increasing flow rate due to the higher average carbon dioxide density at higher flow rates. Similar to the short silica column, the apparent efficiency of anthracene is reduced from 9,000 to 5,200 plates when the shorter 15 cm titania-Lichrospher coupled column is run at 4.0 ml min^{-1} and 125 bar.

3.3.3 Resolution on Packed and Monolithic Columns

Figure 3-3 shows the resolution between the hydrocarbon group-types on the short Lichrospher, Chromolith, and titania-Lichrospher coupled columns. At flow rates higher than 2.0 ml min^{-1}, most group-type resolutions decrease. This is largely due to the decrease in retention factors caused by the higher carbon dioxide density at the higher backpressures. A notable exception is the saturate vs. monoaromatic resolution on the packed columns which has a maximum resolution at 3.5 ml min^{-1} on the Lichrospher column and plateaus at 3.0 ml min^{-1} on the titania-Lichrospher coupled column.

Table 3-1 compares the group-type resolutions for the short packed columns and the Chromolith column with results using longer columns. The short packed Lichrospher and titania-Lichrospher columns produced resolutions 42-51% lower than their longer counterparts. From the discussion of efficiency above, only a 25 to 30% decrease in resolution would be expected. However, some additional loss in resolution occurs due to the lower retention factors at higher flow rates.

Overall the Chromolith column produced the lowest group-type resolutions, due primarily to the low retention of this column. Chromolith columns with higher surface area (mesopore diameters approaching 60 Å) would be required to achieve acceptable resolutions in this application.

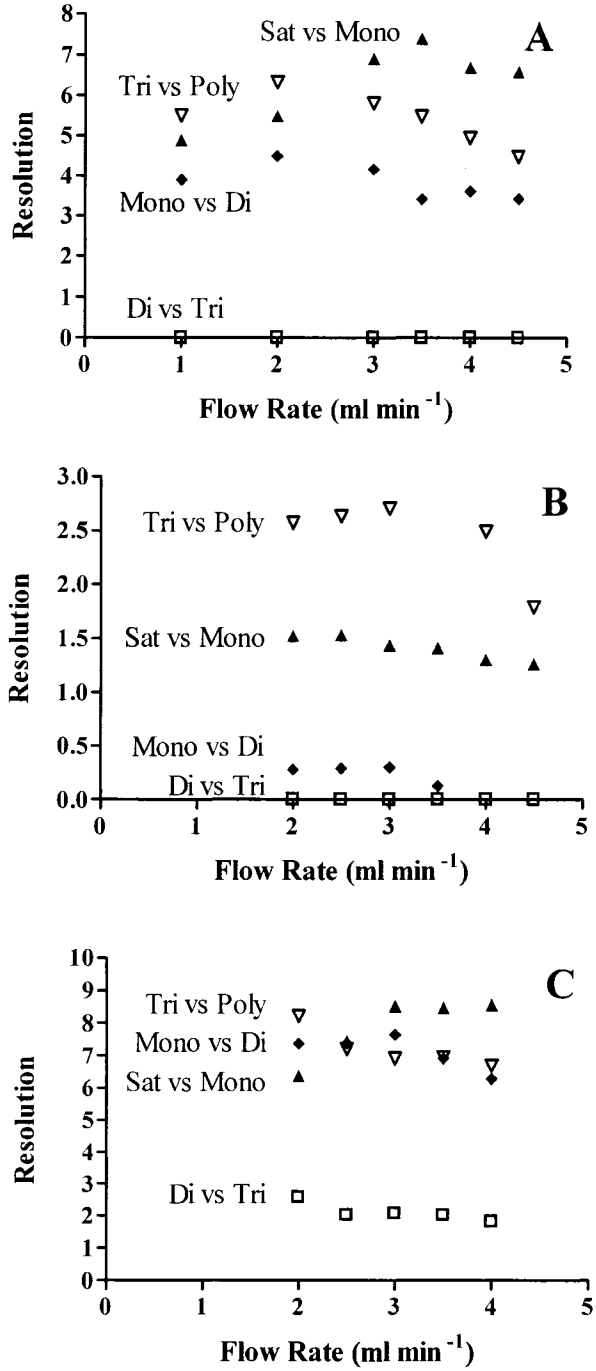

Figure 3-3. Saturate vs. monoaromatic (▲), mono- vs. diaromatic (♦), di- vs. triaromatic (□), and tri- vs. polyaromatic (▽) group-type resolutions versus flow rate at 35°C on (A) a 10 cm Lichrospher column at 125 bar, (B) a 10 cm Chromolith column at 150 bar, and (C) a 15 cm titania-Lichrospher coupled column at 125 bar. Resolution RSD was typically less than 3%.

Table 3-1. Columns tested, group-type resolutions, and pyrene retention times.

Column	Length (x 4.6 mm i.d.)	Diameter, Pore Size	Resolution Sat. vs. Mono.	Mono. vs. Di.	Di. vs. Tri.	Tri. vs. Poly.	Elution Time[a] (min)
Chromolith[b]	100	-	1.3	0	0	1.8	0.54
Three Chromoliths[c,d]	300	-	2.4	0.5	0	2.6	1.7
Short Silica[e]	100	3 μm, 60 Å	6.6	3.4	0	4.5	1.0
Short Titania-Silica[d,f]	150	3 μm, 60 Å	8.6	6.3	1.8	6.7	3.3
Silica Lichrospher[g,h]	250	5 μm, 60 Å	11.6	6.3	0	8.6	6.8
Titania-Lichrospher[d,g,h]	400	3 & 5 μm, 60 Å	14.7	11.9	3.7	12.1	23.7

[a]Based on pyrene retention times
[b]35°C, 150 bar, 4.5 ml min^{-1}
[c]35°C, 150 bar, 4.0 ml min^{-1}
[d]coupled columns
[e]35°C, 125 bar, 4.5 ml min^{-1}
[f]35°C, 125 bar, 4.0 ml min^{-1}
[g]35°C, 150 bar, 2.0 ml min^{-1}
[h]Chapter 2
[i]Chromolith and short silica column resolutions were based on the compounds listed for the HGS column (Figure 2-3).
[j]Short titania-silica coupled column resolutions were based on the compounds listed for the titania-HGS coupled column (Figure 2-3).
[k]Resolution RSD and retention time RSD were typically less than 3% and 0.4% respectively.

Three 10 cm Chromoliths coupled together were studied under various conditions in an effort to achieve higher resolution. The flow rate was varied from 1.0 to 4.0 ml min^{-1} and the pressure from 100 to 200 bar. At 1.0 ml min^{-1}, the extra-column backpressure was insignificant at about 1 bar. This eliminated the lowering of retention by the post-column extra-column backpressure as discussed above. Despite this, the three coupled Chromoliths failed to meet the ASTM method requirements of resolution for the saturates/monoaromatics (4) or the mono-/diaromatics (2) under any of the conditions studied.

3.3.4 Fast Group-Type Analysis of Diesel Samples

The three diesel samples characterized in Chapter 2 were analyzed using the shorter columns at high flow rates. Figure 3-4 shows the light diesel sample separated using the short silica column and the short titania-Lichrospher coupled column under optimal conditions. The integrated FID signal is proportional to hydrocarbon mass. The sudden increases in the UV responses at 254 nm and 300 nm indicate when the monoaromatics and diaromatics begin to elute respectively. The light diesel completely elutes from the short Lichrospher column in 2 min compared to 7 min previously (Figure 2-4A). It elutes from the short titania-Lichrospher coupled column in 3 min compared to 14.5 min previously (Figure 2-4B). The three coupled Chromolith columns eluted the light diesel in 2 min at 4.0 ml min^{-1} and 150 bar (chromatogram not shown), but with inadequate resolution as discussed above.

Figure 3-5 shows a commercial diesel separated in 2 min on the short silica column and 6 min on the titania-Lichrospher coupled column. This compares to 10 min (Figure 2-5A) and 40 min (Figure 2-5B) on the longer columns respectively.

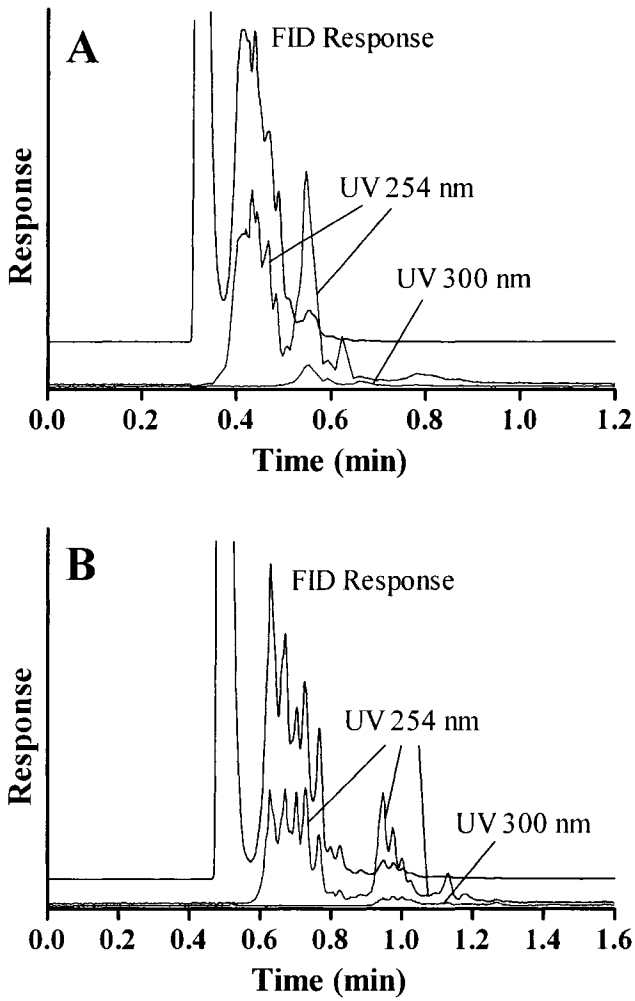

Figure 3-4. FID and UV traces of a Synfuel light diesel separated on (A) a 10 cm Lichrospher silica column at 4.5 ml min^{-1}, 35°C, and 125 bar, and on (B) a 15 cm titania-Lichrospher coupled column at 4.0 ml min^{-1}, 35°C, and 125 bar.

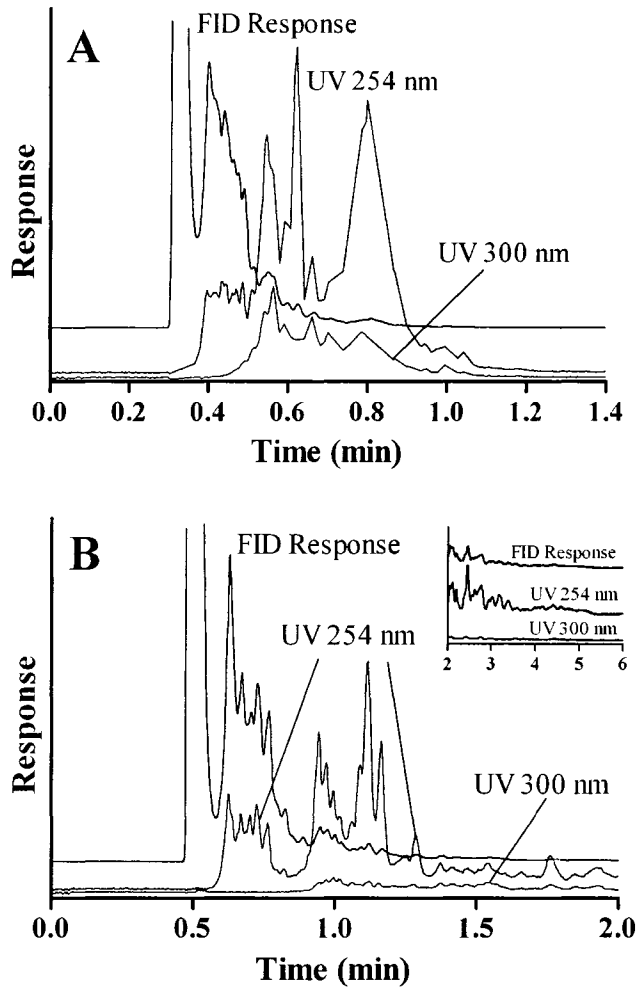

Figure 3-5. FID and UV traces of a commercial Ontario diesel separated on (A) a 10 cm Lichrospher silica column at 4.5 ml min^{-1}, 35°C, and 125 bar, and on (B) a 15 cm titania-Lichrospher coupled column at 4.0 ml min^{-1}, 35°C, and 125 bar.

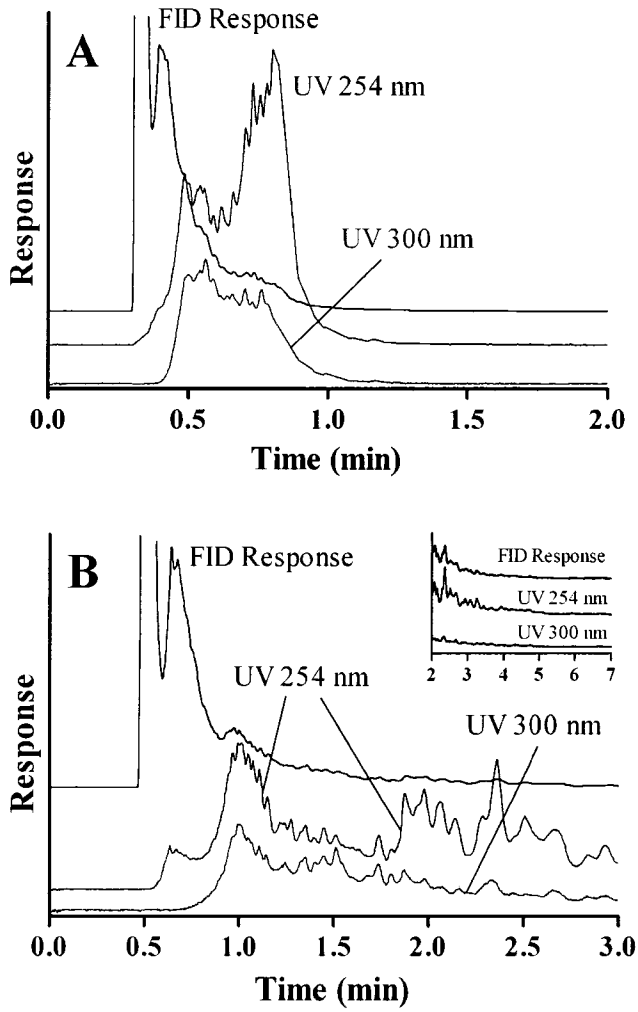

Figure 3-6. FID and UV traces of a diesel blending feedstock separated on (A) a 10 cm Lichrospher silica column at 4.5 ml min^{-1}, 35°C, and 125 bar, and on (B) a 15 cm titania-Lichrospher coupled column at 4.0 ml min^{-1}, 35°C, and 125 bar.

Figure 3-6 shows the heavy diesel blending feedstock separated in 2.5 min on the short silica column and 7 min on the short titania-Lichrospher coupled column. The longer columns require 10 min (Figure 2-6A) and 50 min (Figure 2-6B) for the same separation.

Table 3-2 compares the group-type results from the fast separations to those achieved in Chapter 2. The short packed Lichrospher and titania-Lichrospher columns produce results that compare very favorably with previous results. However, the three coupled Chromolith columns did not yield comparable results for the light diesel sample due to inadequate resolution.

All of the packed column results agree within the ASTM method reproducibility specifications[21] for total aromatic and PAH content with the exception of the short Lichrospher column total aromatic results for the heavy diesel blending feedstock. When the short Lichrospher results are not considered, then the remaining packed column results agree within the reproducibility specifications. This may indicate that for very heavy diesel samples, the 10 cm Lichrospher column may not provide sufficient saturate vs. monoaromatic resolution to achieve comparable results to longer columns. Indeed, the short Lichrospher column monoaromatic and diaromatic results for the heavy diesel blending feedstock displayed the most significant deviations of the packed column results.

Table 3-2. Group-type content of diesel samples reported in mass% (RSD, %)

Sample	Column	Saturates	Mono	Di	Tri	Poly
Synfuel	Chromoliths[a]	62.8 (0.1%)	31.4 (1%)	5.5 (5%)[b]	0.3 (6%)[b]	-
Synfuel	Short Silica	63.0 (0.1%)	35.1 (0.1%)	1.8 (0.9%)[b]	0.14 (25%)[b]	-
Synfuel	Short Ti-Silica	62.9 (0.2%)	35.3 (0.8%)	1.8 (12%)	0.03 (40%)	-
Synfuel	HGS[c]	63.5 (0.1%)	34.7 (0.4%)	1.8 (4%)[b]	0.04 (40%)[b]	-
Synfuel	Ti-HGS[c]	63.5 (0.1%)	34.3 (0.1%)	2.2 (2%)	0.01 (40%)	-
Commercial	Short Silica	69.6 (0.1%)	25.1 (0.2%)	4.5 (0.7%)[b]	0.6 (1%)[b]	0.2 (7%)
Commercial	Short Ti-Silica	69.4 (0.1%)	24.4 (0.3%)	5.3 (0.4%)	0.5 (2%)	0.4 (1%)
Commercial	HGS[c]	70.1 (0.1%)	24.6 (0.2%)	4.7 (0.6%)[b]	0.5 (7%)[b]	0.09 (26%)
Commercial	Ti-HGS[c]	69.8 (0.1%)	23.5 (0.2%)	5.5 (0.6%)	0.6 (6%)	0.6 (9%)
Feedstock	Short Silica	63.2 (0.2%)	24.4 (0.5%)	9.2 (0.2%)[b]	2.1 (0.8%)[b]	1.1 (2%)
Feedstock	Short Ti-Silica	64.0 (0.1%)	20.5 (0.3%)	12.0 (0.6%)	2.2 (2%)	1.3 (2%)
Feedstock	HGS[c]	64.1 (0.1%)	22.7 (0.3%)	11.0 (0.3%)[b]	1.9 (1%)[b]	0.3 (10%)
Feedstock	Ti-HGS[c]	65.6 (0.1%)	19.3 (0.3%)	11.8 (0.2%)	2.0 (0.9%)	1.3 (3%)

[a]Three 10 cm Chromolith bare silica columns coupled in series at 2.0 ml min^{-1}, 35°C, 150 bar.
[b]Silica column results ignore 9,10-dihydroanthracene's (diaromatic) elution after triaromatic model compounds.
[c]Hydrocarbon group separation (HGS) bare silica column and titania-HGS coupled column results (Table 2-3).

3.4 Conclusions

Short packed silica and titania-silica coupled columns achieved 7-fold faster diesel separations than conventional length columns run at typical flow rates, while maintaining more than half of the resolution. Monolithic Chromolith columns achieved 13-fold faster elution times than conventional length packed silica columns run at typical flow rates, but at the expense of significant resolution due to their lower retention. The 15 cm titania-Lichrospher coupled column obtained similar diesel group-type results to much longer columns while reducing the maximum diesel analysis time from 50 min to 7 min.

3.5 References

(1) Chester, T. L.; Pinkston, J. D., *Anal. Chem.* **2002**, *74*, 2801-2812.

(2) Chester, T. L.; Pinkston, J. D., *Anal. Chem.* **2004**, *76*, 4606-4613.

(3) Chester, T. L.; Pinkston, J. D., *Anal. Chem.* **2000**, *72*, 129R-135R.

(4) Honigs, D. E., *Am. Lab.* **1987**, *19*, 48-51.

(5) Wu, N.; Yee, R.; Lee, M. L., *Chromatographia* **2001**, *53*, 197-200.

(6) Cookson, D. J.; Lloyd, C. P.; Smith, B. E., *Energy & Fuels* **1988**, *2*, 854-860.

(7) Cookson, D. J.; Iliopoulos, P.; Smith, B. E., *Fuel* **1995**, *74*, 70-78.

(8) Sato, S.; Sugimoto, Y.; Sakanishi, K.; Saito, I.; Yui, S., *Fuel* **2004**, *83*, 1915-1927.

(9) Sjögren, M.; Li, H.; Rannug, U.; Westerholm, R., *Fuel* **1995**, *74*, 983-989.

(10) de Lucas, A.; Durán, A.; Carmona, M.; Lapuerta, M., *Fuel* **2001**, *80*, 539-548.

(11) Karonis, A.; Lois, E.; Zannikos, F.; Alexandridis, A.; Sarimveis, H., *Energy & Fuels* **2003**, *17*, 1259-1265.

(12) Zannis, T. C.; Hountalas, D. T., *J. Energy Inst.* **2004**, *77*, 16-25.

(13) Ohtsuka, A.; Hashimoto, K.; Akutsu, Y.; Arai, M.; Tamura, M., *J. Jpn. Petrol. Inst.* **2002**, *45*, 24-31.

(14) Li, X.; Gülder, Ö. L., *J. Can. Pet. Technol.* **1998**, *37*, 56-60.

(15) Shimazaki, N.; Tsuchiya, K.; Morinaga, M.; Shibata, M.; Shibata, Y., *SAE Technical Paper* **2002**, *2002-01-2824.*

(16) Mitchell, K., *SAE Technical Paper* **2000**, *2000-01-2890.*

(17) Tanaka, S.; Takizawa, H.; Shimizu, T.; Sanse, K., *SAE Technical Paper* **1998**, *982648.*

(18) Andrews, G. E.; Ishaq, R. B.; Farrar-Khan, J. R.; Shen, Y.; Williams, P. T., *SAE Technical Paper* **1998**, *980527.*

(19) Signer, M.; Heinze, P.; Mercogliano, R.; Stein, H. J., *SAE Technical Paper* **1996**, *961074.*

(20) Mitchell, K.; Steere, D. E.; Taylor, J. A.; Manicom, B.; Fisher, J. E.; Sienicki, E. J.; Chiu, C.; Williams, P. T., *SAE Technical Paper* **1994**, *942053.*

(21) *Method D 5186-03, Annual Book of ASTM Standards*, American Society for Testing and Materials, West Conshohocken, PA, USA, 2003.

(22) Hoke, S. H.; Tomlinson, J. A.; Bolden, R. D.; Morand, K. L.; Pinkston, J. D.; Wehmeyer, K. R., *Anal. Chem.* **2001**, *73*, 3083-3088.

(23) Connolly, D.; Paull, B., *J. Chromatogr. A* **2002**, *953*, 299-303.

(24) Phillips, D. J.; Capparella, M.; Neue, U. D.; El Fallah, Z., *J. Pharm. Biomed. Anal.* **1997**, *15*, 1389-1395.

(25) Gerber, F.; Krummen, M.; Potgeter, H.; Roth, A.; Siffrin, C.; Spoendlin, C., *J. Chromatogr. A* **2004**, *1036*, 127-133.

(26) Wu, N.; Dempsey, J.; Yehl, P. M.; Dovletoglou, A.; Ellison, D.; Wyvratt, J., *Anal. Chim. Acta* **2004**, *523*, 149-156.

(27) Tanaka, N.; Kobayashi, H.; Nakanishi, K.; Minakuchi, H.; Ishizuka, N., *Anal. Chem.* **2001**, *73*, 420A-429A.

(28) Mistry, K.; Grinberg, N., *J. Liq. Chromatogr. Relat. Technol.* **2005**, *28*, 1055-1074.

(29) Cabrera, K.; Lubda, D.; Eggenweiler, H.-M.; Minakuchi, H.; Nakanishi, K., *J. High Resol. Chromatogr.* **2000**, *23*, 93-99.

(30) Hatsis, P.; Lucy, C. A., *Analyst* **2002**, *127*, 451-454.

(31) Murahashi, T., *Analyst* **2003**, *128*, 611-615.

(32) Lesellier, E.; West, C.; Tchapla, A., *J. Chromatogr. A* **2003**, *1018*, 225-232.

CHAPTER FOUR. High Temperature Normal Phase Liquid Chromatography on Bare Zirconia*

4.1 Introduction

In Chapter 2, zirconia and titania exhibited remarkable selectivity for separating aromatics according to aromatic ring number with supercritical fluid chromatography (SFC). One drawback of SFC is that supercritical carbon dioxide is a relatively weak mobile phase compared to those used in normal phase LC. As a result, SFC cannot analyze high boiling oil samples, such as heavy gas oils (boiling range ~350-550°C). However, these samples can be analyzed with normal phase HPLC, typically using mobile phase gradients with hexane and chlorinated solvents. In this chapter, we study the use of elevated temperatures up to 200°C with a thermally stable bare zirconia column to separate aromatic model compounds using a hexane mobile phase.

The benefits of using elevated temperatures in HPLC have recently been reviewed.[1] They include lower mobile phase viscosity and faster diffusion rates. Lower viscosity permits higher flow rates to be used before the pressure limit of the pump is met. Higher diffusion rates move the optimal flow rate of the van Deemter curve to higher values and also flatten the curve at high flow rates.[1,2] These result in better efficiency when operating at relatively high flow rates (mass transfer limited

---

*A version of this chapter will be submitted for publication. Paproski R. E., Liang, C., Lucy C. A., *Journal of Chromatography A* **2007**. R. Paproski co-supervised C. Liang's undergraduate CHEM 403 project on analyte decomposition in high temperature normal phase liquid chromatography (Section 4.3.5).

section of the van Deemter curve). Much faster separations and lower analysis times are thus achieved when elevated temperatures are used with higher flow rates, without sacrificing column efficiency.[1,2]

Elevated temperatures can also be used to decrease retention according to the van't Hoff equation (Equation 4-1).[1]

$$\ln k = \frac{-\Delta H}{RT} + \frac{\Delta S}{R} - \ln \beta \qquad \text{(Equation 4-1)}$$

The retention factor is given by k. ΔH and ΔS are the enthalpy and entropy for the transfer of the analyte from the mobile phase to the stationary phase. R is the gas constant. T is the absolute temperature. β is the phase ratio, equal to void volume of the column divided by the weight of the stationary phase. Changes in selectivity with temperature are possible when there are differences in the enthalpy of different analytes.[1]

While these benefits have been thoroughly documented with reversed phase LC, most studies with normal phase LC were early reports on low efficiency columns[3-13] or open tubular capillary columns.[14-16] These columns are very different from the highly reproducible, commercially prepared, high efficiency columns used in HPLC today. Further, some high temperature normal phase studies employed water saturated mobile phases.[17,18] This can lead to water condensation in detector cells[17] as well as in stationary phase pores,[17,19] resulting in a liquid-liquid partitioning separation mechanism. Normal phase stationary phases studied at elevated temperatures include silicic acid,[3-5,8] magnesium silicate,[3] calcium hydroxide,[4] bare alumina,[6,7] bare silica,[7,9,11-18,20,21] Permaphase ETH (ether bonded silica),[10]

sulphoethyl bonded silica,[14] aminopropyl bonded silica,[14,17,20,22] cyanopropyl bonded silica,[17,18] carbomethoxyethyl bonded silica,[17,18] and diol bonded silica.[23]

In this chapter, the use of elevated temperatures is studied with bare zirconia using carefully dried normal phase solvents. The existing reports of using bare zirconia under normal phase conditions are restricted to near ambient temperatures,[24-33] with some studies using water saturated mobile phases.[26,27] Most of the previous work on normal phase LC at elevated temperatures has focused on temperature's effect on retention, selectivity, and/or efficiency. In addition to these effects, the effect of elevated temperatures on column re-equilibration times following a change in mobile phase and thermal decomposition of a nitrogen containing model compound are also investigated.

4.2 Experimental

4.2.1 Apparatus

A Varian ProStar HPLC system (Varian Palo, Alto, CA) with high pressure mixing was used for all experiments. A schematic of this instrument is shown in Chapter 1 (Figure 1-3), although evaporative light scattering detection (ELSD) was not used in this chapter. Two Varian ProStar 210 pumps provided flow from 0.5 to 6.0 ml min^{-1}. Optima grade hexanes and dichloromethane (Fisher Chemical, Fairlawn, NJ) were pre-dried by adding 50 g of Type 3A, 8-12 mesh, Molecular Sieves (EMD Chemicals, Gibbstown, NJ) directly to a 4 L bottle of solvent at least 24 hours prior to use. Helium used for sparging (<5 ppm water, Praxair, Mississauga, ON) was dried using an in-line Drierite drying tube (W.A. Hammond Drierite Co.

Ltd., Xenia, OH). Open solvent bottles were continuously sparged with dried helium to keep mobile phases free of water, carbon dioxide, and oxygen. The water content in normal phase solvents has a strong effect on retention and efficiency in normal phase LC.[34-36] Carefully dried mobile phases help improve retention time reproducibility.[36] Bare zirconia can adsorb carbon dioxide on its surface.[37,38] The removal of carbon dioxide eliminates atmospheric fluctuations of carbon dioxide as a source of retention time drift. The removal of oxygen reduces the possibility of on-column oxidative reactions involving analytes, the mobile phase, or the stationary phase.

A Varian ProStar 410 Autosampler provided 1 μl sample injections into a 150 × 4.6 mm i.d. column packed with 3 μm zirconia-PHASE particles (Zirchrom Separations Inc., Anoka, MN). A Metalox 200°C High Temperature Column Heater (Quantum Analytics, Foster City, CA) maintained column temperature between 35°C and 200°C. A pre-column heater heated incoming mobile phase. Built-in heat exchangers heated incoming mobile phase while cooling pre-detector effluent. Pre- and post-column thermocouples ensured that axial temperature gradients along the column were within 5°C. Maintaining column temperature gradients within 5°C minimizes thermal mismatch band broadening.[39] Absorbance detection at 254 nm with a 0.1 second rise time was provided by a Knauer Smartline 2500 UV detector (Knauer-ASI, Franklin, MA) using a 2 μl flow cell connected via fiber optic cables. Data acquisition at 20 Hz was provided by Varian Star Chromatography Workstation version 6.20 software. A backpressure regulator was used to apply ~800 psi post-detector pressure to prevent mobile phase boiling at elevated temperatures.

An additional 600 x 0.127 mm i.d. piece of stainless steel tubing submersed in 250 ml of room temperature water was used to cool further the post-column effluent prior to entering the detector cell, as temperature gradients within the detector cell caused significant baseline noise. Figure 4-1 shows how a 7–fold reduction in baseline noise was obtained by using the extra cooling loop with a hexane mobile phase at 200°C and 2.0 ml min^{-1}. Total extra-column volumes including the injector and detector were ~35 μl. Testing confirmed that the addition of the cooling loop did not impact the measured column efficiency for early eluting compounds at 2.0 ml min^{-1}.

4.2.2 Standards and Samples

Twenty five aromatic hydrocarbon model compounds (>90% purity, see Table 4-1) were studied. Model compounds with one to three aromatic rings were dissolved in hexane. Four and five ring model compounds were dissolved in hexane with a minimum amount of dichloromethane or chloroform (Optima grade, Fisher Chemical) added to permit complete dissolution. Carbazole and indole (Sigma-Aldrich, St. Louis, MO) were dissolved in dichloromethane. One ring compounds were prepared at 1.0 mg ml^{-1} and multiple ring compounds were prepared at 0.1 mg ml^{-1}.

4.2.3 Calculations

Retention times and peak widths at half-height were determined using Varian Star Chromatography Workstation version 6.20 software. Retention factors and plate heights were calculated as described in Section 2.2.3. The column void time was based on the baseline deflection observed when an injecton of ACS grade hexane (EMD Chemicals) was made.

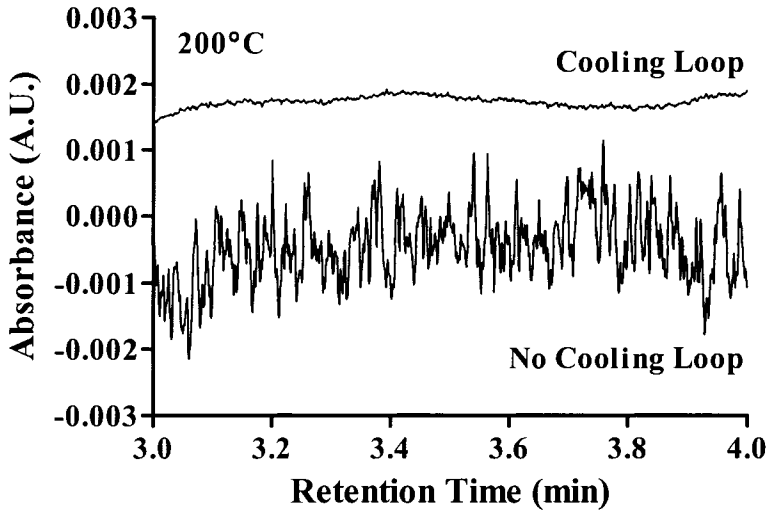

Figure 4-1. Reduction in baseline noise by adding a 600 x 0.127 mm i.d. stainless steel external cooling loop between the column oven outlet and the fiber optic detector cell. Detection at 254 nm. Hexane, 2.0 ml min^{-1}, 200°C.

Table 4-1. Model compounds studied and retention factors with hexane at 2.0 ml min^{-1}.

Compound	Hydrocarbon Group-Type	Retention Factor 35°C	200°C
Toluene[a]	Mono	0.30	0.08
Tetramethylbenzene (1,2,4,5-)[b]	Mono	0.30	0.10
Benzene[c]	Mono	0.27	0.10
n-Butylbenzene[b]	Mono	0.28	0.10
Tetralin[d]	Mono	0.43	0.12
Heptadecylbenzene[b]	Mono	0.15	0.15
Octahydroanthracene (1,2,3,4,5,6,7,8-)[e]	Mono	0.36	0.17
Ethylnaphthalene (2-)[e]	Di	1.88	0.24
Biphenyl[b]	Di, sterically hindered	2.56	0.24
Naphthalene[d]	Di	1.89	0.25
Acenaphthene[b]	Di	2.94	0.30
Dibenzofuran[b]	Di, furan	5.77	0.38
Benzylnaphthalene (1-)[e]	Tri, sterically hindered	5.29	0.43
Fluorene[b]	Di	10.3	0.45
Dibenzothiophene[b]	Di, thiophene	14.1	0.61
Phenanthrene[b]	Tri	20.7	0.67
Phenylanthracene (9-)[b]	Tetra, sterically hindered	10.6	0.69
Anthracene[b]	Tri	22.7	0.72
Dihydrotetracene (5,12-)[b]	Tri	40.4	0.79
Pyrene[b]	Tetra	38.6	1.20
Chrysene[b]	Tetra	I.R.[f]	2.51
Benzanthracene (1,2-)[e]	Tetra	I.R.[f]	2.64
Benzo[A]pyrene[b]	Penta	I.R.[f]	5.04
Perylene[b]	Penta	I.R.[f]	5.09
Dibenzophenanthrene (1,2:7,8-)[e]	Penta	I.R.[f]	11.4

[a]Mallinckrodt Baker, Inc., Phillipsburg, NJ
[b]Sigma-Aldrich, St. Louis, MO
[c]Caledon Laboratories Ltd., Georgetown, ON
[d]Fisher Chemical, Fairlawn, NJ
[e]K&K Laboratories Inc., Carlsbad, CA
[f]Irreversibly retained (k >50)
[g]Retention factor RSD was typically less than 4%.

4.3 Results and Discussion

4.3.1 Effect of Temperature on Retention

Retention for all model compounds decreased with increasing temperature (Table 4-1). This reduction was the most significant for the higher ring number aromatic compounds. Weakly retained compounds such as benzene experienced a less than 3-fold reduction in retention factor (0.27 to 0.10) as temperature was increased from 35°C to 200°C. Meanwhile, strongly retained compounds such as anthracene displayed a more than 30-fold reduction in retention factor (22.7 to 0.72) over the same temperature range. The most highly retained compounds including all five ring compounds were essentially irreversibly retained (k >50) at 35°C. However, these compounds could be eluted within 10 min at 200°C (Table 4-1).

Figure 4-2 shows the van't Hoff plots for a number of representative model compounds. The plots show a certain degree of curvature, which is not unexpected given the heterogenous surface of bare zirconia,[38,40] the multiple enthalpies of different adsorption sites,[41,42] and the general assumptions associated with van't Hoff plots.[41] In addition, others have shown that an adsorbant's surface concentration of both water[13,37,38,40] and polar moderator[7,9,12,19] decrease with increasing temperature. This would cause an increase in the adsorbent's activity with increasing temperature, resulting in higher than expected retention at higher temperatures. This is consistent with the curvature observed here, even though the solvents used were highly anhydrous with no polar moderator added.

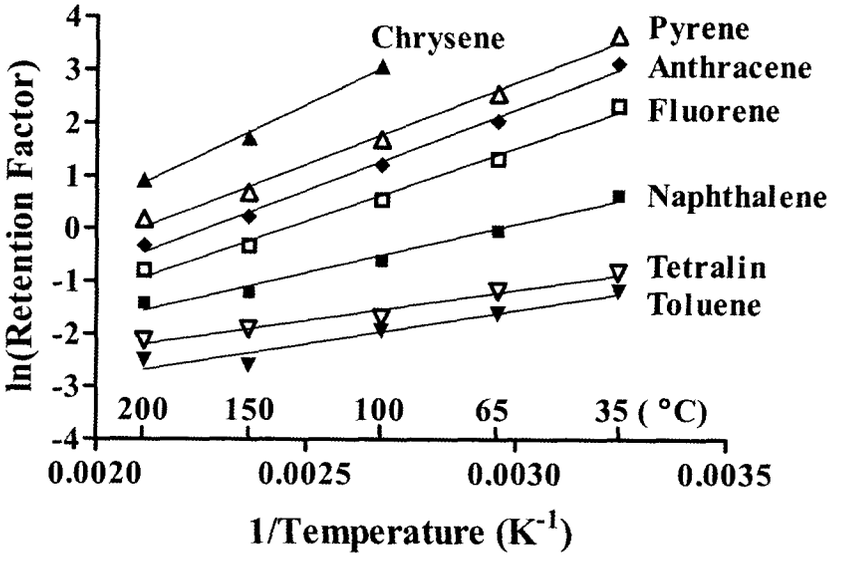

Figure 4-2. Van't Hoff plot for representative model compounds fitted to Equation 4-1. 150 x 4.6 mm i.d., 3 μm, bare zirconia column with a hexane mobile phase at 2.0 ml min^{-1}. Retention factor RSD was typically less than 4%, roughly the size of the data points.

Despite this curvature and the assumptions associated with van't Hoff plots,[41] apparent enthalpies of adsorption, ΔH, can be calculated to illustrate the average enthalpic behavior of each analyte over the temperature range studied. Table 4-2 shows the apparent ΔH for twenty one model compounds. The values range from -6.0 to -33 kJ mol^{-1}, resulting in the sharp changes in retention for the highly retained compounds. For chromatographic systems with comparable ΔS values and phase ratios, ΔH values can be used to compare how much retention factors will decrease with increasing temperature. The normal phase apparent ΔH values compare well with those obtained in reversed phase LC on an octadecylsilane open tubular capilliary (-7.0 to -34 kJ mol^{-1}),[14] carbon-coated zirconia columns (-15 to -23 kJ mol^{-1}),[43] and an octadecylsilane silica column (-8.3 to -31 mol^{-1}),[44] for similar non-polar aromatic hydrocarbons. This shows that comparable decreases in retention are obtained when increasing temperature in both normal phase and reversed phase HPLC.

4.3.2 Group-Type Selectivity

Bare zirconia was found to possess exceptional selectivity for separating aromatics according to ring number in SFC (Chapter 2). This high group-type selectivity is also observed here (Table 4-1) and is ascribed to the presence of Lewis acid sites on zirconia's surface. The strength of this adsorption is expected to be proportional to the number of analyte π-electrons. Figure 4-3 demonstrates the linear relationship between the number of analyte π-electrons and apparent ΔH for planar aromatic compounds. The slope of this plot gives an average apparent $\Delta H_{\pi\text{-electron}}$ of (-2.0 ± 0.1) kJ mol^{-1} for each π-electron.

Table 4-2. Apparent ΔH and (ΔS/R - lnβ) determined from van't Hoff plots with a hexane mobile phase at 2.0 ml min^{-1}. Standard deviations are shown in brackets.

Compound	Hydrocarbon Group-Type	π Electrons	Apparent ΔH (kJ mol^{-1})	(ΔS/R - lnβ)	R^2
Toluene	Mono	6	-10.6 (1.6)	-5.4 (0.5)	0.935
Tetramethylbenzene (1,2,4,5-)	Mono	6	-9.5 (1.7)	-5.0 (0.5)	0.913
Benzene	Mono	6	-8.4 (2.0)	-4.7 (0.7)	0.853
n-Butylbenzene	Mono	6	-8.0 (1.9)	-4.5 (0.6)	0.860
Tetralin	Mono	6	-9.6 (1.0)	-4.6 (0.3)	0.971
Octahydroanthracene (1,2,3,4,5,6,7,8-)	Mono	6	-6.0 (2.1)	-3.5 (0.7)	0.725
Ethylnaphthalene (2-)	Di	10	-15.4 (1.2)	-5.5 (0.4)	0.981
Biphenyl	Di, sterically hindered	12	-17.7 (1.1)	-6.0 (0.4)	0.988
Naphthalene	Di	10	-15.3 (1.2)	-5.5 (0.4)	0.980
Acenaphthene	Di	10	-16.8 (0.9)	-5.6 (0.3)	0.992
Dibenzofuran	Di, furan	12	-20.3 (1.3)	-6.3 (0.4)	0.988
Benzylnaphthalene (1-)	Tri, sterically hindered	16	-18.6 (1.1)	-5.7 (0.3)	0.990
Fluorene	Di	12	-23.0 (1.3)	-6.8 (0.4)	0.991
Dibenzothiophene	Di, thiophene	12	-23.3 (1.3)	-6.6 (0.4)	0.991
Phenanthrene	Tri	14	-25.4 (1.3)	-7.0 (0.4)	0.992
Phenylanthracene (9-)	Tetra, sterically hindered	20	-20.3 (1.3)	-5.7 (0.4)	0.988
Anthracene	Tri	14	-25.4 (1.1)	-6.9 (0.4)	0.994
Dihydrotetracene (5,12-)	Tri	16	-29.2 (1.4)	-7.8 (0.4)	0.994
Pyrene	Tetra	16	-25.7 (1.4)	-6.5 (0.4)	0.992
Chrysene	Tetra	18	-31.7 (2.3)	-7.2 (0.7)	0.995
Benzanthracene (1,2-)	Tetra	18	-33.2 (2.2)	-7.5 (0.6)	0.996

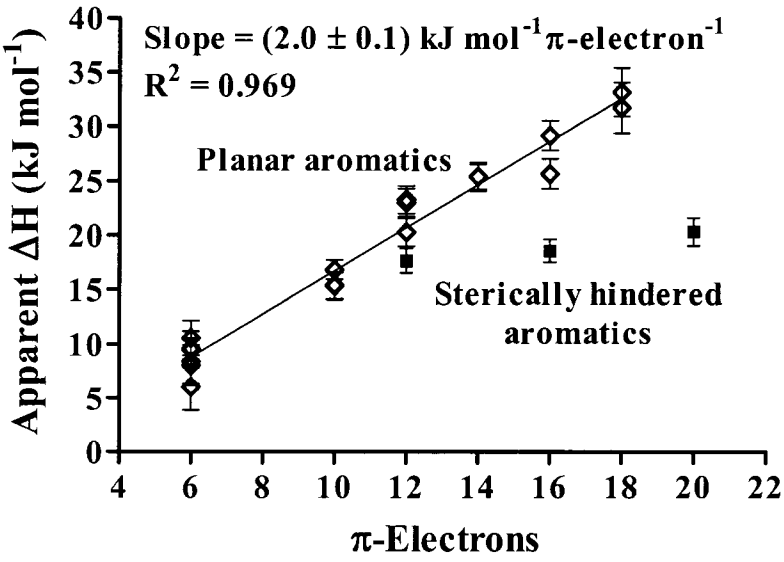

Figure 4-3. Linear relationship between the calculated apparent enthalpies of adsorption and the number of π-electrons for planar aromatic model compounds. Same conditions as Figure 4-2.

This compares with a range of -1.0 to -2.2 kJ mol^{-1} per π-electron for linear aromatic hydrocarbons in reversed phase HPLC.[45] Despite different retention mechanisms between normal phase and reversed phase HPLC, similar apparent $\Delta H_{\pi\text{-electron}}$ were obtained. The three compounds in Figure 4-3 that did not follow this trend were biphenyl, benzylnaphthalene, and phenylanthracene. These compounds possess an aromatic ring with some rotational freedom that inhibits the molecule from adopting a planar structure for ideal surface adsorption. Solid surface-adsorption based stationary phases are known to exhibit such shape selectivity.[46-48] This results in lower than expected apparent ΔH as well as lower overall retention.

Two of these sterically hindered compounds were also not separated according to their ring number compared to other model compounds (Table 4-1). The degree to which these compounds overlapped with smaller aromatic ring group-types was reduced by increasing temperature. Figure 4-4 shows the van't Hoff plot of compounds of different ring number that underwent a change in elution order at elevated temperatures. In all cases, the change in elution order resulted in a larger ring number compound eluting later than a smaller ring number compound as the temperature is increased. Hence, improvements in the aromatic group-type separation selectivity were obtained at higher temperatures. However, even at 200°C, phenylanthracene (tetraaromatic) was still eluting with three ring compounds and benzylnaphthalene (triaromatic) was still eluting with two ring compounds. While higher temperatures could not be explored here due to limitations of our oven, others have assembled home-built instruments capable of temperatures as high as 370°C.[49]

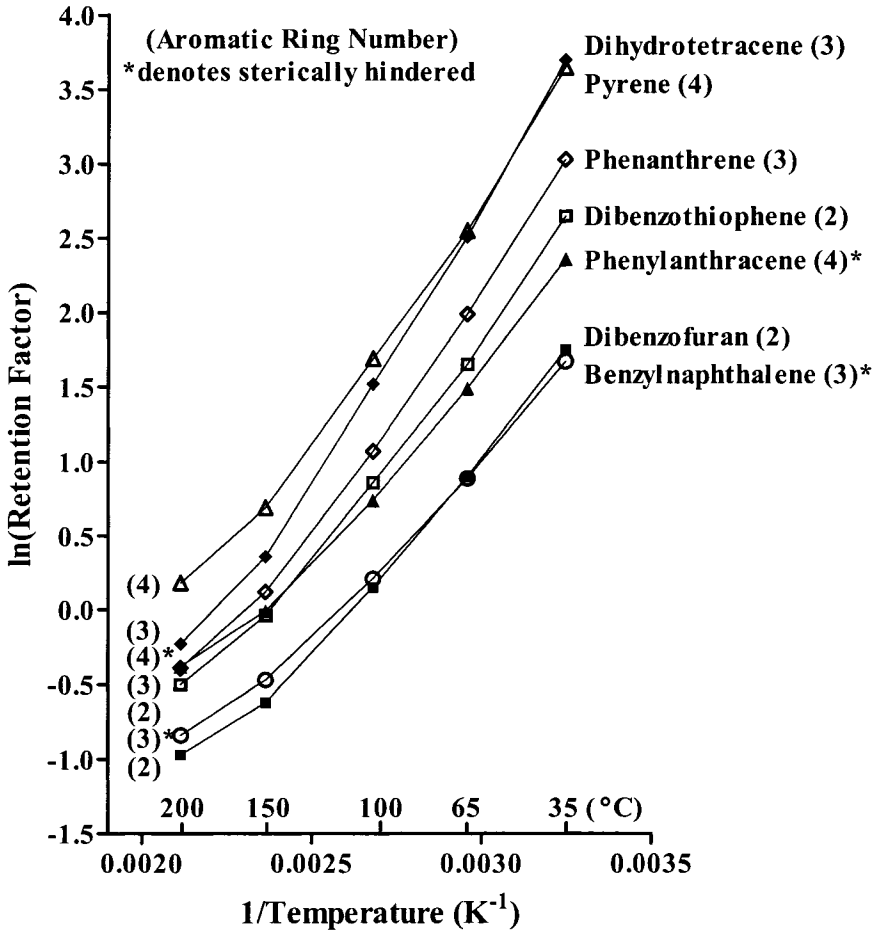

Figure 4-4. Van't Hoff plot of analytes with different aromatic ring numbers that change elution order at elevated temperatures. Aromatic ring numbers are shown in brackets. Same conditions as Figure 4-2. Retention factor RSD was typically less than 4%.

At temperatures and pressures above 234°C and 30 bar (437 psi), hexane becomes a supercritical fluid. Under these conditions, this technique would be defined as supercritical fluid chromatography rather than high temperature HPLC.

4.3.3 Effect of Temperature on Efficiency

Large improvements in both peak shape and plate height were observed at elevated temperatures for moderately and highly retained compounds. Figure 4-5 demonstrates this effect for anthracene. At 35°C, anthracene displays significant tailing along with poor efficiency. At temperatures up to 200°C, peak symmetry and efficiency are markedly improved.

Figure 4-6 shows the plate heights for a representative set of model compounds as a function of temperature. Figure 4-6A shows that under these conditions, monoaromatic compounds have optimal plate heights around 100°C. Figure 4-6B and 4-6C show that plate heights for moderately and highly retained compounds continually improve up to the instrumental limit of 200°C, where reasonable plate heights of less than 35 μm are obtained. While these improvements are very significant, it should be noted that a 3-fold reduction in anthracene concentration at 35°C resulted in a 25% improvement in plate height. Meanwhile, at 200°C, a 30-fold reduction in concentration resulted in less than a 4% improvement in plate height. This indicates that at 35°C analyte concentration is exceeding the linear portion of the adsorption isotherm. At 35°C, isotherm non-linearity for anthracene was found to extend to concentrations approaching the detection limit.

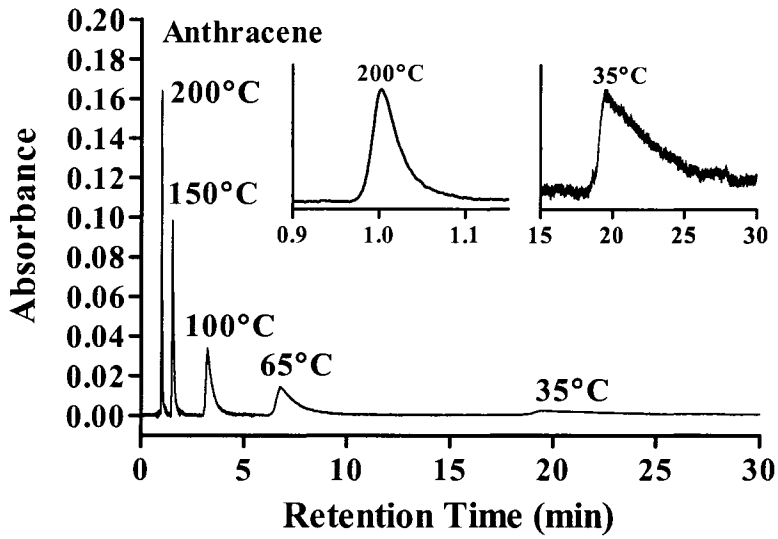

Figure 4-5. Multiple chromatograms of anthracene compiled to demonstrate improved peak shape and efficiency with increasing temperatures up to 200°C. Same conditions as Figure 4-2.

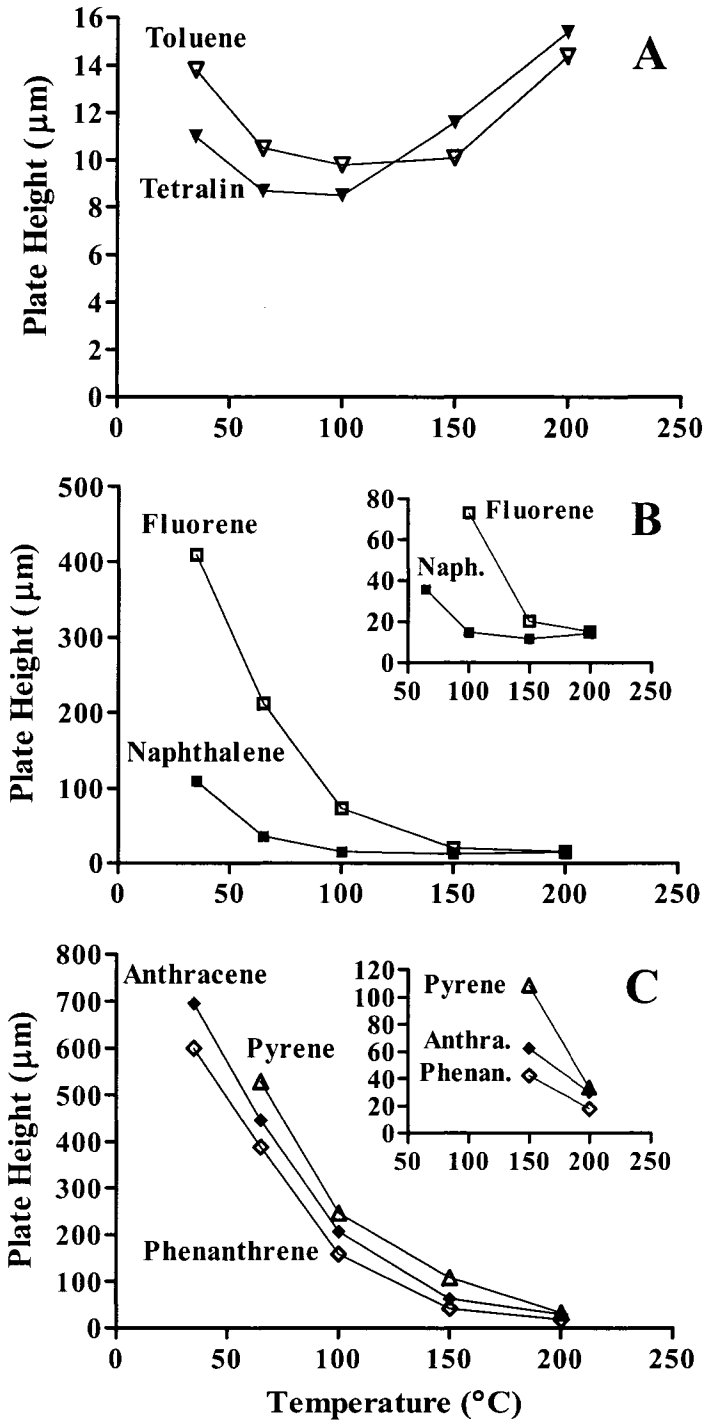

Figure 4-6. Plate height versus temperature for (A) weakly retained monoaromatic compounds, (B) moderately retained diaromatic compounds, and (C) highly retained tri- and tetraaromatic compounds. Same conditions as Figure 4-2. Plate height RSD was typically less than 6%.

This suggests that retention for highly retained compounds is influenced by a small number of highly energetic adsorption sites that are easily overloaded.[50] By increasing temperature, the retention factor is decreased which results in a lower number of adsorbed analytes, and thus less overload. This is the reason for a significant proportion of the improvement in plate height observed here.

Sufficient dichloromethane (17% v/v) was added to the hexane mobile phase at 35°C to mimic the reduction in retention factor observed at 200°C. This removed the effect of retention factor on the observed plate height improvement. As a result, anthracene's efficiency increased 2.2-fold at 200°C compared to 35°C at the same retention factor. This represents the improvement in efficiency that is provided by the increased temperature itself through improved mass transfer and faster desorption kinetics.

Figure 4-7A shows the van Deemter curves for weakly retained butylbenzene at 35°C, 100°C, and 200°C. The maximum reliable operating pressure of most HPLC instruments is 4000 psi. Given the lower mobile phase viscosity at higher temperatures, nearly double the flow rate could be used at 200°C versus 35°C without exceeding 4000 psi of backpressure. Also, a 40% increase in the optimal linear velocity was obtained at 200°C based on the minimum in the van Deemter curve fits (1.3 ml min^{-1} at 35°C versus 1.8 ml min^{-1} at 200°C). While these results represent a significant gain in separation speed, an 80% increase in the minimum plate height was also observed at 200°C compared to 35°C (14.5 μm versus 8.1 μm). A negligible increase in plate height was observed at 100°C compared to 35°C.

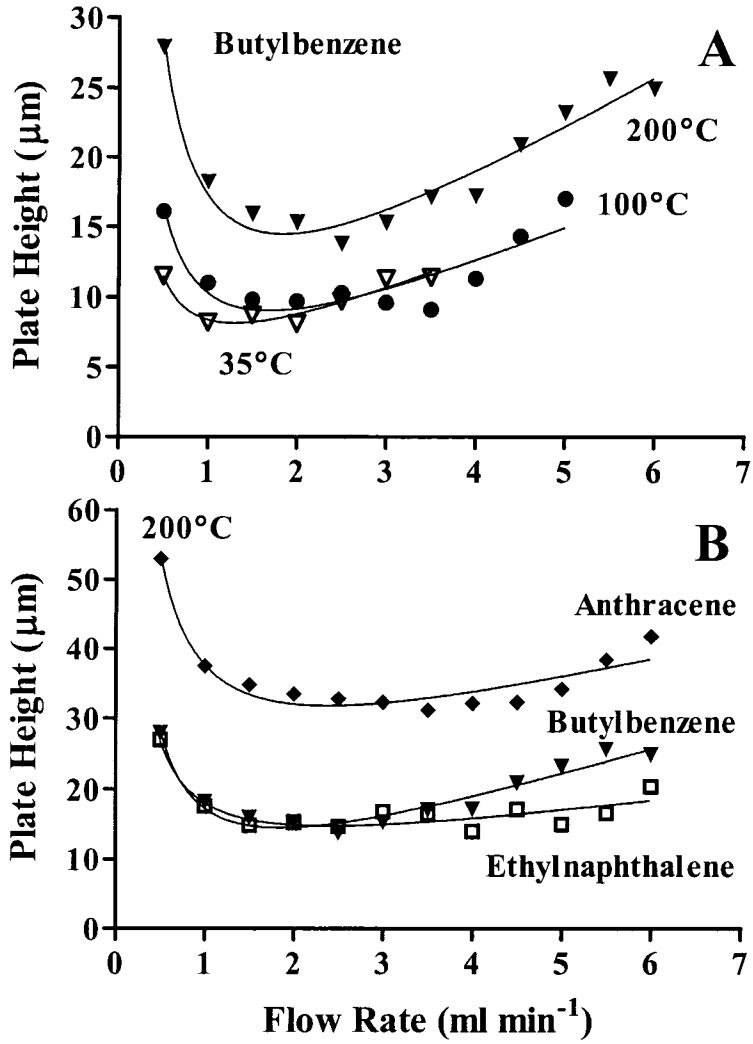

Figure 4-7. Plate height versus flow rate for (A) weakly retained butylbenzene at 35°C and 200°C, and (B) weakly retained butylbenzene, moderately retained ethylnaphthalene, and highly retained anthracene at 200°C. Same conditions as Figure 4-2 except flow rate which was altered between 0.5 to 6.0 ml min^{-1}. Plate height RSD was typically less than 6%.

This represents a loss of efficiency for weakly retained compounds when the temperature is increased above 100°C.

Figure 4-7B compares the van Deemter behavior of weakly retained butylbenzene, moderately retained ethylnaphthalene, and highly retained anthracene at 200°C. The more retained compounds both exhibit very flat van Deemter curves up to 5.0 ml min^{-1}. This flat behavior at high flow rates is an expected benefit of elevated temperatures in HPLC due to the improvements in mass transfer at elevated temperatures.[1,2] The flattened van Deemter curves permit significant increases in flow rate without sacrificing column efficiency due to slow mass transfer. At 200°C, the relatively higher slope for butylbenzene compared to ethylnaphthalene at high flow rates suggests that extra-column band broadening is beginning to limit column efficiency for weakly retained compounds. Another possible cause for the increased van Deemter slope of weakly retained compounds is a limited detector rise time.[51] A rise time of 0.1 second is the limit for most HPLC detectors.

Overall, by increasing the temperature from 35°C to 200°C and the flow rate from 2.0 ml min^{-1} to 6.0 ml min^{-1}, tetraaromatic pyrene's elution time was decreased from 32.6 min to less than 0.5 min. Under these conditions, pyrene's plate height was only 28 μm.

4.3.4 Column Re-Equilibration Time

In gradient elution separations, a significant portion of the overall analysis time can be the time necessary to re-equilibrate the column to the initial weak eluent conditions. It has been shown that re-equilibration times in reversed phase HPLC are not significantly improved by increasing temperature,[52] unless the initial mobile

phase contains less than 10% organic modifier.[53] In normal phase HPLC, larger differences in a mobile phase's affinity for the surface can result in slow desorption kinetics and long re-equilibration times when trying to replace a strong solvent with a relatively weak solvent. Weak solvents compete poorly for the high energy active stationary phase sites. Re-equilibration times as high as 12 hours have been reported in normal phase HPLC.[7-9,19,54] Meyer[55] reported an exception to the commonly observed long re-equilibration times in normal phase HPLC. Fast equilibration times of only a few minutes were reported with hexane and dichloromethane mobile phases on bare silica, despite having not taken any measures to control the water content of either solvent.[55]

To determine the effect of column temperature on equilibration time in normal phase HPLC, the bare zirconia column was equilibrated with the strong eluent dichloromethane. The eluent was then switched to the weak eluent hexane and replicate injections of analytes were performed. Figure 4-8 shows the changes in analyte retention as the column re-equilibrates to the weak eluent. Clearly the equilibration proceeds more quickly at 200°C versus 35°C. Improvements in equilibration time were greater than 5-fold as the column was stabilized in less than 4 min at 200°C compared to 21 min at 35°C. This makes using mobile phase gradients at elevated temperatures more attractive due to the decreased time required to equilibrate the column.

When replacing ethyl acetate, a stronger eluent than dichloromethane, with hexane, retention did not stabilize within 60 min at 35°C or 200°C.

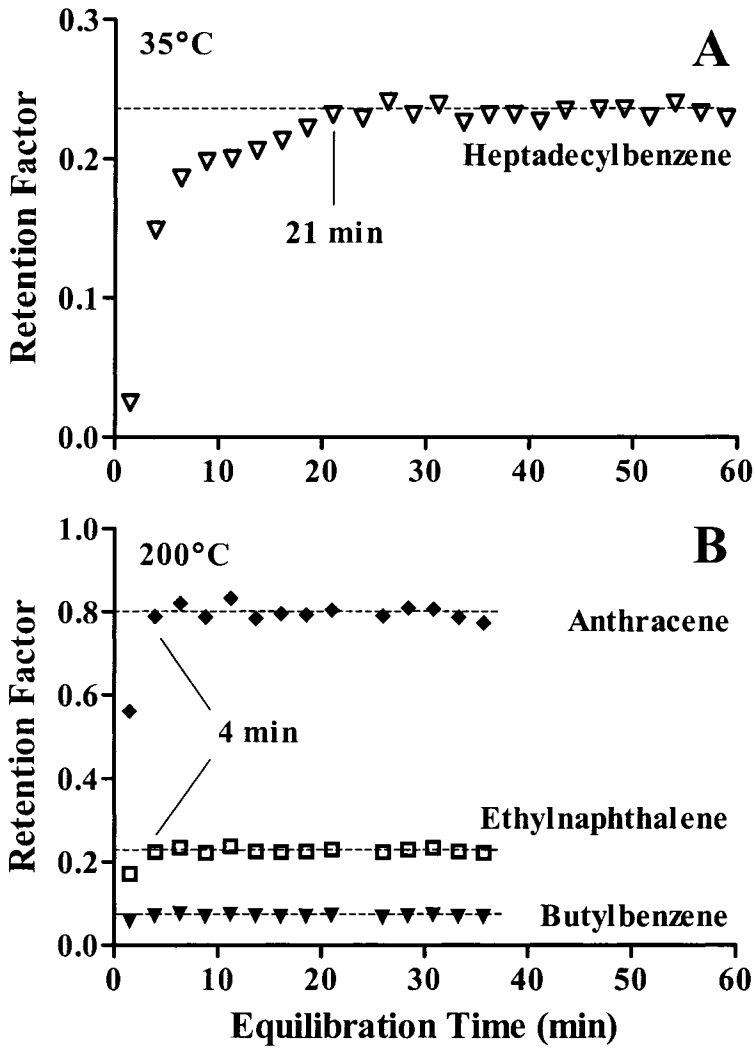

Figure 4-8. Retention factor versus equilibration time. Mobile phase switched immediately to hexane following a rinse with 100 column volumes of dichloromethane (A) at 35°C and (B) at 200°C. Same conditions as Figure 4-2. Retention factor RSD was typically less than 4%.

After 60 min of flushing with hexane, retention factors at both temperatures were between 1.9 and 3.8-fold lower compared to before flushing the column with ethyl acetate. This suggests that residual ethyl acetate remains bound to the stationary phase. Similar experiments replacing isopropanol, the strongest normal phase eluent studied here, with hexane at 35°C and 200°C revealed that the retention does not stabilize within 12 hours. This is not surprising as the time required for column equilibration is proportional to the retention time of the strong eluent being replaced.[9]

As discussed in Section 5.3.5, alcohols could not be eluted from bare zirconia with dichloromethane at 35°C. As a result, we would expect very long equilibration times when replacing relatively polar solvents such as ethyl acetate or isopropanol with hexane. It is clear that elevated temperatures can significantly reduce column re-equilibration times in normal phase HPLC. However, the use of elevated temperatures cannot replace the practice of removing very strong mobile phases with several progressively weaker mobile phases, as opposed to switching directly to a weak mobile phase. Although not studied here, elevated temperatures would be expected to speed up column re-equilibration when switching between three or more solvents.

4.3.5 Thermal Decomposition of Carbazole*

While studying the elution of polar sulfur, nitrogen, and oxygen compounds from zirconia (see Section 5.3.5), two nitrogen compounds, indole and carbazole, were observed to undergo thermal decomposition at temperatures above 100°C in a

*Performed by undergraduate Chen Liang for CHEM 403 under my supervision.

mixed 75:25 hexane and dichloromethane mobile phase. Both carbazole and indole yielded reduced peak areas with increasing column temperature.

On-column decomposition has previously been reported in HPLC, including the decomposition of sugars with normal phase HPLC[56] and pharmaceuticals with reversed phase HPLC.[57] The most common types of on-column reactions are hydrolysis, oxidation, isomerization, and epimerization.[57] Regardless of the type of reaction, such on column reactions are undesirable if they alter the analyte response (as noted above).[57] They can also complicate the separations by generating additional broad peaks. Thus, studies were performed to characterize this decomposition behavior.

Figure 4-9 shows chromatograms for carbazole from 35°C to 160°C. The peak area for carbazole decreases 10-fold as the column temperature is increased to 160°C. A decomposition product peak at lower retention times also becomes more prevalent as the column temperature is increased. Varying carbazole concentration revealed that the initial reaction rate is directly proportional to carbazole concentration (Figure 4-10), suggesting first order kinetics:

$$-\frac{d[A]}{dt} = k_R[A] \qquad \text{(Equation 4-2)}$$

where $[A]$ is the concentration of the reactant, t is reaction time, and k_R is the rate constant.

Alternately the decomposition kinetics can be studied by altering the reaction time, which can be conveniently achieved by varying the flow rate. Figure 4-11 presents the first order kinetic plots based on the integrated first order rate equation:

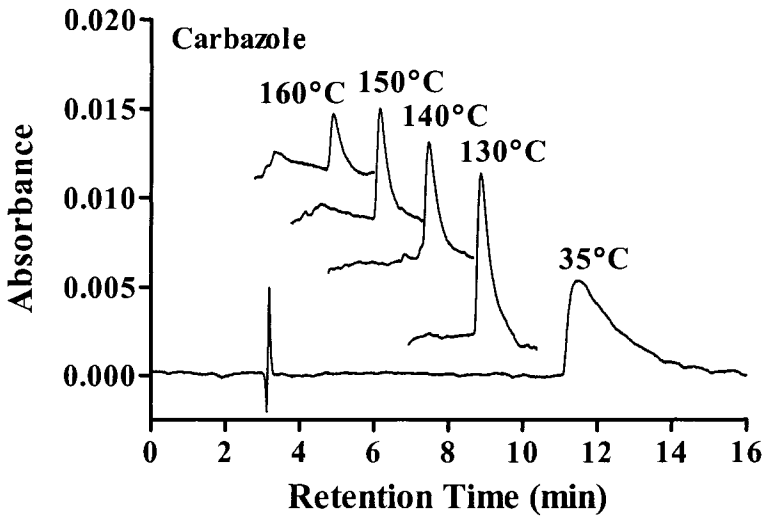

Figure 4-9. Thermal decomposition of carbazole as a function of temperature. Conditions: 75% hexane, 25% dichloromethane, 2.0 ml min^{-1}. Chromatographic traces at elevated temperature are offset in both the x- and y-direction for clarity.

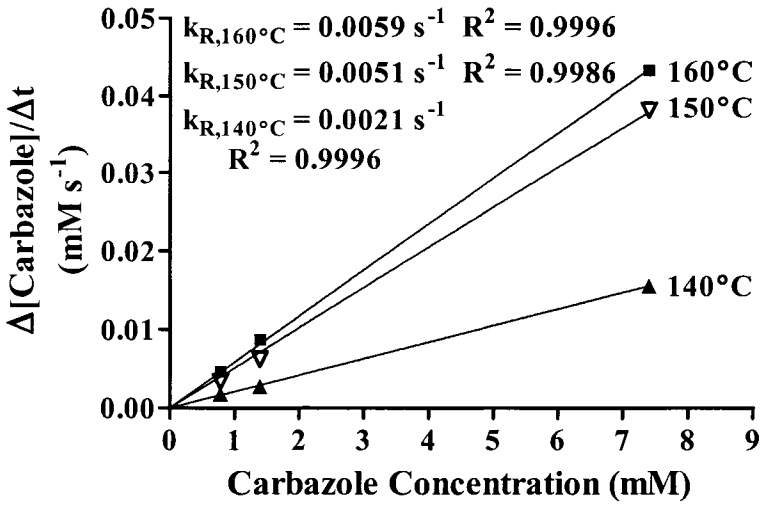

Figure 4-10. Rate of decomposition of carbazole versus carbazole concentration. Mobile phase: 75% hexane, 25% dichloromethane. Plotted rates of decomposition are the average of the rates from data collected at 1.0, 1.5, and 2.0 ml min^{-1} at each specified temperature and carbazole concentration. Rate constant, k_R, determined from the slope. Rate constant standard deviations were less than 0.0001 s^{-1}.

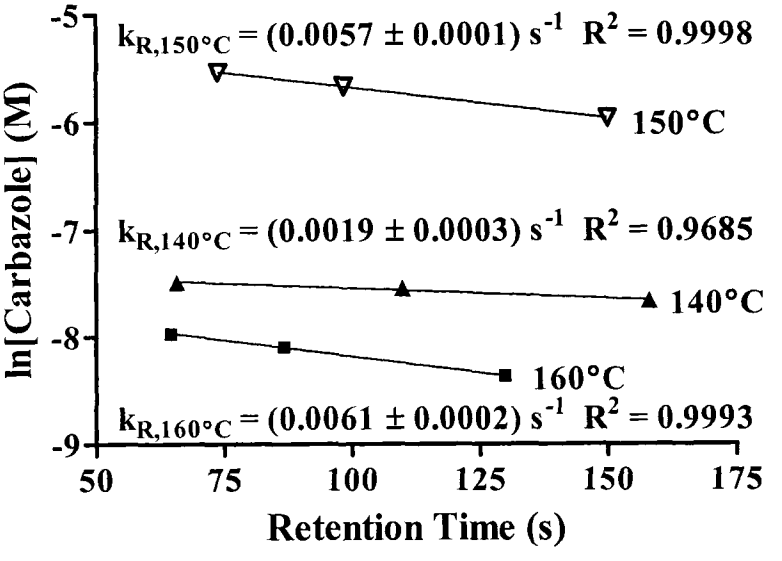

Figure 4-11. Natural logarithm of carbazole concentration versus retention time. Mobile phase: 75% hexane, 25% dichloromethane. Flow rate varied at 1.0, 1.5, and 2.0 ml min^{-1} to alter retention time. Rate constant, k_R, determined from the slope.

$$\ln[A] = -k_R t + Const \qquad \text{(Equation 4-3)}$$

where *Const* is a constant. The plots in Figure 4-11 are reasonably linear, further supporting first order kinetics according to Equation 4-3. Rate constants determined from the slopes of Figure 4-10 and Figure 4-11 yield similar values.

In an effort to identify the decomposition products, a highly concentrated 0.1 g ml^{-1} sample of carbazole was injected using a large 100 µl injection loop at 150°C. Fractions containing the decomposition products were collected and analyzed by mass spectrometry. Several peaks could not be identified. The identified compounds were: naphthalene, biphenyl, 9-methylene-fluorene, methylcarbazole, carbazole, and dichlorodiphenylmethane. However, the first two compounds were observed from fractions collected at 35°C where no decomposition would be expected. Of the remaining compounds detected by GC-MS, a chlorinated decomposition product (dichlorodiphenylmethane) was detected. This suggests involvement of the dichloromethane in the mobile phase within the decomposition mechanism. Preliminary studies using chloroform demonstrated much less decomposition when chloroform was used, further corroborating the involvement of dichloromethane within the decomposition. Further studies would be necessary to fully characterize this behavior.

Regardless, of the thiols, sulfides, thiophenes, pyrroles, furans, ethers, ketones, and esters studied in Chapter 5 and eluted successfully from zirconia, only the two pyrrole compounds showed clear signs of thermal decomposition. Further, preliminary studies suggest that simple modifications of the eluent can suppress this

decomposition. This demonstrates how high temperature normal phase HPLC can be used with a wide variety of non-polar and polar aromatic compounds, with only a few cases where thermal decomposition becomes an issue at temperatures in excess of 100°C.

4.4 Conclusions

The use of elevated temperatures in normal phase HPLC shows considerable promise. Faster elution times, improved peaks shapes, higher efficiency, improved group-type selectivity, and faster re-equilibration times have been demonstrated using a dried hexane mobile phase on a temperature stable bare zirconia column. Bare zirconia shows good group-type selectivity for aromatic compounds in normal phase HPLC as well as SFC as shown in Chapter 2. On-column decomposition was observed for two pyrrole compounds at temperatures above 100°C. However, this decomposition could be minimized by using a chloroform mobile phase instead of dichloromethane, by increasing flow rate, or by limiting column temperature to below 100°C.

4.5 References

(1) Greibrokk, T.; Andersen, T., *J. Chromatogr. A* **2003**, *1000*, 743-755.

(2) Cabooter, D.; Heinisch, S.; Rocca, J. L.; Clicq, D.; Desmet, G., *J. Chromatogr. A* **2007**, *1143*, 121-133.

(3) Strain, H. H., *Ind. Eng. Chem.* **1946**, *18*, 605-609.

(4) LeRosen, A. L.; Rivet, C. A., *Anal. Chem.* **1948**, *20*, 1093-1094.

(5) Chang, L. T., *Anal. Chem.* **1953**, *25*, 1235-1237.

(6) Engelhardt, H., *J. Chromatogr.* **1966**, *21*, 228-238.

(7) Scott, R. P. W.; Lawrence, J. G., *J. Chromatogr. Sci.* **1969**, *7*, 65-71.

(8) Maggs, R. J., *J. Chromatogr. Sci.* **1969**, *7*, 145-151.

(9) Scott, R. P. W.; Lawrence, J. G., *J. Chromatogr. Sci.* **1970**, *8*, 619-624.

(10) Knox, J. H.; Vasvari, G., *J. Chromatogr.* **1973**, *83*, 181-194.

(11) Engelhardt, H., *Z. Anal. Chem.* **1975**, *277*, 267-274.

(12) Kourilova, D.; Krejci, M., *J. Chromatogr.* **1977**, *138*, 329-336.

(13) Kowalczyk, J. S.; Herbut, G., *J. Chromatogr.* **1980**, *196*, 11-20.

(14) Takeuchi, T.; Kumaki, M.; Ishii, D., *J. Chromatogr.* **1982**, *235*, 309-322.

(15) Liu, G.; Djordjevic, N. M.; Erni, F., *J. Chromatogr.* **1992**, *598*, 153-158.

(16) Ryan, K.; Djordjevic, N. M.; Erni, F., *J. Liq. Chromatogr. Relat. Technol.* **1996**, *19*, 2089-2099.

(17) Sisco, W. R.; Gilpin, R. K., *J. Chromatogr. Sci.* **1980**, *18*, 41-45.

(18) Gilpin, R. K.; Sisco, W. R., *J. Chromatogr.* **1980**, *194*, 285-295.

(19) Engelhardt, H., *J. Chromatogr. Sci.* **1977**, *15*, 380-384.

(20) Teramachi, S.; Matsumoto, H.; Kawai, T., *J. Chromatogr. A* **2005**, *1100*, 40-44.

(21) Vanhoenacker, G.; Sandra, P., *J. Chromatogr. A* **2005**, *1082*, 193-202.

(22) Cho, D.; Park, S.; Hong, J.; Chang, T., *J. Chromatogr. A* **2003**, *986*, 191-198.

(23) Im, K.; Park, H.-W.; Kim, Y.; Chung, B.; Ree, M.; Chang, T., *Anal. Chem.* **2007**, *79*, 1067-1072.

(24) Trudinger, U.; Muller, G.; Unger, K. K., *J. Chromatogr.* **1990**, *535*, 111-125.

(25) Whitman, D. A.; Weber, T. P.; Blackwell, J. A., *J. Chromatogr. A* **1995**, *691*, 205-212.

(26) Grün, M.; Kurganov, A. A.; Schacht, S.; Schüth, F.; Unger, K. K., *J. Chromatogr. A* **1996**, *740*, 1-9.

(27) Kurganov, A.; Trüdinger, U.; Isaeva, T.; Unger, K., *Chromatographia* **1996**, *42*, 217-222.

(28) Zhang, Q.-H.; Feng, Y.-Q.; Da, S.-L., *Anal. Sci.* **1999**, *15*, 767-772.

(29) Zhang, Q.-H.; Feng, Y.-Q.; Da, S.-L., *Chromatographia* **1999**, *50*, 654-660.

(30) Winkler, J.; Marmé, S., *J. Chromatogr. A* **2000**, *888*, 51-62.

(31) Shalliker, R. A.; Rizk, M.; Stocksiek, C.; Sweeney, A. P., *J. Liq. Chromatogr. Relat. Technol.* **2002**, *25*, 561-572.

(32) Xiang, D.; Tang, L.; Blackwell, J. A., *J. Chromatogr. A* **2002**, *953*, 67-77.

(33) Zhang, Q.-H.; Feng, Y.-Q.; Da, S.-L., *J. Liq. Chromatogr. Relat. Technol.* **2000**, *23*, 1461-1475.

(34) Berry, L. V.; Engelhardt, H., *J. Chromatogr. A* **1974**, *95*, 27-38.

(35) Szepesy, L.; Combellas, C.; Caude, M.; Rosset, R., *J. Chromatogr.* **1982**, *237*, 65-78.

(36) Jandera, P., *J. Chromatogr. A* **2002**, *965*, 239-261.

(37) Jaroniec, C. P.; Jaroniec, M.; Kruk, M., *J. Chromatogr. A* **1998**, *797*, 93-102.

(38) Nawrocki, J.; Rigney, M. P.; McCormick, A.; Carr, P. W., *J. Chromatogr. A* **1993**, *657*, 229-282.

(39) Thompson, J. D.; Brown, J. S.; Carr, P. W., *Anal. Chem.* **2001**, *73*, 3340-3347.

(40) Nawrocki, J.; Dunlap, C.; McCormick, A.; Carr, P. W., *J. Chromatogr. A* **2004**, *1028*, 1-30.

(41) Gritti, F.; Guiochon, G., *Anal. Chem.* **2006**, *78*, 4642-4653.

(42) Jones, B. A., *J. Liq. Chromatogr. Relat. Technol.* **2004**, *27*, 1331-1352.

(43) Jackson, P. T.; Schure, M. R.; Weber, T. P.; Carr, P. W., *Anal. Chem.* **1997**, *69*, 416-425.

(44) Chmielowiec, J.; Sawatzky, H., *J. Chromatogr. Sci.* **1979**, *17*, 245-252.

(45) Kayillo, S.; Dennis, G. R.; Shalliker, R. A., *J. Chromatogr. A* **2007**, *1145*, 133-140.

(46) Larkins, W. C.; Olesik, S. V., *J. Microcol. Sep.* **1993**, *5*, 543-550.

(47) Kriz, J.; Adamcova, E.; Knox, J. H., *J. Chromatogr. A* **1994**, *663*, 151-161.

(48) West, C.; Lesellier, E., *J. Chromatogr. A* **2005**, *1099*, 175-184.

(49) Kephart, S. T.; Dasgupta, P. K., *Talanta* **2002**, *56*, 977-987.

(50) Fornstedt, T.; Zhong, G.; Guiochon, G., *J. Chromatogr. A* **1996**, *742*, 55-68.

(51) Thompson, J. D.; Carr, P. W., *Anal. Chem.* **2002**, *74*, 4150-4159.

(52) Schellinger, A. P.; Stoll, D. R.; Carr, P. W., *J. Chromatogr. A* **2005**, *1064*, 143-156.

(53) Coym, J. W.; Roe, B. W., *J. Chromatogr. A* **2007**, *1154*, 182-188.

(54) Lee, W.; Cho, D.; Chun, B. O.; Chang, T.; Ree, M., *J. Chromatogr. A* **2001**, *910*, 51-60.

(55) Meyer, V., R., *J. Chromatogr. A* **1997**, *768*, 315-319.

(56) Slimestad, R.; Vagen, I. M., *J. Chromatogr. A* **2006**, *1118*, 281-284.

(57) Thompson, J. D.; Carr, P. W., *Anal. Chem.* **2002**, *74*, 1017-1023.

CHAPTER FIVE. Zirconia, Titania, Silica, and Carbon Columns for the Group-Type Characterization of Heavy Gas Oils using Normal Phase High Temperature Liquid Chromatography*

5.1 Introduction

As the availability of conventional crude oils declines, the use of higher boiling crude oils and bitumens extracted from oilsands will increase.[1] These higher boiling materials are more difficult to process with existing upgrading technologies into the fuels required to meet growing global demand.[1] Having analytical methods available to characterize these high boiling (>350°C) materials is essential to properly evaluate advances in upgrading technologies, including new catalysts used in hydrotreatment and catalytic cracking.[2,3]

Fast analytical methods that can yield hydrocarbon group-type compositions within several minutes can be used to aid decision making when blending heavy gas oil feedstocks or choosing the proper upgrading conditions.[4,5] They can also be used for online process monitoring and product quality monitoring.[4-6]

Existing methods for measuring the group-type composition of high boiling materials include nuclear magnetic resonance (NMR),[4,7,8] multi-dimensional gas chromatography (GC-GC),[8,9] supercritical fluid chromatography (SFC),[7,10] high performance liquid chromatography (HPLC),[2,3,5,7,11-18] and mass spectrometry based

*A version of this chapter will be submitted for publication. Paproski R. E., Liang, C., Lucy C. A., *Energy & Fuels* **2007**. R. Paproski co-supervised C. Liang's undergraduate CHEM 401 project on polar compound analysis by high temperature normal phase liquid chromatography (Section 5.3.5).

methods.[6-10,19] NMR has not been used routinely for this application due to high equipment costs and the high level of required operator expertise. NMR also provides somewhat different information related to the number of aromatic carbon atoms rather than the number of aromatic molecules. GC and SFC based methods can suffer from irreversible adsorption of sample components when the sample material is sufficiently high boiling or contains significant concentrations of polar heteroatom compounds. Mass spectrometry based methods can provide a wealth of qualitative information. However, response factors for compounds within a group-type can vary significantly due to differences in ionization efficiencies.[20] Overall, normal phase HPLC is one of the most widely used techniques for the group-type analysis of high boiling petroleum samples.[10]

In Chapter 2, bare titania and titania-silica coupled columns outperformed conventional columns for the group-type analysis of diesel fuels with SFC. In this chapter, a bare zirconia, bare titania, and carbon coated zirconia column are compared with conventional bare silica and aminopropyl bonded silica columns for their ability to separate model compounds according to their hydrocarbon group-types with normal phase HPLC. Fundamental chromatographic parameters including retention factors, efficiencies, separation selectivities, and group-type resolutions are studied. Their study provides an in depth understanding of each column's strengths and limitations in regards to group-type separations.

Polar sulfur, nitrogen, and oxygen compounds are also studied to evaluate each column's ability to elute and separate various heteroatom compounds naturally present in high boiling heavy gas oils and crude oils. Finally, three heavy gas oil

samples of increasing heteroatom content are separated using two methods. The first method achieves the highest possible group-type resolutions while the second achieves the fastest possible analysis time.

5.2 Experimental

5.2.1 Apparatus

The high temperature HPLC system is described in Section 4.2.1. Mobile phase flow rates were 2.0 ml min^{-1} unless otherwise indicated. An Alltech 500 evaporative light scattering detector (ELSD) (Alltech Associates Inc., Deerfield, IL) was connected to the outlet of the UV detector cell and was used for the detection of saturated hydrocarbons as well as mass quantification of heavy gas oil samples. Nitrogen (Praxair, Mississauga, ON) at a flow rate of 1.2 L min^{-1} was used as the nebulizer gas. The drift tube temperature was held at 45°C. The ELSD detector yielded about 40% lower efficiencies for early eluting compounds compared to the UV detector. This difference in efficiency appeared to be inherent to the ELSD detector. When temperatures higher than the boiling point of the mobile phase were studied, a backpressure regulator was installed between the UV and ELSD detectors to provide ~800 psi of backpressure. The ELSD detector efficiency values were not affected by the presence of the backpressure regulator.

The columns listed in Table 5-1 were studied for their ability to elute non-polar hydrocarbons in hexane (Optima grade, Fisher Chemical, Fairlawn, NJ) and polar sulfur, nitrogen, and oxygen compounds in dichloromethane (Optima grade, Fisher Chemical).

Table 5-1. Columns tested and group-type resolutions achieved with hexane at 2.0 ml min^{-1}.

Column	Length (x 4.6 mm i.d.)	Diameter, Pore Size	Temp. (°C)	Resolution Sat. vs. Mono.	Resolution Mono. vs. Di.	Resolution Di. vs. Tri.	Elution Time[a] (min)
Bare Silica Lichrospher Si 60[b]	100	3 µm, 60 Å	35	14.1	0	0	13.4
Bare Silica Lichrospher Si 60[b]	100	3 µm, 60 Å	65	9.0	0.3	0	6.92
Spherisorb-NH2[c]	150	3 µm, 80 Å	35	9.7	0	0	7.17
Spherisorb-NH2[c]	150	3 µm, 80 Å	65	7.1	0	1.4	4.82
Bare Zirconia PHASE[d]	150	3 µm, 300 Å	35	2.8	8.7	0	32.6
Bare Zirconia PHASE[d]	150	3 µm, 300 Å	100	1.4	7.2	0	4.73
Bare Zirconia PHASE[d]	150	3 µm, 300 Å	200	0	1.6	0	1.28
Bare Titania Sachtopore-NP[d]	150	3 µm, 60 Å	35	9.2	8.6	0	64.5
Bare Titania Sachtopore-NP[d]	150	3 µm, 60 Å	65	6.8	6.3	1.1	20.7
Bare Titania Sachtopore-NP[d]	50	3 µm, 60 Å	35	1.9	3.7	0.3	2.40
Bare Titania Sachtopore-NP[d]	50	3 µm, 60 Å	65	1.7	2.6	0.6	1.23
Bare Titania-Lichrospher[e]	50 + 100	3 µm, 60 Å	35	16.1	0	0	25.0
Bare Titania-Lichrospher[e]	50 + 100	3 µm, 60 Å	65	11.7	1.3	0	12.9
Carbon clad Zirconia-CARB[d]	150	3 µm, 60 Å	-	-	-	-	-

[a]Based on pyrene retention times
[b]Thermo Electron, Waltham, MA, USA
[c]Waters, Milford, MA, USA
[d]Zirchrom, Anoka, MN, USA
[e]Coupled columns
[d]Resolution RSD and retention time RSD were typically less than 3% and 2% respectively.

Chloroform (Optima grade, Fisher Chemical, Fairlawn, NJ), tetrahydrofuran (OmniSolv grade, EMD Chemicals, Gibbstown, NJ), and toluene (ChromAR grade, Mallinckrodt Baker, Inc., Phillipsburg, NJ), were also used in the study of the carbon coated zirconia column. All solvents were pre-dried and degassed according to the procedure outlined in Section 4.2.1.

5.2.2 Standards and Samples

Table 5-2 lists the twenty seven non-polar aromatic hydrocarbon model compounds (>90% purity) that were studied. In addition, twenty three sulfur, nitrogen, and oxygen containing polar model compounds were also studied (>90% purity, Table 5-3). These samples were prepared as described in Section 4.2.2.

Three heavy gas oil (HGO) samples (Syncrude Canada Ltd.) that were subjected to varying severities of hydrotreating were analyzed (Table 5-4). Each heavy gas oil was diluted with hexane prior to analysis. For the high resolution analysis method (Section 5.2.4), heavy gas oils were prepared at 0.050 g ml^{-1}. Due to the higher peak heights, heavy gas oils were prepared at 0.010 g ml^{-1} for the fast analysis method (Section 5.2.5). No precipitation or phase separation of the diluted samples was observed over several months of storage.

5.2.3 Calculations

Retention times and peak widths at half-height were determined using Varian Star Chromatography Workstation version 6.20 software. Retention factors, plate heights, and group-type resolutions were calculated as described in Section 2.2.3. The column void time was based on the baseline deflection observed when an injecton of ACS grade hexane (EMD Chemicals) was made.

Table 5-2. Non-polar model compounds studied and retention times (min) with hexane at 65°C and 2.0 ml min^{-1}.

Compound	Hydrocarbon Group-Type	Bare Titania 5 cm	Bare Silica 10 cm
Hexanes (dead time)	-	0.28	0.64
Hexadecane[a]	Saturate	0.26	0.56
Tetracosane[a]	Saturate	0.26	0.54
n-Butylbenzene[a]	Mono	0.34	1.87
Heptadecylbenzene[a]	Mono	0.34	1.34
Benzene[b]	Mono	0.34	2.22
Toluene[c]	Mono	0.34	2.48
Tetramethylbenzene (1,2,4,5-)[a]	Mono	0.37	3.55
Tetralin[d]	Mono	0.38	2.73
Octahydroanthracene (1,2,3,4,5,6,7,8-)[e]	Mono	0.40	2.42
Ethylnaphthalene (2-)[e]	Di	0.46	3.58
Naphthalene[d]	Di	0.47	3.63
Biphenyl[a]	Di, sterically hindered	0.55	5.45
Acenaphthene[a]	Di	0.58	4.77
Dibenzofuran[a]	Di, furan	0.74	6.49
Fluorene[a]	Di	0.81	9.09
Dibenzothiophene[a]	Di, thiophene	0.88	7.30
Benzylnaphthalene (1-)[e]	Tri, sterically hindered	0.91	>20
Phenanthrene[a]	Tri	0.92	7.36
Anthracene[a]	Tri	1.01	7.04
Pyrene[a]	Tetra	1.23	6.92
Phenylanthracene (9-)[a]	Tetra, sterically hindered	1.46	18.1
Dihydrotetracene (5,12-)[a]	Tri	1.99	>20
Benzanthracene (1,2-)[e]	Tetra	3.09	15.0
Chrysene[a]	Tetra	3.41	23.3
Perylene[a]	Penta	5.41	16.6
Benzo[A]pyrene[a]	Penta	5.89	45.8
Dibenzophenanthrene (1,2:7,8-)[e]	Penta	28.5	40.7

[a]Sigma-Aldrich, St. Louis, MO
[b]Caledon Laboratories Ltd., Georgetown, ON
[c]Mallinckrodt Baker, Inc., Phillipsburg, NJ
[d]Fisher Chemical, Fairlawn, NJ
[e]K&K Laboratories Inc., Carlsbad, CA
[f]Retention time RSD was typically less than 2%.

Table 5-3. Polar heteroatom model compound retention times (min) with dichloromethane at 35°C and 2.0 ml min^{-1}.

Compound	Hydrocarbon Group-Type	Bare Silica 100 mm	Silica-NH_2 150 mm	Zirconia 150 mm	Titania 50 mm
Hexanes (dead time)	-	0.58	0.84	0.82	0.28
Benzylmethyl sulfide[a]	S, sulfide	0.66	0.89	0.85	0.30
Phenyl sulfide[b]	S, sulfide	0.96	0.94	0.89	0.47
Benzothiophene[c]	S, thiophene	0.65	0.90	0.86	0.32
Dibenzothiophene[b]	S, thiophene	0.65	0.90	0.88	0.32
p-Methylthiophenol[d]	S, thiol	0.68	1.06	0.83	0.32
Naphthalenethiol (2-)[b]	S, thiol	8.24	4.89	0.89	0.56
Indole[b]	N, pyrrole	0.88	1.21	1.01	0.30
Carbazole[d]	N, pyrrole	1.07	1.30	1.07	0.40
Tetrahydrocarbazole (1,2,3,4-)[b]	N, pyrrole	0.80	1.15	1.23	0.31
Benzo[def]carbazole[b]	N, pyrrole	0.80	1.15	2.72	0.53
Quinoline[e]	N, pyridine	I.R.[h]	8.12	I.R.[h]	I.R.[h]
Acridine[d]	N, pyridine	I.R.[h]	8.42	I.R.[h]	I.R.[h]
Aniline[f]	N, amine	I.R.[h]	1.98	I.R.[h]	0.48
Benzylamine[b]	N, amine	I.R.[h]	1.45	I.R.[h]	0.32
Aminonaphthalene (2-)[b]	N, amine	I.R.[h]	2.20	I.R.[h]	I.R.[h]
Aminopyrene (1-)[b]	N, amine	I.R.[h]	1.70	I.R.[h]	I.R.[h]
Anisole[b]	O, ether	0.69	0.89	0.85	0.30
Phenyl ether[b]	O, ether	1.06	0.94	0.85	4.84
Benzofuran (2,3-)[b]	O, furan	0.67	0.92	0.86	0.32
Dibenzofuran[b]	O, furan	0.70	0.92	0.86	0.32
Acetophenone[g]	O, ketone	4.87	1.45	6.92	I.R.[h]
Methylbenzoate[g]	O, ester	2.34	1.18	1.43	2.47
Benzyl alcohol[b]	O, alcohol	20.0	4.68	I.R.[h]	I.R.[h]

[a]Alfa Aesar, Ward Hill, MA
[b]Sigma-Aldrich, St. Louis, MO
[c]Acros Organics, Morris Plains, NJ
[d]Eastman Chemical Company, Arlington, VA
[e]Matheson, Coleman & Bell, East Rutherford, NJ
[f]Anachemia Chemicals Inc., Rouses Point, NY
[g]Fisher Chemical, Fairlawn, NJ
[h]Irreversibly retained (k >50)
[i]Retention time RSD was typically less than 2%.

Table 5-4. Elemental analysis and simulated distillation results for three heavy gas oils studied with high resolution and fast analysis methods (Sections 5.2.4 and 5.2.5).

	HGO-A	HGO-B	HGO-C
Sulfur (ppm)	550	1040	3860
Nitrogen (ppm)	400	820	1980
Initial Boiling Point (°C)	142	117	146
T10% (°C)	257	285	312
T50% (°C)	392	404	416
T90% (°C)	492	499	506
Final Boiling Point (°C)	584	588	592

[a]Elemental analysis and simulated distillation (ASTM D2887-04a) were performed by Syncrude Canada Ltd.

5.2.4 High Resolution Method for Heavy Gas Oil Analysis

The high resolution separation of heavy gas oils was achieved with the instrumental setup shown in Figure 5-1. The separation used two columns, two switching valves, and separate hexane to dichloromethane gradients on each column. The 5 cm bare titania column (dimensions are shown in Table 5-1) was heated to 65°C and was placed upstream of the 10 cm bare silica column (22°C). Two 7010 Rheodyne valves (Rheodyne, Rohnert Park, CA) were used to either by-pass a column or to allow mobile phase to flow through a column. All tubing connections were made with the shortest possible lengths of 0.127 mm i.d. stainless steel tubing. No backflushing was used as the solvent flow was always in the forward direction for both columns. Table 5-5 shows the gradient and valve switching timings. All valve switching was performed manually to within one second of the timings listed in Table 5-5.

Cut-points between the different group-types were made at the minimum between the corresponding peaks in the ELSD chromatogram (Figure 5-2). Typically, the saturate vs. monoaromatic cut-point was made at 1.3 min. The mono- vs. diaromatic cut-point was made via the first valve switching. This resulted in the monoaromatics eluting between 1.3 min and 10 min after eluting from both the bare titania and bare silica columns. The diaromatics eluted from the bare titania column between 23 min and 23.4 min following additional valve switching.

The di- vs. triaromatic cut-point was made at the minimum between the two group-types at 23.4 min. The heteroatom compounds were eluted from the bare titania column when the gradient to 100% dichloromethane was made at 33 min.

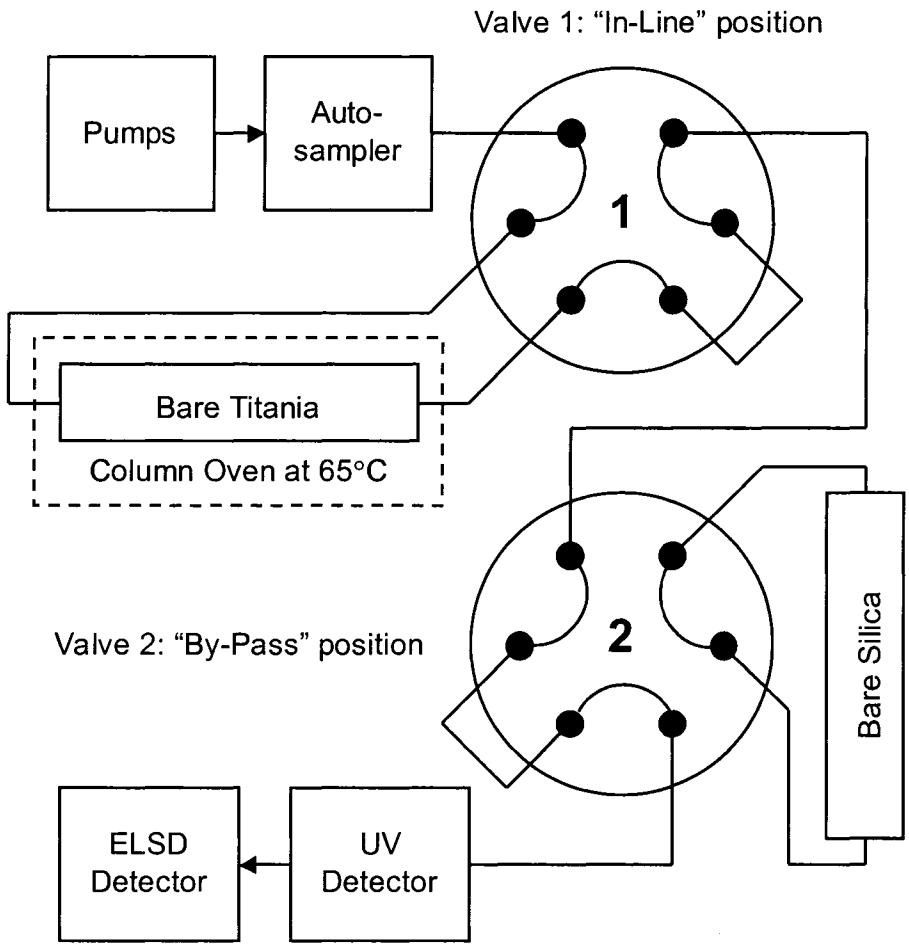

Figure 5-1. Schematic of the valves and columns for the high resolution heavy gas oil analysis method.

Table 5-5. Gradient and valve switching timings for the high resolution heavy gas oil analysis method.[a]

Time (min:seconds)	%Hexane	%Dichloro-methane	Valve 1 (5 cm Titania)	Valve 2 (Bare Silica)
0:00	100	0	In-line	In-line
0:30	100	0	By-pass	In-line
10:00	100	0	By-pass	In-line
10:10	0	100	By-pass	In-line
20:00	0	100	By-pass	By-pass
20:30	0	100	By-pass	By-pass
21:00	100	0	By-pass	By-pass
23:00	100	0	In-line	By-pass
33:00	100	0	In-line	By-pass
33:10	0	100	In-line	By-pass
88:00	0	100	In-line	By-pass
88:30	100	0	In-line	By-pass
90:00	100	0	In-line	In-line
100:00	100	0	In-line	In-line

[a]A linear gradient was used when switching solvents. See Section 5.2.4 for experimental conditions.

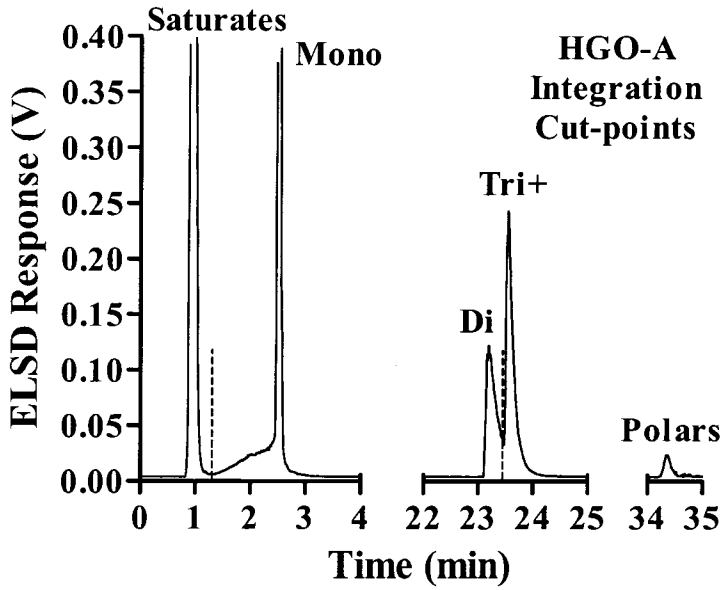

Figure 5-2. Integration cut-points for HGO-A sample separated on a 5 cm bare titania column (65°C) coupled to a 10 cm bare silica column (22°C) using two switching valves and hexane to dichloromethane gradients at 2.0 ml min^{-1} (Section 5.2.4 high resolution analysis method). ELSD detection. See Table 5-5 for valve switching and gradient timings.

The gradient to 100% dichloromethane was performed to speed up the analysis by eluting the highly retained compounds more quickly with the stronger mobile phase.

5.2.5 Fast Gradient Method for Heavy Gas Oil Analysis

A method for the rapid separation of heavy gas oils was developed using a 5 cm bare titania column at 65°C and a mobile phase flow rate of 5.0 ml min^{-1}. Due to the exceptionally high flow rate, a T-joint was used to split the flow to the ELSD detector such that only 2.9 ml min^{-1} was reaching the detector. This flow did not result in any additional baseline noise that would be expected if undried droplets were reaching the light scattering cell.[21,22] Table 5-6 shows the conditions for the gradient method starting with 100% hexane, a linear gradient to 100% dichloromethane from 20 to 30 seconds, followed by a return to 100% hexane at 2 min for column re-equilibration. The gradient to 100% dichloromethane was made following the elution time of pyrene.

The cut-points for the fast heavy gas oil analysis method were determined empirically to yield similar group-type results to the high resolution heavy gas oil analysis method results for HGO-C. In this way, the fast analysis method results are calibrated to the high resolution analysis results using HGO-C. The saturate vs. monoaromatic cut-point was 0.16 min. The mono- vs. diaromatic cut-point was 0.18 min. The di- vs. triaromatics cut-point was 0.20 min.

The cut-point between the triaromatics and heteroatom compounds was 0.87 min.

Table 5-6. Gradient timings for the fast heavy gas oil analysis method.[a]

Time (min:seconds)	%Hexane	%Dichloromethane
0:00	100	0
0:20	100	0
0:30	0	100
2:00	0	100
2:10	100	0
3:10	100	0

[a]A linear gradient was used when switching solvents. See Section 5.2.5 for experimental conditions.

Due to small, random variability in the retention times of the fast heavy gas oil chromatograms, the cut-points were manually corrected for each chromatogram according to the degree in which the retention time of the peak maximum for replicate injections differed from their average retention time. This cut-point time correction greatly improved the precision of the fast group-type results by reducing the average relative standard deviation from 8.0% to 3.9%. The average retention time correction was only 0.6 seconds in magnitude. For routine analysis, software could be programmed to either align the retention time data automatically or adjust the cut-points automatically.

5.2.6 Quantification of Heavy Gas Oil Group-Types with ELSD Detection

Quantification of heavy gas oil group-types was performed by integrating the area under the ELSD chromatograms. The ELSD response was calibrated using six representative compounds: dodecylcyclohexane (saturate, Koch-Light Laboratories Ltd., Colnbrook, Bucks, England), heptadecylbenzene (monoaromatic, Sigma-Aldrich), 1,2,3,6,7,8-hexahydropyrene (diaromatic, K&K Laboratories Inc.), 9-methyl anthracene (triaromatic, Sigma-Aldrich), chrysene (tetraaromatic, Sigma-Aldrich), and carbazole (heteroatom compound, Eastman Chemical Company). Each compound was prepared at three concentrations and was detected by the ELSD detector using the gradient method described in Section 5.2.4. The logarithm of the ELSD response is directly proportional to the logarithm of sample concentration.[21-24] Figure 5-3 shows the logarithmic calibration curve for the non-polar compounds and carbazole. Similar compounds can have a single calibration curve.[10,22] This was the case for the non-polar compounds.

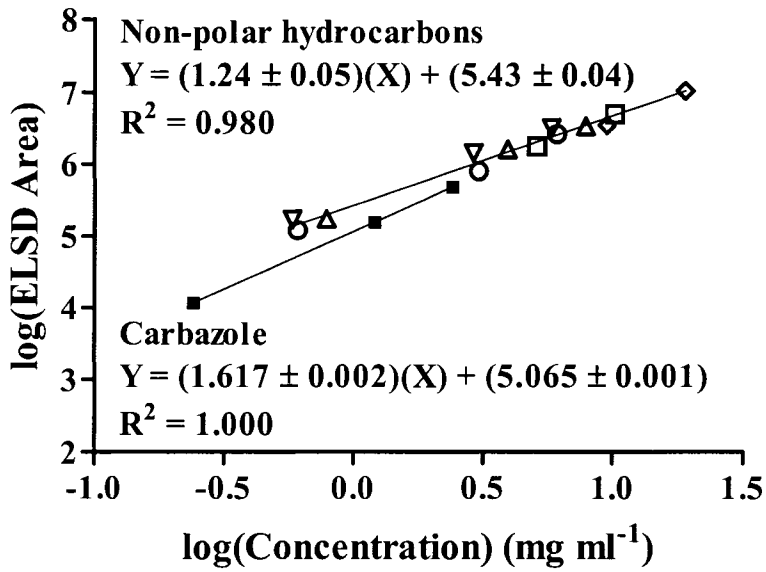

Figure 5-3. ELSD calibration curve for non-polar model compounds: dodecylcyclohexane (saturate, Δ), heptadecylbenzene (monoaromatic, ∇), 1,2,3,6,7,8-hexahydropyrene (diaromatic, □), 9-methylanthracene (triaromatic, ◊), and chrysene (tetraaromatic, ○), as well as the calibration curve for carbazole (heteroatom compound, ■). ELSD response RSD was typically less than 3%.

As a result, a single calibration curve was used for all non-polar group-types. Carbazole gave a statistically different response. Thus, the carbazole calibration curve was used to quantify the polar group-type. It should be noted that carbazole was found to be stable at temperatures up to 100°C in Chapter 4, and thus should be stable at 65°C here. ELSD detectors do not provide a response for material that boils below 315°C.[10]

As a result, only the material that boils above this temperature is actually detected by ELSD. 10-20% of the material in the heavy gas oil samples studied here boiled below 315°C, and thus was not quantified. This lighter boiling material was produced during sample hydrotreatment and falls below the boiling range of the high boiling materials (>350°C) intended for this method.

5.3 Results and Discussion

5.3.1 Retention

The degree to which each hydrocarbon group-type is retained by a column largely dictates how well the column will separate the group-types within a reasonable amount of time. Ideally, saturated compounds would be minimally retained while monoaromatic compounds would be sufficiently retained to permit an adequate separation between the two group-types. Likewise, larger aromatic ring group-types should display progressively higher retention than the monoaromatics, without yielding overly high retention times to minimize analysis time.

For almost all of the columns studied, the saturated model compounds showed very little retention with retention factors less than 0.12 in hexane at 35°C. The only

exception was the carbon coated zirconia column where a slightly higher retention factor of 0.44 was observed for tetracosane. The retention of the monoaromatic model compounds varied more significantly across the different columns. Bare zirconia displayed the weakest monoaromatic retention with retention factors in the range of 0.15 to 0.43. Bare titania and aminopropyl bonded silica exhibited intermediate monoaromatic retention factors from 0.72 to 3.0. Bare silica yielded high monoaromatic retention factors from 1.8 to 9.3. As would be expected, a bare titania-silica coupled column displayed retention factors from 1.5 to 7.0, which are intermediate values between those for bare titania and bare silica separately. Carbon coated zirconia completely retained the monoaromatic model compounds with hexane as the eluent at 35°C. Very high retention is characteristic of carbon based columns.[25] The high amount of π-π interactions involved with retention on carbon based columns[25] accounts for the very high separation selectivity between saturates (no π-electrons) and monoaromatics. This very high retention is similar to the results obtained when testing a carbon coated zirconia column with SFC in Section 2.3.2.

These results suggest that bare zirconia would provide the worst saturates vs. monoaromatics separation due to the limited retention of monoaromatic compounds. Owing to the much higher retention of monoaromatics, bare silica would be expected to provide the best saturate vs. monoaromatic separation. Carbon coated zirconia however would be expected to provide the best separation if a gradient were used. A stronger mobile phase such as dichloromethane was successful at eluting the monoaromatic model compounds from the carbon coated zirconia column with small retention factors (less than 0.1) at 35°C. This permits full control of the

monoaromatic retention by varying the amount of dichloromethane in the mobile phase.

With the numerous benefits of using elevated temperatures in normal phase HPLC presented in Chapter 4, elevated temperatures were also studied here. However, the silica based columns used in this study were not prepared with high temperature applications in mind. When working with a completely non-aqueous mobile phase, dissolution of the silica is not expected to be an issue at temperatures approaching 200°C. However, high temperature applications place additional burdens on the mechanical stability of the chromatographic bed.[26] During column preparation, higher than normal column packing pressures are required to avoid problems with bed settling and void formation.[26] Commercially prepared columns that are not intended for use at high temperatures (>65°C) may not be packed at sufficiently high pressures to ensure bed stability during periods of thermal stress. For this reason, the silica based columns were not studied above 65°C. Bare titania was studied up to 200°C, although as discussed in Section 5.3.3 below, a permanent loss of column efficiency was experienced after working at 100°C and 200°C.

Increasing column temperature was found to decrease retention for all model compounds studied on all columns. When increasing temperature from 35°C to 65°C in hexane, anthracene retention factors decreased 1.5-fold on the aminopropyl bonded silica, 2.1-fold on the titania-silica coupled column, 2.2-fold on bare silica, 3.0-fold on bare zirconia, and 3.9-fold on bare titania. These represent significant decreases in retention when considering the relatively small 30°C increase in temperature. Table 5-1 lists the retention time of pyrene for each column with hexane at 2.0 ml min^{-1}.

Under isocratic conditions, these values can be considered proportional to the analysis time for a given sample. Pyrene elution times decreased with increasing temperature in similar proportions to the decrease in anthracene retention factors discussed above. Pyrene elution times at 65°C range from as little as 4.82 min on aminopropy bonded silica to as high as 20.7 min on bare titania. Bare zirconia, bare silica, and the titania-silica coupled column yielded intermediate elution times at 65°C. However, pyrene's retention time on bare zirconia was only 1.28 min at 200°C. As a result, bare zirconia would be expected to yield the shortest analysis time under isocratic conditions at 200°C. At 65°C, the aminopropyl bonded silica would be expected to give the shortest analysis time.

Due to the very high retention of the carbon coated zirconia column with hexane as the eluent, dichloromethane was also studied as an eluent with this column. With dichloromethane at 35°C, the mono-, di-, and triaromatic model compounds could be eluted with an anthracene retention time of 22.3 min. However, most four- and five-ring aromatics could not be eluted under these conditions. When the temperature was increased to 200°C with dichloromethane, all of the four-ring model compounds could be eluted with a pyrene retention time of 9.13 min, although the five-ring compounds still could not be eluted. Other solvents were studied that are considered strong mobile phases for carbon based columns.[27,28] Tetrahydrofuran was found to provide a similar mobile phase strength to dichloromethane at 35°C. Chloroform was found to be a slightly stronger mobile phase than dichloromethane, but it also failed to elute the five-ring model compounds even at 200°C. Only an aromatic solvent such as toluene was found to elute the five-ring compounds

(dibenzophenanthrene retention time of 13.7 min at 35°C). The relative strengths of these mobile phases are similar to those reported on other carbon based columns.[27,28] Unfortunately, with the use of toluene, detection of monoaromatics at 254 nm becomes impossible. Also, the very long column re-equilibration times (in excess of 12 hours) prevent the use of toluene as an eluent in any gradient separation. As a result, the 15 cm carbon coated zirconia column was not amenable for use in this application.

A short 1 cm carbon coated zirconia guard column was briefly studied in an effort to overcome the long retention times discussed above. While it became possible to elute four-ring aromatics with dichloromethane at 35°C (pyrene retention time of 4.77 min), five-ring compounds could not be eluted without the use of an aromatic mobile phase.

5.3.2 Group-Type Selectivity

It is highly desirable to find a combination of columns and conditions that yield good group-type separation selectivity. Ideally, each of the twenty seven model compounds studied would be eluted in order of increasing aromatic ring number. Higher group-type selectivities result in fewer compounds eluting with the wrong group-types. This results in a better group-type separation and less systematic errors when integrating sample chromatograms.

With hexane at 35°C, the saturated model compounds eluted before the monoaromatic model compounds for all of the columns studied. While achieving the proper saturate vs. monoaromatic selectivity is relatively easy, no column completely separated all of the triaromatic model compounds from the tetraaromatic model

compounds under any condition studied. In the case of bare silica, aminopropyl bonded silica, bare titania, and the titania-silica coupled column, pyrene was found to elute earlier than the latest eluting triaromatic compound. In the case of bare zirconia, the sterically hindered phenylanthracene eluted before some triaromatic compounds (as discussed in Section 4.3.2). With the carbon coated zirconia column using dichloromethane as the mobile phase, phenylanthracene eluted before some triaromatic model compounds. Thus, no column provided adequate tri- vs. tetraaromatic separation selectivity. As a result no effort was made to quantify the degree of their separation or to determine these group-types separately.

To evaluate the mono- vs. diaromatic selectivity and di- vs. triaromatic selectivity, a van't Hoff plot containing the latest eluting monoaromatic compound, the earliest and latest eluting diaromatic compound, and the earliest eluting triaromatic compound were plotted for each column studied. Figure 5-4 shows this plot for aminopropyl bonded silica, the most commonly reported column used for this application.[2,3,5,7,11-18]

At 35°C, the latest eluting monoaromatic compound (octahydroanthracene) elutes later (higher retention factor) than the earliest eluting diaromatic compound (naphthalene). Similarly, the latest eluting diaromatic (fluorene) is eluting later than the earliest eluting triaromatic (anthracene). This means that these group-types are overlapping under these conditions. Thus, depending on where the integration cut-points are made on a sample chromatogram, some monoaromatics would be integrated as diaromatics and vice versa. The same would be true with di- and triaromatics.

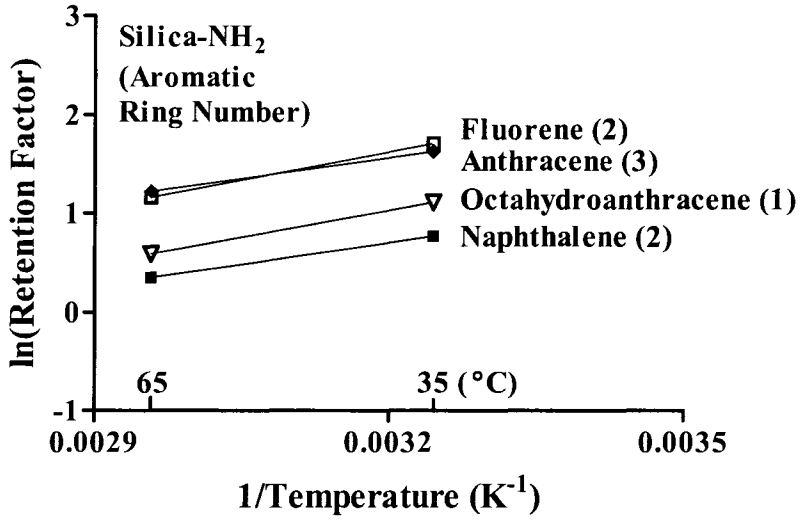

Figure 5-4. Van't Hoff plot of the latest eluting monoaromatic compound, earliest and latest eluting diaromatics compound, and earliest eluting triaromatic compound. 150 x 4.6 mm i.d., 3 μm, aminopropyl bonded silica column, with a hexane mobile phase at 2.0 ml min^{-1}. Retention factor RSD was typically less than 4%.

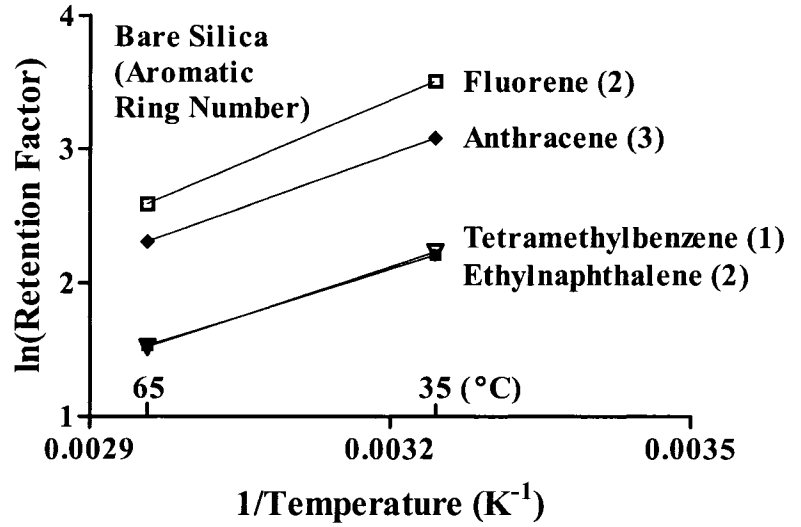

Figure 5-5. Van't Hoff plot of the latest eluting monoaromatic compound, earliest and latest eluting diaromatics compound, and earliest eluting triaromatic compound. 100 x 4.6 mm i.d., 3 μm, bare silica column, with a hexane mobile phase at 2.0 ml min^{-1}. Retention factor RSD was typically less than 4%.

However, when the temperature is increased from 35°C to 65°C with aminopropyl bonded silica, an elution order change occurred where fluorene (diaromatic) elutes slightly earlier than anthracene (triaromatic). This represents an improvement in group-type selectivity with increasing temperature, as was observed with bare zirconia in Section 4.3.2. Poor mono- vs. diaromatic and di- vs. triaromatic group-type selectivity at 35°C is also evident with the bare silica column (Figure 5-5). At 65°C, the di- vs. triaromatic selectivity appears to improve due to an elution order change of fluorene and anthracene. However, the difference in retention time of these two compounds on bare silica is within experimental error.

Figure 5-6 shows that all monoaromatic compounds elute before the diaromatic compounds on the bare titania column. However, at 35°C, dibenzothiophene (diaromatic) elutes later than phenanthrene (triaromatic). At 65°C, this elution order also changes resulting in better di- vs. triaromatic selectivity. Figure 5-7 shows the plot for the titania-silica coupled column. This coupled column shows identical behavior to bare silica where di- vs. triaromatic selectivity is poor at both temperatures while mono- vs. diaromatic selectivity is poor at 35°C, but improves at 65°C. The elution order changes on the titania and titania-silica coupled columns were confirmed with multiple chromatograms.

Figure 5-8 shows the plot for bare zirconia. Mono- vs. diaromatic selectivity is good at all temperatures studied (35°C to 200°C). Di- vs. triaromatic selectivity is poor even though fewer compounds from different group-types are overlapping at 200°C compared to 35°C as discussed in Section 4.3.2. Figure 5-9 shows the selectivity plot for carbon coated zirconia using a dichloromethane mobile phase.

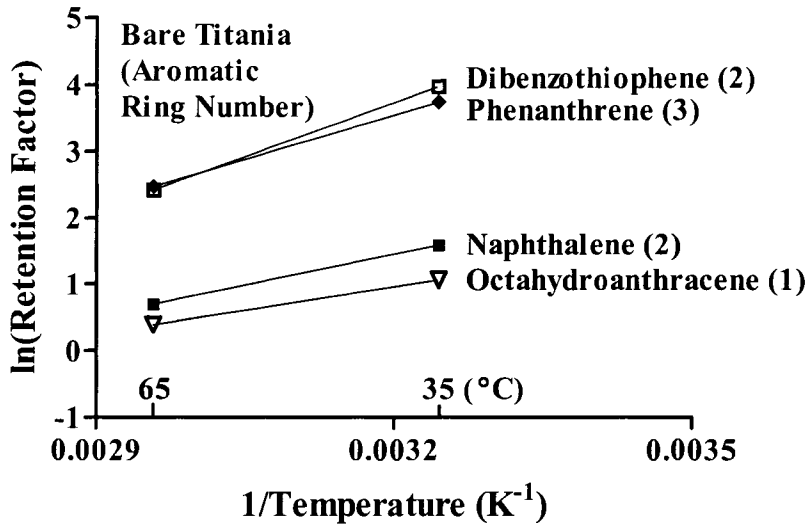

Figure 5-6. Van't Hoff plot of the latest eluting monoaromatic compound, earliest and latest eluting diaromatics compound, and earliest eluting triaromatic compound. 150 x 4.6 mm i.d., 3 μm, bare titania column with a hexane mobile phase at 2.0 ml min^{-1}. Retention factor RSD was typically less than 4%.

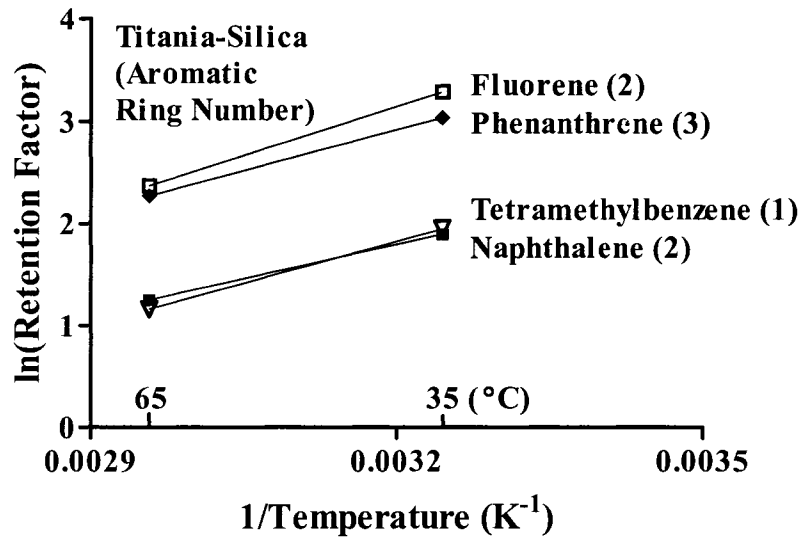

Figure 5-7. Van't Hoff plot of the latest eluting monoaromatic compound, earliest and latest eluting diaromatics compound, and earliest eluting triaromatic compound. (50 + 100) x 4.6 mm i.d., 3 μm, titania-silica coupled column with a hexane mobile phase at 2.0 ml min^{-1}. Retention factor RSD was typically less than 4%.

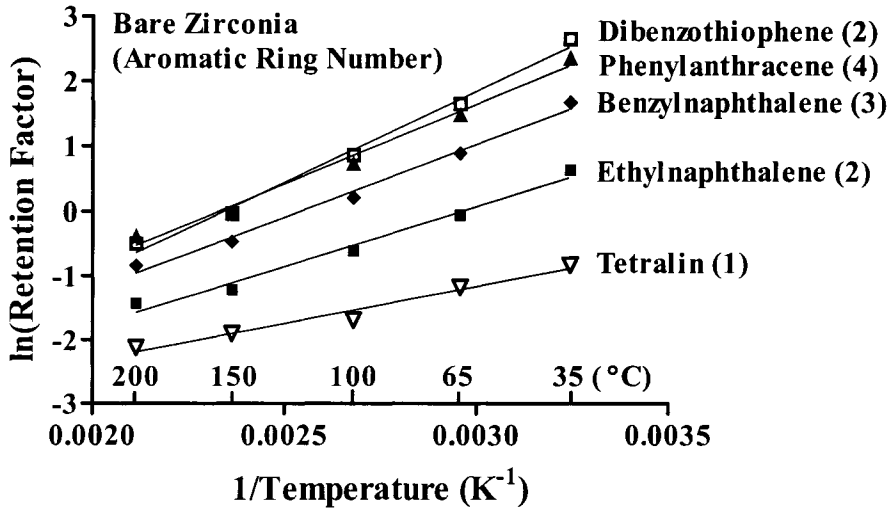

Figure 5-8. Van't Hoff plot of the latest eluting monoaromatic compound, earliest and latest eluting diaromatics compound, and earliest eluting triaromatic compound. 150 x 4.6 mm i.d., 3 μm, bare zirconia column with a hexane mobile phase at 2.0 ml min^{-1}. Retention factor RSD was typically less than 4%.

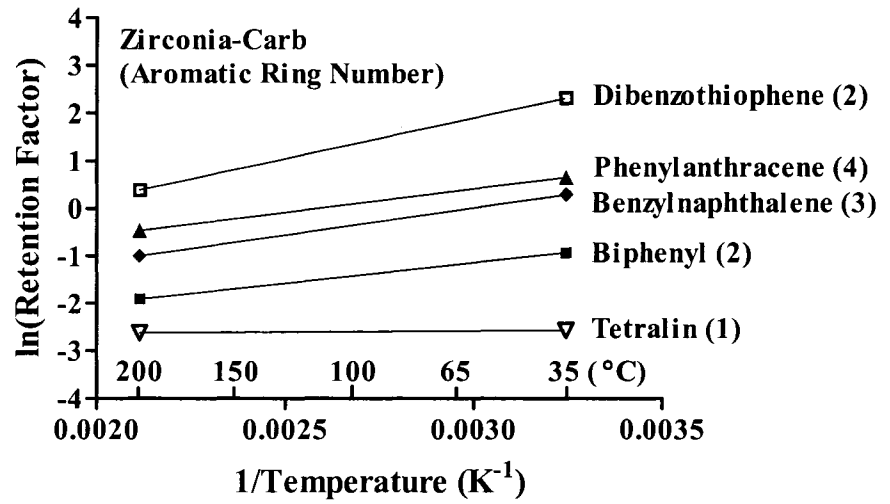

Figure 5-9. Van't Hoff plot of the latest eluting monoaromatic compound, earliest and latest eluting diaromatics compound, and earliest eluting triaromatic compound. 150 x 4.6 mm i.d., 3 μm, carbon coated zirconia column with a dichloromethane mobile phase at 2.0 ml min^{-1}. Retention factor RSD was typically less than 4%.

While the mono- vs. diaromatic selectivity is good at both 35°C and 200°C, di- vs. triaromatic selectivity is poor at both temperatures due to the sterically hindered compounds benzylnaphthalene (triaromatic) and phenylanthracene (tetraaromatic) eluting before dibenzothiophene (diaromatic). The carbon coated zirconia column was the only column studied where no improvement in the group-type selectivity was observed with increasing temperature.

Overall, the bare titania column at 65°C was the only column to provide good group-type separation selectivity for saturates vs. monoaromatics, mono- vs. diaromatics, and di- vs. triaromatics. This high aromatic group-type selectivity is similar to the results observed with SFC in Section 2.3.2. An interesting difference however is that the titania-silica coupled column achieved good di- vs. triaromatic selectivity with SFC (Section 2.3.3), but poor di- vs. triaromatic selectivity here with normal phase HPLC. This worsened selectivity was not a result of expanding the number of model compounds studied with normal phase HPLC (twenty seven) compared to SFC (twenty) as both compounds involved in the di- vs. triaromatic overlap with normal phase HPLC were also studied with SFC. While separation trends are similar with SFC and normal phase HPLC when using the same columns, notable differences are also evident.

5.3.3 Efficiency

In Section 4.3.3, significant improvements in efficiency were observed with increasing temperature up to 200°C on bare zirconia (Figure 4-6). Similar improvements were also observed here when the column temperature was increased from 35°C to 65°C. Figure 5-10 shows the improvement in plate height with

increasing temperature for four representative aromatic compounds on bare silica. Anthracene's plate height was 1.9-fold lower at 65°C, resulting in nearly double the efficiency and a reasonable plate height of 28 μm. Figure 5-11 shows the same plot for aminopropyl bonded silica. This column gave an excellent anthracene plate height of 14 μm at 35°C. A 20% reduction in plate height was obtained at 65°C, yielding a plate height of 11 μm.

On bare titania (Figure 5-12) the plate height for anthracene improved 3.2-fold at 65°C compared to 35°C. However, when column temperature was increased to 100°C, about half of the efficiency for early eluting model compounds was lost. This suggests that column stability is an issue for the bare titania column at temperatures approaching 100°C. At 200°C, catastrophic loss of peak efficiency was observed, confirming the thermal instability of the bare titania column despite operating under non-aqueous conditions.

Titania has excellent chemical stability.[29-32] As a result, the titania particles themselves are not expected to dissolve at elevated temperatures, especially in non-aqueous solvents. Further, a capillary column packed in-house with C18-modified titania particles was found to be stable at 160°C with an acetonitrile-water mobile phase (reversed phase conditions).[33] Given the high chemical and thermal stability of titania particles, bed instability is believed to be the cause of the efficiency loss.[26] Chromatographic beds can settle and form voids when exposed to elevated temperatures.[26] These voids can cause a non-uniform flow profile through the column which results in broad, non-Gaussian peak shapes and poor column efficiency.

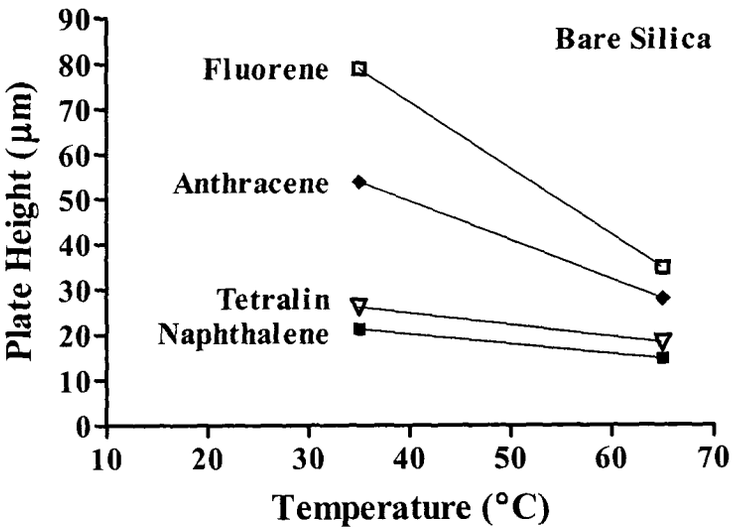

Figure 5-10. Plate height versus temperature for four representative model compounds. 100 x 4.6 mm i.d., 3 µm, bare silica column with a hexane mobile phase at 2.0 ml min^{-1}. Plate height RSD was typically less than 6%.

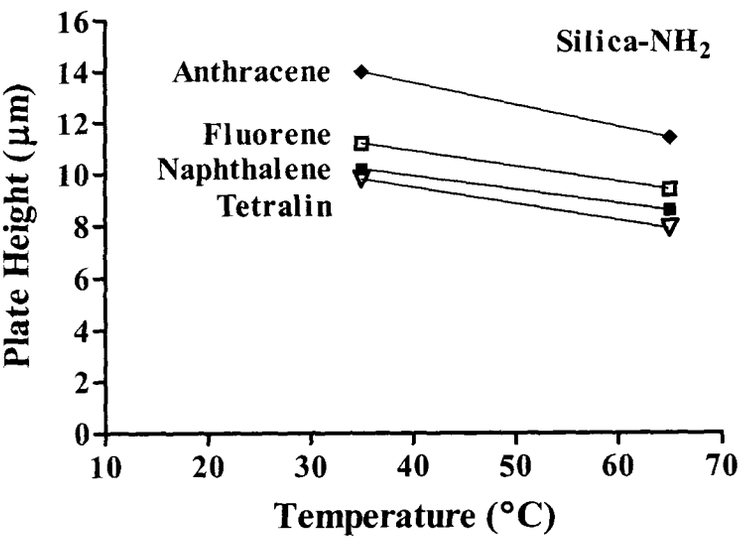

Figure 5-11. Plate height versus temperature for four representative model compounds. 150 x 4.6 mm i.d., 3 µm, aminopropyl bonded silica column with a hexane mobile phase at 2.0 ml min^{-1}. Plate height RSD was typically less than 6%.

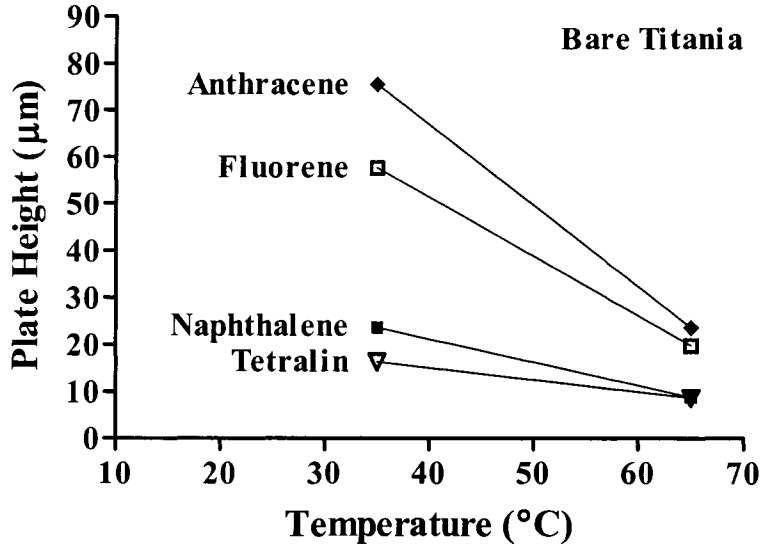

Figure 5-12. Plate height versus temperature for four representative model compounds. 150 x 4.6 mm i.d., 3 µm, bare titania column with a hexane mobile phase at 2.0 ml min^{-1}. Plate height RSD was typically less than 6%.

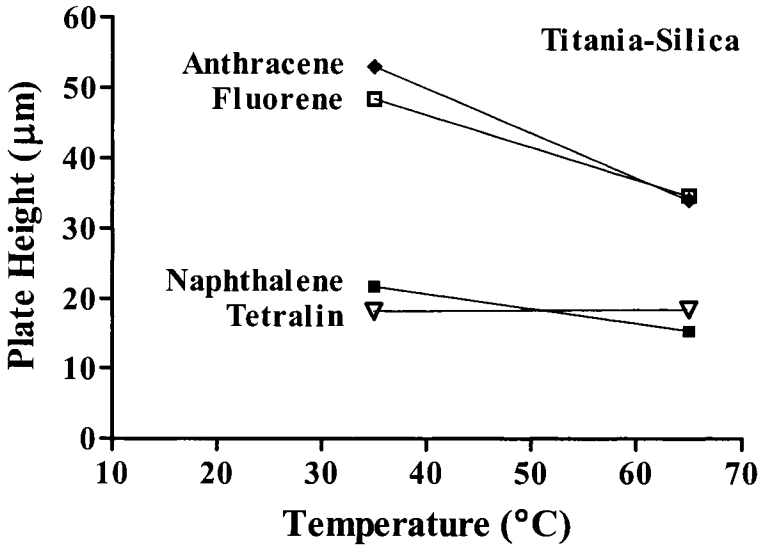

Figure 5-13. Plate height versus temperature for four representative model compounds. (50 + 100) x 4.6 mm i.d., 3 µm, titania-silica coupled column with a hexane mobile phase at 2.0 ml min^{-1}. Plate height RSD was typically less than 6%.

Figure 5-13 shows a 1.6-fold improvement in plate height for anthracene at 65°C on the titania-silica coupled column. This resulted in an anthracene plate height of 34 μm. Figure 5-14 shows the plate height for anthracene with the carbon coated zirconia column using dichloromethane as the mobile phase. At 200°C, anthracene's plate height decreased nearly 38-fold, yielding a plate height of 54 μm.

The very poor efficiency at 35°C is likely due to the low capacity of carbon based columns.[25] This leads to sample overload for highly retained compounds, and poor efficiency and peak shape as a result. This is very similar to the drastic improvements in plate height observed at elevated temperatures with bare zirconia in Section 4.3.3. Overall, aminopropyl bonded silica displayed the best efficiency while the bare titania and the bare silica columns displayed reasonable efficiencies at 65°C.

5.3.4 Group-Type Resolution

Table 5-1 lists the group-type resolutions for each column studied with a hexane mobile phase at 2.0 ml min^{-1}. The best overall resolutions were obtained at elevated temperatures due to the improvements in separation selectivity with increasing temperature. Figure 5-15 compares the resolutions at elevated temperatures for each column. At 65°C, the highest saturate vs. monoaromatic resolution was obtained on the titania-silica coupled column with a value of 9.7, while the bare silica column alone provided a resolution of 9.0. The lowest saturate vs. monoaromatic resolutions were observed on the bare zirconia column and the short 5 cm bare titania column.

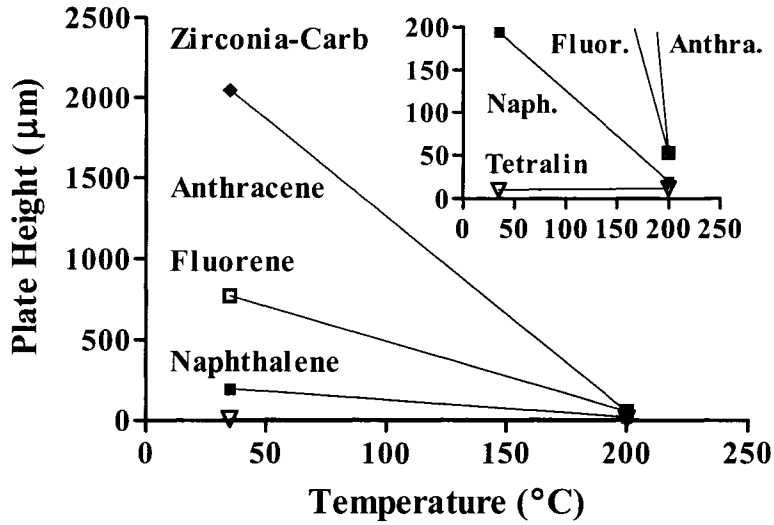

Figure 5-14. Plate height versus temperature for four representative model compounds. 150 x 4.6 mm i.d., 3 µm, carbon coated zirconia column with a dichloromethane mobile phase at 2.0 ml min^{-1}. Plate height RSD was typically less than 6%.

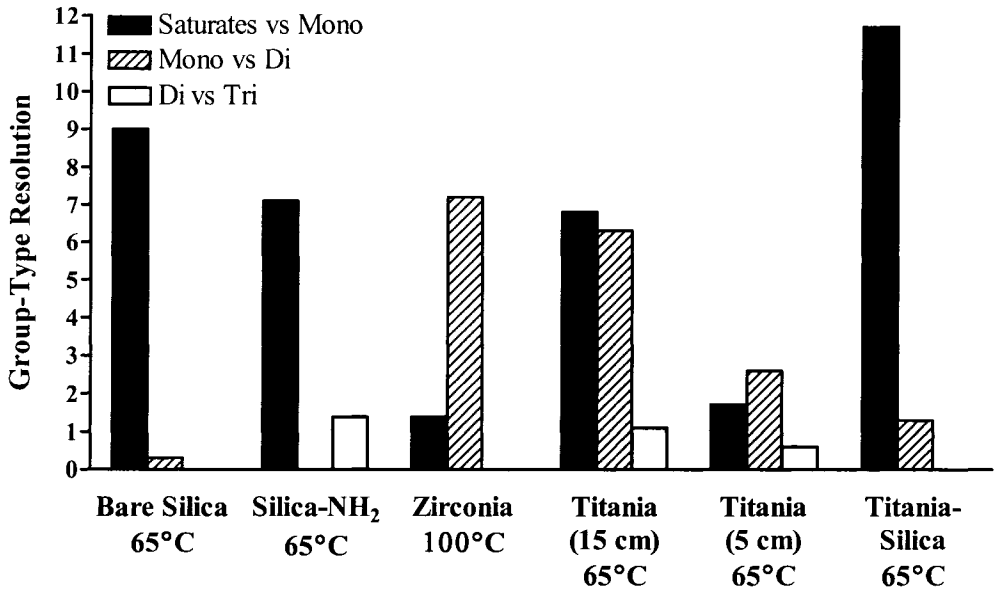

Figure 5-15. Group-type resolutions on various columns with a hexane mobile phase at 2.0 ml min^{-1}. See Table 5-1 for column dimensions and numerical resolution values. See Figures 5-4, 5-5, 5-6, 5-7, and 5-8 for the compounds used to determine the aromatic group-type resolutions for each column. All saturate vs. monoaromatic resolutions were based on tetracosane and heptadecylbenzene. The only exception was the 15 cm titania column, which was based on tetracosane and benzene. Resolution RSD was typically less than 3%.

The highest mono- vs. diaromatic resolution was obtained on the bare zirconia column, with the 15 cm bare titania column also providing high mono- vs. diaromatic resolution. The aminopropyl bonded silica column provided no mono- vs. diaromatic resolution. However, the aminopropyl bonded silica column did yield the highest di- vs. triaromatic resolution, followed by the 15 cm and 5 cm bare titania columns. The bare silica, bare zirconia, and titania-silica coupled column gave no di- vs. triaromatic resolution. Overall, the best group-type resolutions were obtained with the 15 cm bare titania column at 65°C.

One aspect of the analysis that is not taken into account by Figure 5-15 is the analysis times associated with each column. Figure 5-16 shows the group-type resolutions for each column divided by pyrene's retention times (Table 5-1). This is one way to measure the amount of resolution produced by each column per unit time. From this we can see that the short 5 cm bare titania column produces the highest overall group-type resolutions per unit time compared to the other columns studied, including the 15 cm bare titania column.

There are two reasons why the 5 cm titania column produced a higher resolution per unit time compared to the 15 cm titania column. The first reason is fundamental to chromatography. Retention time scales with the length of the column. Thus, a 3-fold reduction in column length results in a 3-fold reduction in retention time. However, resolution scales with the square root of the column length. This is due to the linear relationship between resolution and the square root of efficiency (Equation 1-9) as well as the linear relationship between efficiency and the column length (Equation 1-8).

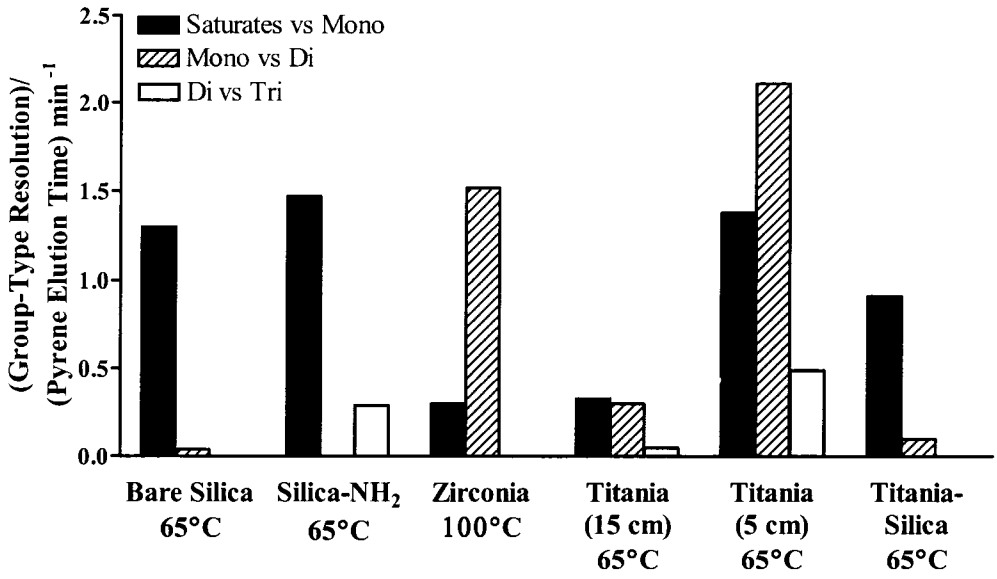

Figure 5-16. Group-type resolutions divided by pyrene elution time (min) on various columns with a hexane mobile phase at 2.0 ml min^{-1}. See Table 5-1 for column dimensions, numerical resolution values, and pyrene elution times. Resolution RSD and retention time RSD were typically less than 6% and 2% respectively.

Thus, as we decrease the column length 3-fold, we would expect a $(3)^{1/2}$-fold improvement in the resolution per unit time. The second reason for the improvement is more circumstantial. The 5 cm bare titania column was significantly less retentive with a retention factor for anthracene being 5.5-fold lower than the 15 cm bare titania column at 65°C.

The reason for this is that the resolution data for the short 5 cm titania column was collected following the study of polar heteroatom compounds, some of which did not elute from the column (see Section 5.3.5). These irreversibly retained compounds block some of the high energy adsorption sites on the stationary phase surface, making it less retentive. This makes the resolution and pyrene retention time results for the 5 cm bare titania column more typical for a column that had been previously used for the analysis of heavy gas oils containing polar compounds. When analyzing high boiling samples with a high heteroatom content, some initial conditioning of a new column is to be expected. Some initial sample retention time drift is common, followed by stable retention times once the column has reached an equilibrium state with the polar components in the sample. In Section 2.3.5, a bare titania column displayed this conditioning behavior upon repeat injections of diesel samples containing polar compounds.

5.3.5 Elution of Sulfur, Nitrogen, and Oxygen Compounds*

Heavy gas oils can contain varying amounts of polar heteroatom compounds depending on the source and upgrading history of the material. In crude oils, sulfur content can range from 0.05 to 14% w/w.[34] Nitrogen content in crude oils is often

*Performed by undergraduate Chen Liang for CHEM 401 under my supervision.

much lower with a range from a few ppm to 2% w/w.[7,34] Oxygen compounds are also found in low concentrations (<1%) in most crude oils.[34] For a given crude oil, the sulfur content increases roughly linearly with boiling temperature.[34] Nitrogen and oxygen content also increase with boiling temperature, but are only prominent in materials that boil above 345°C.[34]

Table 5-3 shows the twenty three polar model compounds that were studied on each column with a dichloromethane mobile phase. The goals of studying polar model compounds were two-fold. The first goal was to determine which model compounds could be eluted from each column using dichloromethane as the mobile phase. Irreversible retention (under experimental conditions) of any compounds would necessitate a periodic cleansing of the column with a strong solvent such as dried methanol to avoid long term changes in column performance. The second goal was to determine if the studied columns offered any interesting selectivity towards polar compounds. It would be highly desirable to be able to separate polar compounds of different heteroatoms (e.g. sulfur vs. nitrogen compounds) or separate different compound types within the same elemental group of compounds (e.g. pyrroles vs. amines vs. pyridines).

Only the aminopropyl bonded silica column displayed elution of all polar compounds studied using a dichloromethane mobile phase at 35°C. The bare silica column irreversibly retained (k >50) the pyridine and amine compounds under these conditions. The bare zirconia column irreversibly retained (k >50) the pyridine compounds, half of the amine compounds, acetophenone (ketone), and benzyl alcohol. The pyridine compounds, amine compounds, and benzyl alcohol were not

eluted (k >50) from the bare titania column under these conditions. As a result, only the aminopropyl bonded silica column could be used for the routine analysis of high boiling samples rich in heteroatom compounds without the need to periodically cleanse the column of irreversibly retained components. These results are not surprising as bonded phases are known to be less retentive towards highly polar compounds than the solid adsorption phases used in normal phase separations.[7,13] However, others have shown that pyridine and amine compounds can be eluted from bare titania with either a hexane[29,30] or heptane[31] mobile phase moderated with 0.5% isopropanol.

From Table 5-3, it is clear that no column studied was capable of completely separating the polar compounds according to heteroatom (e.g. sulfur vs. nitrogen). The wide range of polarities for the various sulfur, nitrogen, and oxygen compounds makes their separation difficult. Often ligand-exchange columns based on bare silica impregnated with either palladium chloride[35,36] or silver nitrate[7] are required to separate sulfur compounds from non-polar compounds.

The aminopropyl bonded silica column was the only column to show interesting selectivity towards separating compounds of the same element. Pyrrole, amine, and pyridine compounds were successfully separated using this column with dichloromethane at 35°C. A previous study found that an aminopropyl bonded silica column was well suited for separating pyrrole and pyridine compounds using a dichloromethane mobile phase.[37] Surprisingly, the elution order of the pyrrole and pyridine compounds was reversed in that study compared to this one.[37] It is unclear what could cause this difference in elution order.

Figure 5-17 shows highest sulfur and nitrogen content heavy gas oil sample HGO-C separated on the aminopropyl silica column using a dichloromethane mobile phase at 35°C. Regions where the various pyrrole, amine, and pyridine compounds would be expected to elute are indicated. Non-polar aromatic compounds are contributing to the UV signal in Figure 5-17. In order to quantify the various nitrogen compound group-types, a selective detector such as a chemiluminescent nitrogen detector would be required.[10,38,39] While the chromatogram in Figure 5-17 does not distinguish between non-polar and nitrogen compounds, it does show that compounds are indeed eluting within the expected ranges for all three nitrogen group-types.

5.3.6 High Resolution Heavy Gas Oil Analysis

Table 5-1 shows how the best saturate vs. monoaromatic resolution was obtained with a titania-silica coupled column at low temperatures (35°C), while the best aromatic group-type resolutions were obtained with a bare titania column at 65°C. Unlike with SFC in Chapter 2, coupling a bare titania column in series with a bare silica column did not yield good overall group-type resolutions in normal phase HPLC.

As a result, a useful approach for achieving good overall group-type separation is to use valve switching. Valve switching is a common way of improving group-type separations by directing different group-types to different columns.[7,9] This takes advantage of the unique selectivity of different columns toward specific group-types, even if each column alone does not provide good overall group-type separations.

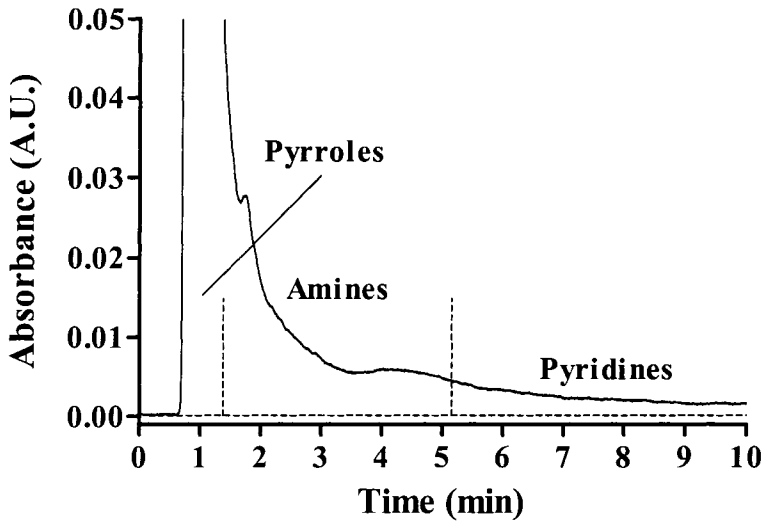

Figure 5-17. Chromatogram of HGO-C separated on an aminopropyl bonded silica column with a dichloromethane mobile phase at 35°C and 2.0 ml min^{-1}. UV detection at 254 nm. HGO-C sample diluted with hexane to 50% w/w. The regions where different polar nitrogen compound group-types would be expected to elute are indicated. See Table 5-3 for nitrogen compound retention times.

Here, the separation of the saturates and monoaromatics was performed on bare titania and bare silica columns coupled serially, while the di-, triaromatic, and polar group-types were separated on the bare titania column alone. For this separation the 5 cm bare titania column (heated to 65°C) was placed upstream of the 10 cm bare silica column (Figure 5-1). Because higher saturate vs. monoaromatic resolution was obtained at lower temperatures (Table 5-1), the bare silica column was kept at room temperature (22°C). Table 5-5 shows the timings for the valve switching as well as the hexane to dichloromethane gradients.

To summarize the overall separation process, the heavy gas oil sample is first partially separated on the 5 cm bare titania at 65°C. The saturates and monoaromatics are swept through this column and onto the bare silica column. At 30 seconds, the bare titania column is by-passed and thus isolated from the flow path. The timing for this valve switch corresponds with the beginning of the elution of the first diaromatic model compound (ethylnaphthalene). The use of this as a cut-point between the mono- and diaromatics is similar to the cut-point used in Chapters 2 and 3 to separate the same group-types in diesel fuels.[40] Following the isolation of the di-, triaromatics, and polar group-types on the bare titania column, the saturates and monoaromatics are separated on the bare silica column with hexane as the eluent. Thus, the saturates and monoaromatics are separated on both columns, yielding a high degree of separation.

Figure 5-18 shows the chromatogram for a high heteroatom content heavy gas oil (HGO-C) using the high resolution analysis method.

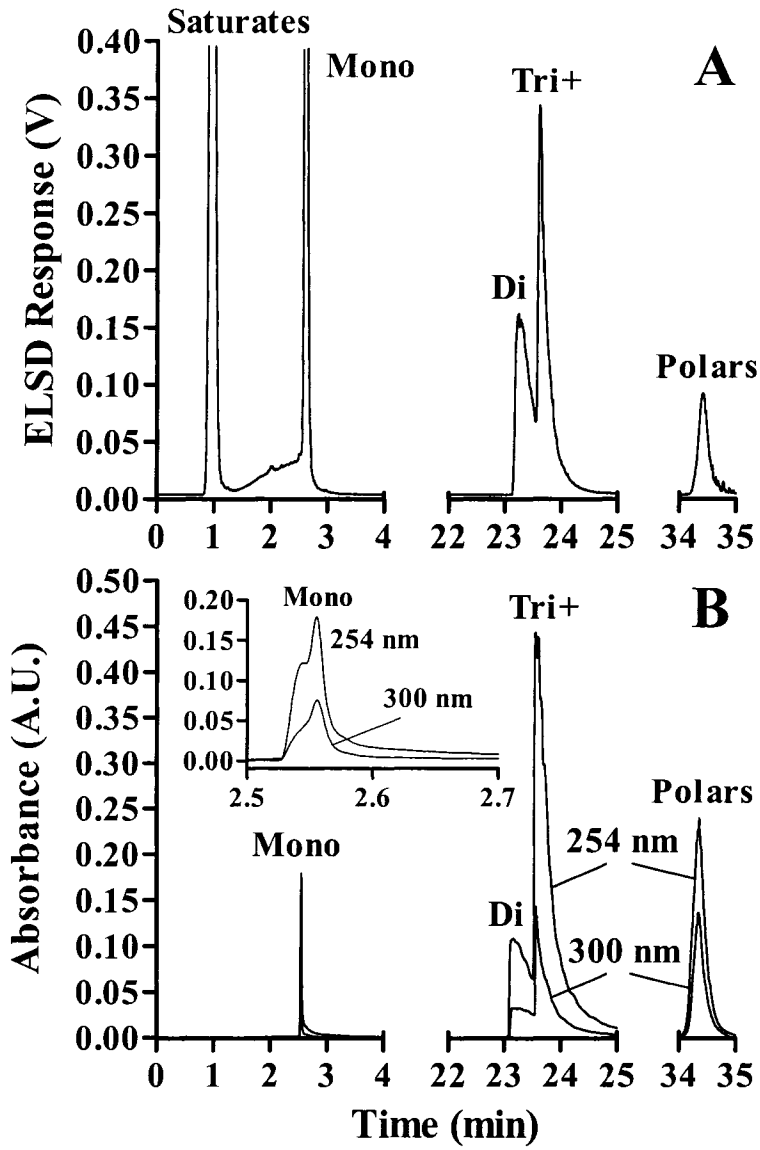

Figure 5-18. Chromatogram of HGO-C sample separated on a 5 cm bare titania column (65°C) coupled to a 10 cm bare silica column (22°C) using two switching valves and hexane to dichloromethane gradients at 2.0 ml min^{-1} (Section 5.2.4 high resolution analysis method). ELSD detection (A) and UV detection at 254 nm and 300 nm (B). See Table 5-5 for valve switching and gradient timings.

To ensure complete elution of the saturates and monoaromatics from the bare silica column, a 10-second linear gradient from 100% hexane to 100% dichloromethane was performed at 10 min. At 20 min, the bare silica column was by-passed (both columns now by-passed). At 20.5 min the mobile phase was returned to 100% hexane to flush the lines and prepare for the elution of the remaining di-, triaromatic, and polar group-types from the by-passed bare titania column.

At 23 min, the bare titania column was switched back inline. The diaromatics eluted, followed quickly by the triaromatics. Using the bare titania column to separate the di- vs. triaromatic group-types takes advantage of the high group-type resolution bare titania exhibited towards these group-types (Figure 5-15). A visible minimum was obtained between the di- and triaromatics which serves as a convenient cut-point between these two group-types (Figure 5-18). A second hexane to dichloromethane gradient was used at 33 min to flush the polar compounds from the bare titania column.

It should be noted that some non-polar aromatic compounds with five or more rings are expected to co-elute with the polar group-type. Also, some polar heteroatom compounds, especially sulfur compounds, often elute within the aromatic group-type that matches their aromatic ring number. Thus, complete separation of non-polar compounds vs. polar compounds was not achieved. This is often the case with normal phase separations,[7] unless ligand-exchange columns are used.[7,35,36] Close inspection of Figure 5-18 reveals that complete separation of mono- and diaromatic compounds is not achieved. The monoaromatic group-type gives a response at 300 nm. This shows that some diaromatics are being eluted in the

monoaromatic group-type, despite the very high mono- vs. diaromatic resolution provided by the bare titania column. This is likely due to a high degree of alkylation with the high boiling diaromatic compounds.[6] This extensive alkylation can result in steric effects preventing effective adsorption of the sample compounds onto the bare titania surface. This in turn reduces their retention.

Figures 5-19 and 5-20 show the ELSD chromatogram for heavy gas oil samples of low (HGO-A) and intermediate (HGO-B) heteroatom content, respectively. Both chromatograms show similar peak shapes to HGO-C (Figure 5-18). The quantitative results for the group-types are given in Table 5-7. Due to the long analysis time of the high resolution method, only the high heteroatom content HGO-C sample was run in triplicate. Precision for the group-type results varied from 0.6% to 3.1%. This precision is good for an ELSD detector. Upper limits of reported ELSD precision range from 2.8% to 10.3%.[41-44] While UV detectors provide a more reproducible response that scales linearly with concentration, response factors for various aromatic compounds of the same group-type can vary significantly at a given wavelength. As a result, UV detection cannot be used for the quantification of hydrocarbon group-types without making perilous assumptions regarding response factors.

5.3.7 Fast Heavy Gas Oil Analysis

High resolution analysis methods work well at determining the group-type composition of heavy gas oils with a high degree of confidence. This is due to the high degree of separation achieved between the various group-types.

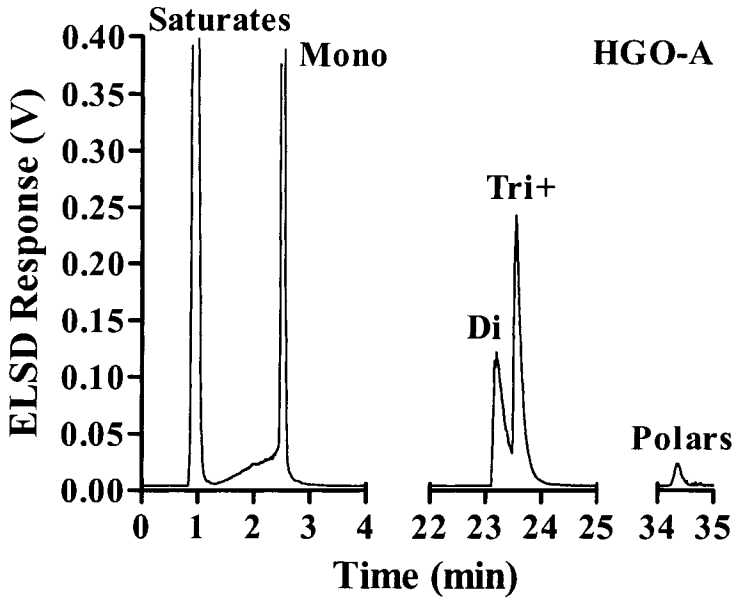

Figure 5-19. Chromatogram of HGO-A sample separated on a 5 cm bare titania column (65°C) coupled to a 10 cm bare silica column (22°C) using two switching valves and hexane to dichloromethane gradients at 2.0 ml min^{-1} (Section 5.2.4 high resolution analysis method). ELSD detection. See Table 5-5 for valve switching and gradient timings.

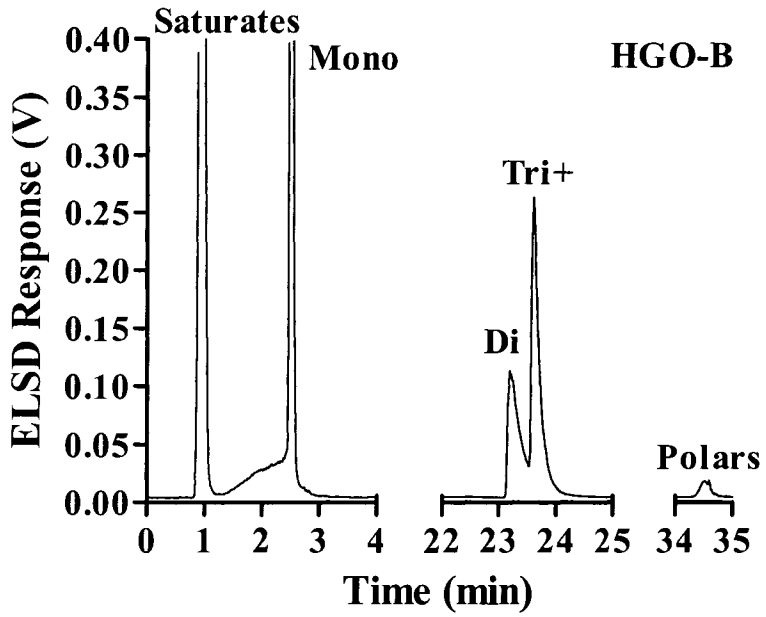

Figure 5-20. Chromatogram of HGO-B sample separated on a 5 cm bare titania column (65°C) coupled to a 10 cm bare silica column (22°C) using two switching valves and hexane to dichloromethane gradients at 2.0 ml min^{-1} (Section 5.2.4 high resolution analysis method). ELSD detection. See Table 5-5 for valve switching and gradient timings.

Table 5-7. Group-type content of heavy gas oil samples reported in mass% (RSD, %).

Sample	Column	Saturates	Mono.	Di.	Tri.+	Polars
HGO-A	Titania-Silica[a]	39.7	31.3	10.7	15.0	3.3
HGO-A	Titania[b]	35.5 (4.8%)	30.6 (1.7%)	14.1 (2.9%)	16.5 (5.2%)	3.3 (7.8%)
HGO-B	Titania-Silica[a]	36.9	33.5	10.3	15.8	3.5
HGO-B	Titania[b]	36.0 (3.3%)	31.6 (0.8%)	14.0 (5.1%)	15.0 (2.9%)	3.4 (14%)
HGO-C	Titania-Silica[a]	32.1 (2.0%)	27.0 (2.9%)	13.7 (1.5%)	18.8 (0.6%)	8.4 (3.1%)
HGO-C	Titania[b]	32.5 (2.4%)	26.5 (1.9%)	13.2 (2.0%)	19.2 (1.0%)	8.6 (2.7%)

[a]High resolution heavy gas oil (HGO) analysis method. 50 mm bare titania column (65°C) coupled to 100 mm bare silica column (22°C) via two switching valves. Hexane to dichloromethane gradients, 2.0 ml min^{-1}. See Table 5-5 for valve switching and gradient timings. Due to long analysis times, only HGO-C was run in triplicate with the high resolution HGO analysis method.

[b]Fast HGO analysis method. 50 mm bare titania column, hexane to dichloromethane gradient, 65°C, 5.0 ml min^{-1}. See Table 5-6 for gradient timings. All fast HGO analysis method results were run in triplicate.

However, for online process monitoring and product quality monitoring, fast analysis methods that can achieve results within minutes are required.[45]

Section 5.3.4 discussed how the 5 cm bare titania column provided the highest group-type resolutions per unit time (Figure 5-16). In this section this column was used at high flow rates (5.0 ml min^{-1}) to separate the heavy gas oil samples in the shortest possible time. A hexane to dichloromethane gradient was used to further reduce analysis time. Table 5-6 shows the gradient timings. The total analysis time including column re-equilibration was 3.2 minutes.

Figures 5-21 5-22, and 5-23 show the ELSD and UV chromatograms for HGO-A, HGO-B, and HGO-C respectively. Complete elution of the samples was achieved in only 1 min, with an additional 2 min required to ensure complete elution of the sample as well as column re-equilibration. While no obvious separation of the group-types is visible in the ELSD chromatogram, the area under the curve can still be divided into separate group-types. Using the HGO-C results obtained from the high resolution analysis method (Table 5-7), the fast analysis method cut-points were empirically determined to provide similar group-type results for HGO-C. In this way, the fast analysis group-type results were calibrated to the high resolution group-type results using the HGO-C sample.

This should permit a higher degree of accuracy than would otherwise be possible by using the retention times of model compounds for the determination of the cut-points. The fast analysis method cut-points are listed in Section 5.2.5. The fast analysis results for HGO-A and HGO-B (based on HGO-C cut-points) agreed reasonably well with the high resolution results (Table 5-7).

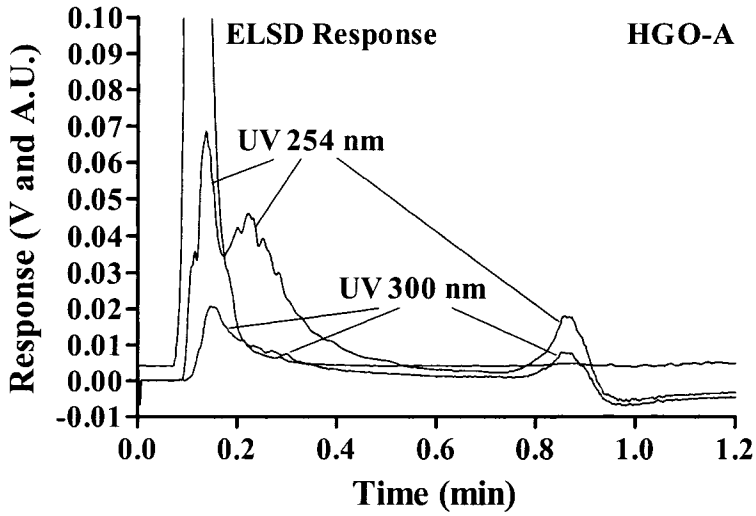

Figure 5-21. Chromatogram of HGO-A sample separated on a 5 cm bare titania column (65°C) with a hexane to dichloromethane gradient at 5.0 ml min^{-1} (Section 5.2.5 fast analysis method). ELSD and UV detection at 254 nm and 300 nm. See Table 5-6 for gradient timing.

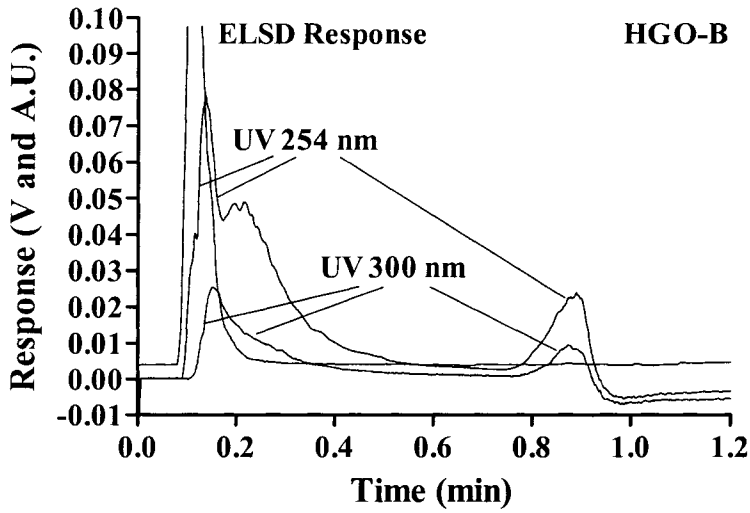

Figure 5-22. Chromatogram of HGO-B sample separated on a 5 cm bare titania column (65°C) with a hexane to dichloromethane gradient at 5.0 ml min^{-1} (Section 5.2.5 fast analysis method). ELSD and UV detection at 254 nm and 300 nm. See Table 5-6 for gradient timing.

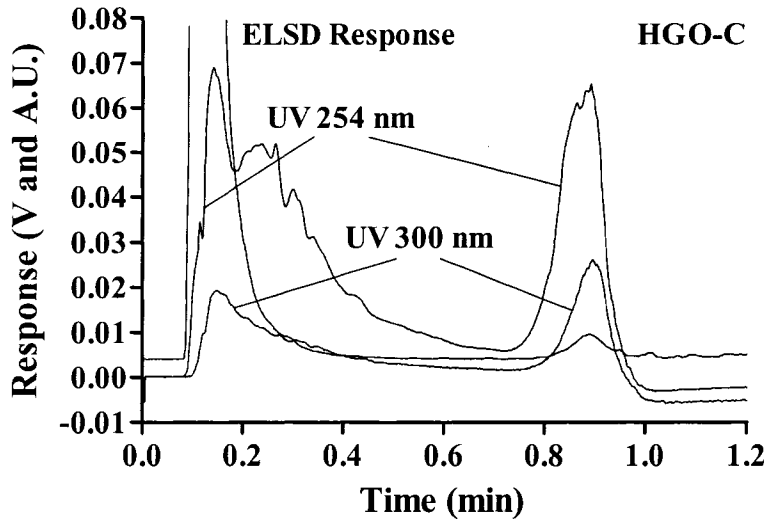

Figure 5-23. Chromatogram of HGO-C sample separated on a 5 cm bare titania column (65°C) with a hexane to dichloromethane gradient at 5.0 ml min^{-1} (Section 5.2.5 fast analysis method). ELSD and UV detection at 254 nm and 300 nm. See Table 5-6 for gradient timing.

Differences between the high resolution and fast analysis method results for HGO-A and HGO-B varied from zero to 4.2% w/w. This is quite good considering the short 3.2 min total analysis time. Precision for the fast analysis method results was good (3.9% RSD average variation) when small, random retention time shifts were corrected by adjusting the cut-points accordingly (see Section 5.2.5).

5.4 Conclusions

Bare zirconia, bare titania, bare silica, aminopropyl bonded silica, and carbon coated zirconia columns were compared for their ability to separate model compounds representing saturate, mono-, di-, tri-, and tetraaromatic hydrocarbon group-types found in heavy gas oils. The retention, efficiency, separation selectivity, and group-type resolutions of model compounds were studied to permit an in depth understanding of the factors that influence each column's ability to separate hydrocarbon group-types. A bare titania column was found to provide the best overall separation of the hydrocarbon group-types, while a titania-silica coupled column provided the best saturate vs. monoaromatic separation. A study of polar compounds revealed that only the aminopropyl bonded silica column could elute all of the studied sulfur, nitrogen, and oxygen model compounds with a dichloromethane mobile phase. The aminopropyl bonded silica column was also successful at separating pyrrole-, amine-, and pyridine-type compounds.

A high resolution heavy gas oil analysis method based on valve switching and gradients was developed using bare titania and bare silica columns. A fast heavy gas

oil analysis method using a bare titania column was also developed that had a total analysis time of only 3.2 min. Both methods yielded results with good precisions.

5.5 References

(1) Fu, J.; Klein, G. C.; Smith, D. F.; Kim, S.; Rodgers, R. P.; Hendrickson, C. L.; Marshall, A. G., *Energy & Fuels* **2006**, *20*, 1235-1241.

(2) Woods, J. R.; Kung, J.; Pleizier, G.; Kotlyar, L. S.; Sparks, B. D.; Adjaye, J.; Chung, K. H., *Fuel* **2004**, *83*, 1907-1914.

(3) Woods, J. R.; Kung, J.; Adjaye, J.; Kotlyar, L. S.; Sparks, B. D.; Chung, K. H., *Pet. Sci. Technol.* **2004**, *22*, 347-365.

(4) Kapur, G. S.; Chopra, A.; Sarpal, A. S., *Energy & Fuels* **2005**, *19*, 1065-1071.

(5) Robbins, W. K., *J. Chromatogr. Sci.* **1998**, *36*, 457-466.

(6) Kaminski, M.; Kartanowicz, R.; Gilgenast, E.; Namiesnik, J., *Crit. Rev. Anal. Chem.* **2005**, *35*, 193-216.

(7) Lundanes, E.; Greibrokk, T., *J. High Resol. Chromatogr.* **1994**, *17*, 197-202.

(8) Barman, B. N., *Anal. Chem.* **2001**, *73*, 2791-2804.

(9) Beens, J.; Brinkman, U. A. T., *Trends Anal. Chem.* **2000**, *19*, 260-275.

(10) Barman, B. N.; Cebolla, V. L.; Membrado, L., *Crit. Rev. Anal. Chem.* **2000**, *30*, 75-120.

(11) Ali, M. A., *Pet. Sci. Technol.* **2003**, *21*, 963-970.

(12) Fan, T.; Buckley, J. S., *Energy & Fuels* **2002**, *16*, 1571-1575.

(13) Felix, G.; Thoumazeau, E.; Colin, J.-M.; Vion, G., *J. Liq. Chromatogr.* **1987**, *10*, 2115-2132.

(14) Pasadakis, N.; Gaganis, V.; Varotsis, N., *Fuel* **2001**, *80*, 147-153.

(15) Sarowha, S. L. S.; Sharma, B. K.; Sharma, C. D.; Bhagat, S. D., *Energy & Fuels* **1997**, *11*, 566-569.

(16) Akhlaq, M. S., *J. Chromatogr.* **1993**, *644*, 253-258.

(17) Grizzle, P. L.; Sablotny, D. M., *Anal. Chem.* **1986**, *58*, 2389-2396.

(18) Pasadakis, N.; Varotsis, N., *Energy & Fuels* **2000**, *14*, 1184-1187.

(19) Stanford, L. A.; Rodgers, R. P.; Marshall, A. G., *Energy & Fuels* **2007**, *21*, 973-981.

(20) Wang, F. C.-Y.; Qian, K.; Green, L. A., *Anal. Chem.* **2005**, *77*, 2777-2785.

(21) Young, C. S.; Dolan, J. W., *LCGC* **2003**, *21*, 120-128.

(22) Young, C. S.; Dolan, J. W., *LCGC* **2004**, *22*, 244-250.

(23) Guiochon, G.; Moysan, A.; Holley, C., *J. Liq. Chromatogr.* **1988**, *11*, 2547-2570.

(24) Mengerink, Y.; De Man, H. C. J.; Van Der Wal, S., *J. Chromatogr.* **1991**, *552*, 593-604.

(25) Weber, T. P.; Jackson, P. T.; Carr, P. W., *Anal. Chem.* **1995**, *67*, 3042-3050.

(26) Kirkland, J. J.; DeStefano, J. J., *J. Chromatogr. A* **2006**, *1126*, 50-57.

(27) Colin, H.; Guiochon, G.; Jandera, P., *Chromatographia* **1982**, *15*, 133-139.

(28) Hazotte, A.; Libong, D.; Chaminade, P., *J. Chromatogr. A* **2007**, *1140*, 131-139.

(29) Grün, M.; Kurganov, A. A.; Schacht, S.; Schüth, F.; Unger, K. K., *J. Chromatogr. A* **1996**, *740*, 1-9.

(30) Kurganov, A.; Trüdinger, U.; Isaeva, T.; Unger, K., *Chromatographia* **1996**, *42*, 217-222.

(31) Winkler, J.; Marmé, S., *J. Chromatogr. A* **2000**, *888*, 51-62.

(32) Nawrocki, J.; Dunlap, C.; McCormick, A.; Carr, P. W., *J. Chromatogr. A* **2004**, *1028*, 1-30.

(33) Kephart, S. T.; Dasgupta, P. K., *Anal. Chim. Acta* **2000**, *414*, 71-78.

(34) Altgelt, K. H.; Boduszynski, M. M., *Composition of Heavy Petroleum Fractions*, Marcel Dekker, Inc., New York, 1994.

(35) Ma, X.; Sakanishi, K.; Isoda, T.; Mochida, I., *Fuel* **1996**, *76*, 329-339.

(36) Sripada, K.; Andersson, J. T., *Anal. Bioanal. Chem.* **2005**, *382*, 735-741.

(37) Carlsson, H.; Ostman, C., *J. Chromatogr. A* **1997**, *790*, 73-82.

(38) Navas, M. J.; Jimenez, A. M., *Crit. Rev. Anal. Chem.* **2000**, *30*, 153-162.

(39) Fujinari, E. M.; Courthaudon, L. O., *J. Chromatogr.* **1992**, *592*, 209-214.

(40) *Method D 5186-03, Annual Book of ASTM Standards*, American Society for Testing and Materials, West Conshohocken, PA, USA, 2003.

(41) Megoulas, N. C.; Koupparis, M. A., *J. Pharm. Biomed. Anal.* **2004**, *36*, 73-79.

(42) Foglia, T. A.; Jones, K. C.; Phillips, J. G., *Chromatographia* **2005**, *62*, 115-119.

(43) Xie, Z.; Jiang, Y.; Zhang, D.-q., *J. Chromatogr. A* **2006**, *1104*, 173-178.

(44) Muller, A.; Ganzera, M.; Stuppner, H., *J. Chromatogr. A* **2006**, *1112*, 218-223.

(45) Honigs, D. E., *Am. Lab.* **1987**, *19*, 48-51.

CHAPTER SIX. Conclusions and Future Work

6.1 Conclusions

This thesis explored the use of unconventional columns and operating conditions to improve the resolution and speed of group-type separations (saturates, mono-, di-, tri-, and polyaromatics) of middle distillates (175-350°C) with SFC and high boiling materials (>350°C) with HPLC.

6.1.1 Supercritical Fluid Chromatography

With SFC, bare titania columns provided higher aromatic group-type resolutions compared to conventional silica based columns. A bare titania column coupled in series to a bare silica column yielded the highest overall group-type resolution based on twenty model compounds. Short (10 to 15 cm) columns with small 3 μm diameter packing were compared with monolithic silica columns as two approaches for decreasing the time necessary for diesel group-type analysis. High carbon dioxide flow rates up to 5.0 ml min^{-1} were used with both approaches to significantly reduce analysis times. Monolithic columns achieved 13-fold lower elution times, but gave poor group-type resolution due to their lower surface area. Short packed columns achieved 7-fold lower elution times while maintaining high group-type resolution.

Three diesel samples of increasing boiling range and PAH content were studied using both high resolution (Chapter 2) and high speed (Chapter 3) SFC methods. Achieving near-baseline separation between the group-types became more difficult as the boiling range and PAH content of the diesel samples increased. As a

result, the group-type results for the higher boiling samples became more sensitive to both column choice and instrumental conditions. Diesel analysis times using high resolution (40 cm) titania-silica coupled columns with a typical 2.0 ml min^{-1} flow rate ranged between 14.5 and 50 min. Analysis times using a shorter 15 cm titania-silica coupled column at a high 4.0 ml min^{-1} flow rate reduced these analysis times to between 3 and 7 min. Group-type results obtained under high resolution and high speed conditions compared favorably.

6.1.2 High Temperature High Performance Liquid Chromatography

In Chapter 4, the use of elevated temperatures (up to 200°C) in normal phase HPLC was explored with a thermally stable bare zirconia column for the separation of aromatic compounds using a hexane mobile phase. The benefits of using higher temperatures with bare zirconia based on twenty five model compounds include faster elution times, improved peak shapes, higher efficiency, improved aromatic group-type selectivity, and faster column re-equilibration times. One drawback of using higher column temperatures is that on-column decomposition of thermally labile analytes can occur. This was observed with two pyrrole compounds at temperatures above 100°C in a hexane/dichloromethane mobile phase. Thermal decomposition could be minimized by replacing the dichloromethane with chloroform, increasing flow rate to reduce reaction time, or by limiting column temperature to 100°C.

In Chapter 5, bare titania, bare zirconia, and carbon coated zirconia columns were compared with conventional bare silica and aminopropyl bonded silica columns for the group-type separation of heavy gas oils (>350°C). Generally, group-type separations improved at higher column temperatures. A bare titania column at 65°C

provided the highest overall group-type resolutions based on twenty seven non-polar model compounds. A titania-silica coupled column held at 35°C provided the best saturate vs. monoaromatic separation, but provided poor aromatic group-type resolutions (unlike the results with SFC). As a result, a high resolution two column, dual valve, dual gradient method was developed. A titania-silica coupled column was used to separate the saturates and monoaromatics. Meanwhile, the silica column was by-passed to allow the aromatic group-types to be separated on the bare titania column alone. Three heavy gas oils of increasing sulfur and nitrogen content were separated using this method. Visible minimums were achieved between the group-types.

A fast analysis method was developed using a short 5 cm bare titania column with a high 5.0 ml min^{-1} flow rate. Analysis time could be reduced to only 3 min, including column re-equilibration time following the hexane to dichloromethane gradient. Cut-points for the fast analysis method were calibrated using the high resolution results from a heavy gas oil sample. The high resolution and fast analysis method results for two other heavy gas oil samples were in good agreement. Good precision for both methods was also obtained.

In summary, group-type separations were improved by using bare titania columns in both SFC and HPLC. Analysis times were significantly reduced by using shorter columns with high flow rates without adversely impacting quantitative group-type results. The main advantage of using SFC for the analysis of light boiling materials (<350°C) is that flame ionization detection (FID) may be used to provide reliable mass quantification.[1-4] A second advantage is the 3-fold faster separations

that SFC provides over HPLC when near-ambient column temperatures are used.[5] The main disadvantage of SFC is the inability to use organic solvents with the FID detector due to high background signals. This results in the inability to use a mobile phase stronger than non-polar supercritical carbon dioxide. Thus, the elution of high boiling materials and highly retained polar compounds is difficult with SFC-FID.

One advantage of normal phase HPLC is the ability to elute high boiling materials (>350°C) as well as polar compounds using either chlorinated solvents or more polar mobile phases. A second advantage is the over 30-fold decrease in elution time for highly retained compounds when thermally stable columns are used at temperatures up to 200°C. The main disadvantage of normal phase HPLC is the lack of an ideal detector for the detection of hydrocarbons, as discussed in the following section.

6.2 Future Work

6.2.1 Improvements in HPLC Detection Systems

While flame ionization detection provides reliable mass quantification of hydrocarbon samples with GC and SFC,[1-4] HPLC has no such ideal universal detector. The currently available detection systems for HPLC have significant drawbacks when applied to hydrocarbon analysis. Refractive index detection (RID) is universal in that any analyte with a different refractive index than the mobile phase will provide a response. However, mobile phase gradients cannot be used due to significant baseline deflections.[1,6,7] Also, RID yields non-uniform response factors

for hydrocarbons,[1] and cannot detect compounds with refractive indexes that match the mobile phase.

UV absorbance detection does not provide a response for analytes that lack a chromophore. As a result, saturated compounds cannot be detected.[1,7] Further, UV response factors for aromatic compounds can vary significantly, depending on chemical structure.[1,6,7] Evaporative light scattering detection (ELSD) does not detect volatile compounds.[1] It also provides a logarithmic relationship between analyte concentration and detector response, making quantification more difficult.[1,8,9]

Flame ionization detection has been adapted for HPLC by using rotating disks, moving wires, and rotating belts to dry the organic mobile phase prior to introduction into the flame.[1] While these avoid large background signals due to the carbon content in the organic mobile phase, these interfaces generally lack reproducibility due to variations in the rate of effluent deposition.[1] They can also exhibit memory effects and cannot be used for volatile samples.[7] The need remains for a universal HPLC detector that provides uniform response factors for the various hydrocarbon group-types.

A promising new detection method called acoustic flame detection (AFD) has been developed by Thurbide and co-workers.[6,10,11] First studied as a novel GC detector,[10] and more recently used with HPLC[6] and SFC,[11] this detector employs a hydrogen/oxygen premixed flame that burns in an oscillating manner at the end of a capillary. These oscillations produce an audible sound that changes in frequency as the burn velocity is altered by carbonaceous analytes entering the flame. This results in an easily measured signal. An advantage of AFD is that it responds universally

and uniformly to the carbon content in a sample (similar to FID).[6,11] AFD also provides a linear relationship between signal and concentration over three orders of magnitude (comparable to or better than ELSD and RID).[6,11] Further, the use of organic mobile phases does not result in a high background signal (unlike FID) as the change in baseline can be compensated by adjusting the oxygen flow.[6,11] Finally, the equipment required to setup an AFD detector is an order of magnitude less expensive than other HPLC detectors.[6] A disadvantage of AFD is that it is less sensitive than RID and UV detection, although it is more sensitive than ELSD.[6] Another disadvantage is that mobile phase gradients cannot be used due to large baseline shifts.[6]

In Chapter 4, the use of elevated temperature was shown to significantly reduce retention in normal phase separations. The use of thermal gradients rather than mobile phase gradients with AFD would allow faster analysis times while avoiding baseline shifts. Other approaches that could be taken include adding a reversed mobile phase gradient to the post-column effluent to maintain a stable carbon mass flux through the detector. Alternately, the oxygen flow rate during a separation could be programmed to compensate for the mobile phase gradient.[6] Further, a series of mobile phases could be identified that differ in elution strengths but yield very similar carbon mass fluxes through the flame.[6] This would permit mobile phase gradients to be used with manageable deflections in the baseline. Solvents that are either fully fluorinated or chlorinated should allow gradients to be used as the AFD responds only to reduced carbon.[6] However, these mobile phases can be expensive and would require careful venting of the AFD exhaust due to the

formation of hydrofluoric acid and hydrochloric acid. Also, fully fluorinated or chlorinated hydrocarbons are generally weaker mobile phases than hexane and dichloromethane respectively.[12] As a result, it could be difficult to elute highly retained compounds with such solvents.

Further studies in this area would help encourage the commercialization of AFD, which would be a prerequisite for its widespread acceptance and use. Until AFD or other universal detection systems become commercially available, reliable quantification of hydrocarbon samples by HPLC will remain problematic.

6.2.2 Two Dimensional HPLC of High Boiling Materials

Multidimensional chromatographic separations are used for the analysis of complex samples when one dimensional separations fail to provide sufficient separation. While GC x GC has established a niche for the analysis of petroleum samples,[1,13,14] conventional gas chromatography based methods have an upper sample boiling limit of ~540°C.[1] Above this, irreversible sample adsorption and thermal cracking of sample compounds can become an issue.[1]

Two dimensional HPLC techniques have not yet been widely adopted. There are considerable challenges to performing two dimensional HPLC. In order to characterize the entire sample in a single separation, all the material eluted from the first column must be transferred quantitatively to the second column. This is known as comprehensive two dimensional HPLC. Next, to preserve the separation achieved on the first column, each peak must be sampled three or more times by the second column. Thus, several separations on the second column must take place in the time it takes one peak to elute from the first column. Due to excessively long re-

equilibration times in normal phase HPLC, gradients would be difficult to use to speed up the second dimension separation. Using a very strong mobile phase would also be problematic as most early eluting compounds would be unretained, leading to no benefit of using the second column for most compounds.

In Chapter 4, faster separation times could be obtained with normal phase chromatography at elevated temperatures. High temperature normal phase HPLC could be used to provide faster separations of high boiling samples (>350°C) with low polar content. However, isocratic normal phase HPLC would be difficult to use as the second dimension for samples with highly retained polar compounds due to long separation times (Table 5-3).

For the comprehensive two dimensional HPLC analysis of polymers, a size exclusion chromatography (SEC) column has been used as the second dimension.[15] Size exclusion chromatography separates molecules based on their exclusion from a porous packing. Sample molecules that are too large to enter the porous particles elute from the column first at the total exclusion limit. Very small molecules that can diffuse into the particles through even the smallest pores elute last at the total permeation limit. Molecules of intermediate sizes elute at intermediate times based on what fraction of the pore volume they are excluded from. Under ideal conditions, interactions between the sample molecules and the stationary phase surface are insignificant. Thus, the latest eluting compounds elute at the permeation limit, which corresponds to the dead time in normal phase chromatography. This permits very fast elution times to be achieved. Synovec and co-workers demonstrated the fast SEC separation of toluene and a 500 000 g mol^{-1} polystyrene polymer in only 3 seconds.[16]

Further, the use of elevated temperatures up to 150°C with higher flow rates resulted in 4-fold shorter analysis times.[17]

SEC has yet to be used as the second dimension in two dimensional comprehensive HPLC separations of high boiling oil samples. Based on results in Chapter 5, a bare titania column, held at 65°C for better group-type resolutions, could be used as the first dimension to separate samples according to aromatic ring number. An ideal second dimension column would be a short SEC column operated at high flow rates and elevated temperature to permit very fast separations (<15 seconds). The SEC column would separate compounds according to size (e.g., high and low molecular weight saturates). A procedure for selecting the optimal experimental conditions and column dimensions for comprehensive two dimensional HPLC was recently published.[18] Additional benefits of using elevated temperature with SEC for high boiling materials are enhanced sample solubility[19] and less aggregation of the highest molecular weight compounds known as asphaltenes.[19,20] The ability to perform comprehensive two dimensional HPLC on high boiling materials would allow a higher degree of separation than previous obtained.

6.2.3 Size Exclusion Chromatography

Typical SEC columns are based on polystyrene-divinylbenzene or silica when additional mechanical strength is required. However, aromatic hydrocarbons and polar compounds typically display significant retention on such phases in most solvents.[1,21] As a result, the use of conventional SEC columns for separating oil samples may lead to significant interactions between the sample and the SEC stationary phase. This leads to samples being separated by both size and

thermodynamic retention simultaneously. Thus, accurate molecular weight determinations become very difficult.[1,21] In Chapters 4 and 5, elevated temperatures were shown to reduce retention in normal phase HPLC. Similar reductions in the retention of analytes on SEC columns would be expected, making SEC separations less skewed by undesirable retention. Commercial high temperature SEC instruments exist. They were designed for separating polymers that are not soluble at ambient temperatures. They could also be used to reduce interactions between the sample and the stationary phase.

Another way of reducing undesirable retention would be to develop SEC columns based on fluorinated stationary phases. Fluorinated solvents are known to be among the weakest normal phase solvents.[12] Additionally, perfluoroalkane modified silica exhibits low retention to non-fluorinated molecules due to its very weak surface interactions.[22,23] Polymeric SEC columns could be made from fluorinated monomers or could be fluorinated after particle formation, although the mechanical strength of such a phase could be suspect. Efforts to reduce interactions between sample compounds and the column packing material would improve the accuracy of molecular weight determinations by SEC.

The other major limitation of SEC separations of oil samples is calibration of elution time to molecular weight. Typically, polystyrene standards are used to perform this calibration. These long linear polymers are not representative of the compounds observed in high boiling materials.[1,24,25] The lack of truly representative model compounds complicates molecular weight distribution determinations. Mass spectrometry can be used with various ionization methods to determine molecular

weight accurately.[24] However, obtaining quantitative data with such methods is difficult as discussed in Section 5.1. Reduced sample-surface interactions and improved calibration methods would be needed to improve the accuracy of SEC methods towards the separation of high boiling oil samples.

6.2.4 Appropriate Application of Analytical Methods

The discussion in this section is more philosophical in nature. Analytical chemists have long concerned themselves with characterizing samples using a wide variety of available techniques. We try to answer the questions "what is in the sample?" and "how much is there?" with higher accuracy, better precision, in less time, and for less money. A review of the literature might leave one with the impression that analytical chemists are concerned with generating or improving analytical methods with little thought of solving real-world problems. While this is not entirely true, the amount of effort that we apply to developing or optimizing methods for the same problems is disproportionate to the effort applied to problems that have no existing analytical solution. This represents a missed opportunity as an analytical method is only as valuable as the problems that it can solve. There will always be a need to improve upon existing methods. However, a concerted effort must also be made to determine what problems confront our society for which there are currently no suitable methods.

An improvement in the appropriate application of analytical methods in the oil industry is no exception. Problems that currently challenge the oil industry include determining the conditions in upgrading units that result in increased levels of fouling or catalyst deactivation. Process streams need to be studied carefully to determine

what chemical markers signify favorably or unfavorable reactor conditions. Pattern recognition software could be used when trends are not obvious.[26,27] Suitable on-line process monitoring methods must then be developed to help mitigate unfavorable conditions. Most processes are currently operated with minimal on-line chemical monitoring.[28]

As existing industrial processes are continually improved upon and new processes are developed, our analytical methods must also adapt. We must never stop searching for novel applications of analytical methods (both existing and as yet non-existent) to solve the persistent chemical problems that face our society.

6.3 References

(1) Barman, B. N.; Cebolla, V. L.; Membrado, L., *Crit. Rev. Anal. Chem.* **2000**, *30*, 75-120.

(2) Thiébaut, D. R. P.; Robert, E. C., *Analusis* **1999**, *27*, 681-690.

(3) DiSanzo, F. P.; Yoder, R. E., *J. Chromatogr. Sci.* **1991**, *29*, 4-7.

(4) M'Hamdi, R.; Thiébaut, D.; Caude, M., *J. High Resol. Chromatogr.* **1997**, *20*, 545-554.

(5) Chester, T. L.; Pinkston, J. D., *Anal. Chem.* **2002**, *74*, 2801-2812.

(6) Thurbide, K., B.; Xia, Z., *Anal. Chem.* **2004**, *76*, 5459-5464.

(7) Kaminski, M.; Kartanowicz, R.; Gilgenast, E.; Namiesnik, J., *Crit. Rev. Anal. Chem.* **2005**, *35*, 193-216.

(8) Young, C. S.; Dolan, J. W., *LCGC* **2003**, *21*, 120-128.

(9) Young, C. S.; Dolan, J. W., *LCGC* **2004**, *22*, 244-250.

(10) Thurbide, K., B.; Wentzell, P., D.; Aue, W., A., *Anal. Chem.* **1996**, *68*, 2758-2765.

(11) Xia, Z.; Thurbide, K., B., *J. Chromatogr. A* **2006**, *1105*, 180-185.

(12) Lundanes, E.; Greibrokk, T., *J. High Resol. Chromatogr.* **1994**, *17*, 197-202.

(13) Beens, J.; Brinkman, U. A. T., *Trends Anal. Chem.* **2000**, *19*, 260-275.

(14) Barman, B. N., *Anal. Chem.* **2001**, *73*, 2791-2804.

(15) van der Horst, A.; Schoenmakers, P. J., *J. Chromatogr. A* **2003**, *1000*, 693-709.

(16) Renn, C. N.; Synovec, R. E., *Anal. Chem.* **1988**, *60*, 200-204.

(17) Renn, C. N.; Synovec, R. E., *Anal. Chem.* **1992**, *64*, 479-484.

(18) Schoenmakers, P. J.; Vivo-Truyols, G.; Decrop, W. M. C., *J. Chromatogr. A* **2006**, *1120*, 282-290.

(19) Carbognani, L.; Orea, M., *Pet. Sci. Technol.* **1999**, *17*, 165-187.

(20) Espinat, D.; Fenistein, D.; Barre, L.; Frot, D.; Briolant, Y., *Energy & Fuels* **2004**, *18*, 1243-1249.

(21) Andersen, S. I., *J. Liq. Chromatogr.* **1994**, *17*, 4065-4079.

(22) Glatz, H.; Blay, C.; Engelhardt, H.; Bannwarth, W., *Chromatographia* **2004**, *59*, 567-570.

(23) Ecknig, W.; Trung, B.; Radeglia, R.; Gross, U., *Chromatographia* **1982**, *16*, 178-182.

(24) Mullins, O. C., *Fuel* **2007**, *86*, 309-312.

(25) Sarowha, S. L. S., *Pet. Sci. Technol.* **2005**, *23*, 573-578.

(26) Johnson, K. J.; Synovec, R. E., *Chemom. Intell. Lab. Syst.* **2002**, *60*, 225-237.

(27) Synovec, R. E., *J. Chromatogr. A* **2005**, *1096*, 1.

(28) Robbins, W. K., *J. Chromatogr. Sci.* **1998**, *36*, 457-466.